ABSTRACT

Title of Document: PHYTOPLANKTON AND NUTRIENT DYNAMICS WITH A FOCUS ON NITROGEN FORM IN THE ANACOSTIA RIVER, IN WASHINGTON, D.C. AND WEST LAKE, IN HANGZHOU, CHINA

Melanie L. Jackson, Master of Science, 2016

Directed By: Patricia M. Glibert, Professor
Marine Estuarine Environmental Science

Nutrient loading has been linked with severe water quality impairment, ranging from hypoxia to increased frequency of harmful algal blooms (HABs), loss of fisheries, and changes in biodiversity. Waters around the globe are experiencing deleterious effects of eutrophication; however, the relative amount of nitrogen (N) and phosphorus (P) reaching these waters is not changing proportionately, with high N loads increasingly enriched in chemically-reduced N forms. Research involving two urban freshwater and nutrient enriched systems, the Anacostia River, USA, a tributary of the Potomac River feeding into the Chesapeake Bay, and West Lake, Hangzhou, Zhejiang Province, China, was conducted to assess the response of phytoplankton communities to changing N-form and N/P-ratios. Field observations involving the characterization of ambient phytoplankton communities and N-forms, as well as experimental (nutrient enrichment) manipulations were used to understand shifts in phytoplankton community composition with increasing NH_4^+ loads. In both locations, a >2-fold increase in ambient NH_4^+:NO_3^- ratios was followed by a shift in the phytoplankton community, with diatoms giving way to chlorophytes and cyanobacteria. Enrichment experiments mirrored this, in that samples enriched with NH_4^+ lead to increased abundance of chlorophytes and cyanobacteria. This

work shows that in both of these systems experiencing nutrient enrichment that NH_4^+ supports communities dominated by more chlorophytes and cyanobacteria than other phytoplankton groups.

PHYTOPLANKTON AND NUTRIENT DYNAMICS WITH A FOCUS ON NITROGEN FORM IN THE ANACOSTIA RIVER, IN WASHINGTON, D.C. AND WEST LAKE, IN HANGZHOU, CHINA

By

Melanie Leigh Jackson

Thesis submitted to the Faculty of the Graduate School of the
University of Maryland, College Park and University of Maryland Center for Environmental Science, in partial fulfillment
of the requirements for the degree of
Master of Science
2016

Advisory Committee:
Professor Dr. Patricia M. Glibert, Chair
Professor Dr. Jeffrey Cornwell
Professor Dr. Caroline M. Solomon
Assistant Professor Dr. Alexander E. Parker

ACKNOWLEDGEMENTS

I would like to express the deepest appreciation to my committee chair Professor Patricia Glibert for her motivation, guidance, and support through the learning process of this master thesis. Without her patience and willingness to help, this thesis project and my ability to pursue a career in oceanography would not have been possible.

I would like to thank my committee members, Professor Jeffrey Cornwell, Professor Caroline Solomon, and Assistant Professor Alexander Parker for their contributions and assistance to help me complete this thesis. In particular, I am extremely grateful for Dr. Solomon's help coordinating the fieldwork in the Anacostia River and the Anacostia Riverkeeper for allowing me to join.

I would also like to thank Professor Mengmeng Tong for her hospitality and advice while I was in China, as well as the students Jingjing Yang and Youmai Li for their assistance with fieldwork and sample analysis. In addition, without the help of Peipei Qu I would have never found my way around the Zhejiang University Campus and felt so comfortable in China.

I am grateful for the support from the NSF EAPSI summer fellowship, as well as support from Zhejiang University (ZJU) and the State Oceanic Administration (SOA) in Hangzhou, China. Many thanks to ZJU and SOA for providing advice and technical support. I am also grateful for the Waterfowl Chesapeake Board of Directors and the Explorers Club Washington Group exploration grant for their financial support. I thank Harry Nelson and Fluid Imaging Technologies for their assistance and use of the FlowCAM for sample analysis.

I am especially thankful to Jeffrey Alexander for his support and guidance from the start. In addition, I thank HPL Analytical Services for their help analyzing samples in such a timely manner. I thank my fellow labmates, students, and friends at HPL for moral support and interesting discussions. Finally, I would like to thank my family and fiancé, from whom I rely on for calming words and encouragement.

TABLE OF CONTENTS

LIST OF TABLES

LIST OF FIGURES

Chapter 1: Nitrogen form determining recent phytoplankton dynamics and community structure in the urbanized Anacostia River, Washington, D.C.

INTRODUCTION

An estimated 5-fold increase in reactive nitrogen (N) use compared to pre-industrial time in the United States has led to the enrichment of N relative to phosphorus (P; increased N:P) in many coastal waters (Houlton *et al.*, 2013, Peñuelas *et al.*, 2013, Glibert *et al.*, 2014). Imbalances in N:P loading have been identified as having direct and indirect effects on organismal metabolism, species composition, and ultimately food webs (Sterner and Elser, 2002, Hall, 2009, Glibert *et al.*, 2011, Peñuelas *et al.*, 2013). Despite knowledge that increased N:P loading is occurring worldwide, disproportionate changes in N forms reaching many coastal waters are also occurring, specifically increasing loads of chemically reduced (e.g. NH_4^+, organic N) relative to oxidized N (e.g. NO_3^-; Glibert *et al.*, 2014a, 2016). Although NO_3^- is the dominant N form contributing to eutrophication in many systems, there are many sources of NH_4^+ that are on the increase, therefore it is important to determine the role of relative NH_4^+:NO_3^- ratios in determining the composition of primary producers and productivity in coastal systems.

Over the last half-century, escalating N use has been attributed to the substantial increase in fertilizer usage, sewage effluent, and atmospheric deposition (Vitousek *et al.*, 1997, Galloway and Cowling, 2002, EPA, 2011, Glibert *et al.*, 2014a). Nutrient loading is associated with detrimental effects of eutrophication, including increased algal growth and development of high biomass blooms, changes in species diversity of both primary and secondary producers, reductions in dissolved oxygen resulting in fish kills, and

increased frequency of harmful algal blooms (HABs; Nixon, 1995, Cloern, 2001, Glibert and Burkholder, 2006, Heisler *et al.*, 2008, Glibert *et al.*, 2010). Not only is N loading rising, but the form of N nutrient delivered to many coastal marine and freshwater systems is changing, with coastal systems across the globe experiencing sustained and elevated concentrations (>5 μM) of NH_4^+ (Glibert *et al.*, 2016). Increasing NH_4^+ loads can be attributed to sewage treatment plant upgrades releasing large quantities of NH_4^+ (NRC, 2000) and global fertilizer usage shifting to more urea use than NO_3^- (Glibert *et al.*, 2006, 2014a). Following shifts in N form from NO_3^- to NH_4^+, numerous systems have observed shifts in phytoplankton community composition from those dominated by diatoms to flagellates and cyanobacteria, and ultimately shifts in the composition of higher food webs (Legendre and Rassoulzadegan, 1995, Glibert, 1998, Mousseau *et al.*, 2001, Berg *et al.*, 2003, Heil *et al.*, 2007, Glibert *et al*. 2016).

Algal blooms occur when there are sufficient nutrients to support growth and biomass; however, some phytoplankton functional groups and species have preferences for different nutrient forms (Glibert *et al.*, 2016 and references therein). A central tenet in phytoplankton physiology has classically considered NH_4^+ the preferred form of N for phytoplankton uptake (McCarthy, 1981, Raven *et al.*, 1992), a function of its favorable energetics and the repression of NO_3^- uptake by NH_4^+ (Dortch, 1990). For instance, systems impacted by NH_4^+ (4-10 μM) from sewage effluent, such as the San Francisco Bay Delta, have observed the repression of NO_3^- uptake by NH_4^+ (Dugdale *et al.*, 2007, Glibert *et al.*, 2014c). Likewise, in the San Francisco Bay Delta, the loss of diatoms following mesocosm enrichment experiments enriched with NH_4^+ has been observed (Glibert *et al.*, 2014c). Work in the Baltic Sea and the southwest Florida shelf has found

that dinoflagellates are associated with N concentrations dominated by reduced forms rather than NO_3^- (Berg *et al.*, 2003, Heil *et al.*, 2007). The effect of NH_4^+ and relative changes in NH_4^+:NO_3^- on phytoplankton community composition has been more difficult to appreciate in systems experiencing chronic nutrient loading.

One of the most contaminated rivers in the USA, the Anacostia River (SRC, 2000), running from Bladensburg, MD to Washington, D.C., experiences significant and consistent N pollution from point and nonpoint sources (Miller *et al.*, 2013). The Anacostia is in a highly urbanized area of the Chesapeake Bay watershed and is listed as impaired in Maryland's 305b report with selected fish-consumption advisories in effect (MDE, 2012). Based on the river's long history of pollution contributing to its degradation from industrial and urban sources (Hwang and Foster, 2006), it has been designated one of the three highest priority regions of concern within the Chesapeake Bay region (CBP, 2002). The majority of the literature on the Anacostia River consists of reports on pollutants such as toxic chemicals (e.g. Hwang and Foster, 2006, Velinsky *et al.*, 2011). However, sources of pollution such as leaking sewer infrastructure, outfalls from industry and sewage-treatment plants, landfills, fertilizer runoff from lawns, gardens and atmospheric deposition all contribute to N pollution that reaches the Anacostia River (Miller *et al.*, 2013). Sewage effluent is of particular concern, considering approximately 1.3 billion gallons of untreated sewage mixed with storm water is released into the river each year from combined sewer overflow (CSO) outfalls (DC Water, 2016). Although it is understood that sewage effluent and other sources are contributing to N pollution in the Anacostia River, it is not well known how nutrient pollution and the different forms (i.e., NO_3^- and NH_4^+) vary temporally or spatially or their effects on primary producers.

The Anacostia River is in one of the most densely populated watersheds in the Chesapeake Bay drainage basin with over 800,000 residents (EPA, 2016). As a result, development and associated increases in impervious surfaces cause storm discharges to be flashy, thus enhancing downstream fluxes of N (Miller *et al.*, 2013). In hopes of improving water quality in the Anacostia River, a multi-billion dollar project is underway that will reduce CSO overflows (DC Water, 2016), along with many other restoration projects throughout the watershed; although the CSO project will be fully implemented in October 2016, based on responses following nutrient reductions in other parts of the Chesapeake Bay, it is expected that it will take time for the system to respond (Kemp *et al.,* 2005).

Given the increasing number of restoration efforts and investments being made in the watershed, it is essential to understand the effect of N form on phytoplankton community composition. The overall goal of this study was to evaluate the impact of NH_4^+ compared to NO_3^- on the phytoplankton community composition and productivity. The nutrient dynamics, productivity, and phytoplankton community assemblage were characterized along the river differentially impacted by varying NH_4^+ levels. Even against a background of elevated nutrient concentrations, it was hypothesized that sites characterized by higher NH_4^+ levels would have a community dominated by cyanobacteria and other NH_4^+-tolerant flagellates. Contrastingly, areas with lower NH_4^+:NO_3^- would consist of mostly diatoms. In addition to characterizing differences in the river, enclosure experiments with river water were conducted with either NH_4^+ or NO_3^- enrichments to assess the role of these different forms of N in the growth of different phytoplankton groups. The enclosure experiments were expected to mirror and

extend the ambient community observations, with additions of NH_4^+ supporting a greater proportion of cyanobacteria and chlorophytes, and NO_3^- additions supporting more diatoms. Finally, a series of enrichment experiments in which samples were collected from contrasting sites in terms of NH_4^+ were conducted to determine the concentration of NH_4^+ addition required to repress NO_3^- metabolism when nutrients concentrations were elevated. This tested the hypothesis that in waters with higher NO_3^- concentrations, higher concentrations of NH_4^+ are required to repress NO_3^- uptake than waters with lower NO_3^- concentrations.

MATERIAL AND METHODS

Study Site and Available Data

The Anacostia River is one of the largest tributaries of the Potomac River, with a watershed area of 456 km^2 (MDE, 2010), draining portions of Maryland and the District of Columbia. The river is on average 1.2 m deep at the Bladensburg Bridge in the north to 5.6 m at the confluence with the Potomac (Fig. 1). The river is ~10 km long and is about 60 m wide at the northerly end and 500 m wide at the mouth. The water level varies by approximately a meter with a semidiurnal tide up to Bladensburg, and responds similar to a standing wave (Behm *et al.*, 2003, Tetra Tech, 2014), since the tide changes occur almost simultaneously throughout the estuary based on friction and the "funnel-like" shape of the river (Friedrichs and Aubrey, 1994). The entire river is freshwater, with discharges from the Northeast and Northwest Branch making up ~77% of the total discharge in the river with the balance of the flow from tributaries (Warner *et al.*, 1997), such as Watts Branch, Hickey Run, Beaverdam Creek, CSO outfalls, overland flow, groundwater seepage and precipitation. The water entering from the NE and NW

Branches of the Anacostia river discharged on average 3.6 m^3 s^{-1} during 2014 and 2015 (USGS Stations 01649500 and 01650500; www.waterdata.usgs.gov). The coarse sediments in the upper portion of the river are more suitable for groundwater seepage (average of 0.125 m^3 s^{-1}), but this only contributes 4% of the average NE and NW Branch average discharge (Logan, 1999, Miller *et al.*, 2013, Tetra Tech, 2014). There are currently 14 CSOs concentrated in the lower portion of the Anacostia that discharge a mixture of sewage and stormwater into the surface of the tidal river during storm events.

The analysis herein is based on a combination of data collected by the Chesapeake Bay Program and sampling efforts from 2013 to 2015 (http://www.chesapeakebay.net/data). Samples were collected primarily bimonthly during the summer and once a month during the winter. This work focuses on data collected at 9 sites along the Anacostia River from Bladensburg Bridge down to the confluence of the Potomac River (ANA0082, ANA01, ANA03, ANA08, ANA13, ANA14, ANA15, ANA17, and ANA22; Fig. 1).

Sample Collection and Analytical Protocols

During bimonthly sampling efforts from 2013 to 2015, a transect from the upper river (ANA0082) at the Bladensburg Bridge to the confluence of the Potomac (ANA22) was conducted (Table 1). Sampling occurred prior to high tide in the morning before 10am. At each station measurements of temperature, salinity, and dissolved oxygen were measured using a YSI-85 sonde for 2013-2014 and YSI Pro 2030 for 2015. Surface water was collected using a clean bucket for nutrients, chlorophyll *a* (chl *a*) and phytoplankton enumeration. Water was collected from each site and returned to the laboratory (within ~4 h) on ice for analysis.

Samples were analyzed in the laboratory of Gallaudet University or University of Maryland Center for Environmental Science. The same protocols and analysis methods were used throughout sampling dates for all nutrients. Samples were immediately filtered through Whatman GF/F filters (nominally 0.7 μm; precombusted 2 h 450 °C) for pigment analysis and for the determination of total chl *a*. The GF/F filtrate was stored frozen for later nutrient analysis of NH_4^+, NO_3^-, PO_4^{3-}.

Concentrations of NH_4^+ were analyzed according to Parsons *et al.* (1984). Concentrations of NO_3^- were analyzed according to Jones (1984) for uptake measurements, while ambient NO_3^- concentrations were determined at Gallaudet University according to Miranda *et al.* (2001) and Doane and Horwáth (2003). PO_4^{3-} was determined at Horn Point Laboratory Analytical Services following Bran and Luebbe (1999) Method G-175-96. Urea was analyzed according to Revilla *et al.* (2005). Samples for chl *a* were analyzed using a Turner Designs Model 10-AU fluorometer following acetone extraction and acidification as described by Parsons *et al.* (1984).

Community Composition

The phytoplankton community composition was enumerated from samples collected within the transect on the Anacostia River during the summer of 2014 using an image particle analyzer (FlowCAM; Fluid Imaging Technologies®), whereas shifts in phytoplankton community composition were assessed over the course of the year in 2015 using accessory pigments. In 2014 (July 9, July 23, and August 7), samples were collected from ANA0082, ANA03, ANA08, ANA13, ANA22 and returned to University of Maryland Center for Environmental Science. On July 9 and July 23, extra samples were taken for phytoplankton enumeration based on the presence of a surface feature

between the upper river and middle of the river (between ANA0082 and ANA03). Samples for assemblage analysis were kept cool until analysis by FlowCAM. A 10X objective (UPlan FLN, Olympus®) and 100 μm field-of-view flow cell were used. Approximately 10 mL of sample were run through the system, and cells were counted through Auto Image mode with a peristaltic pump rate of approximately 0.3 ml min^{-1} (according to manufacturer specifications). The Visual Spreadsheet program (Fluid Imaging®) was used to create libraries to identify cells by genus-level, removing bubbles, particles, and debris. Only a portion of the volume moving through the flow cell is in the field of view; therefore, the concentration of cells was automatically calculated using the total number of particles counted, field of view dimensions, depth of the flow cell, and total number of images collected. The spreadsheet program was checked manually after sorting with libraries to remove any invalid images or bubbles.

In 2015, community composition was determined using accessory pigments. The samples from 2015 were frozen at -80°C until analysis, and processed by High Performance Liquid Chromatograph (Agilent) following the protocols of Van Heukelem and Thomas (2001). Each of the pigments were used for the chemosystematic identification of five algal functional groups: chl *b* as an indicator of chlorophytes, alloxanthin as an indicator of cryptophytes, fucoxanthin as an indicator of diatoms, peridinin as an indicator of peridinin-containing dinoflagellates, and zeaxanthin as an indicator of cyanobacteria (Jeffrey and Wright, 1994, Jeffrey and Vesk, 1997, Glibert *et al.*, 2004).

Experimental Treatments

A series of enrichment experiments were performed to test the hypothesis that changes in either phytoplankton community composition or N-metabolism with the addition of different N-forms. Enrichment experiments in 2014 were conducted to address whether the addition of different N-forms would support differing phytoplankton community compositions even in the presence of N levels that were already enriched. A second set of enrichment experiments was conducted in 2015 using ^{15}N tracer techniques (Glibert and Capone 1993) to measure N uptake rates and to determine the concentration of NH_4^+ that would be required to repress NO_3^- uptake.

During the first set of experiments (June 30, 2014) water was collected from the site closest to the confluence with the Potomac River (ANA22) and returned to the University of Maryland Center for Environmental Science for the initiation of enrichment experiments. Samples were enriched with 10, 20, and 30 μM NO_3^- or NH_4^+. The N-enrichment was targeted to create a gradient of N conditions and ensure that concentrations were >20 μM, allowing for NH_4^+ concentrations to be >2-fold larger than the mean concentration observed at ANA22 from 2013 to 2014 (18.6 μM). The incubations were placed in water-filled enclosures to maintain ambient temperatures and covered with a single layer of neutral density screening to simulate 60% of neutral irradiance. The community composition was tracked for 24 hours using the FlowCAM protocol described above. The statistical difference between the community composition between NH_4^+ and NO_3^- treatments was calculated using an unpaired, two sample Welch's t-test, using the statistical computing and graphics software R base and statistics packages (R Core Team, 2014). This statistical analysis was chosen to compare the

means of NH_4^+ and NO_3^- treatments, since there was no replication of the concentration gradient additions.

For the second set of enrichment experiments (April 16, April 29, May 13, and May 27, 2015), ~5 L of water were collected from ANA0082 and ANA22 (upper river and lower river) and were returned to University of Maryland Center for Environmental Science and were both enriched with 10 and 25 μM NH_4^+. Similar to the enrichment experiments in 2014, the additions were targeted to ensure that resulting NH_4^+ concentrations were >20 μM, which were approximately 2-fold greater than the ambient conditions at ANA22. At the same time in order to determine N uptake rates, an additional 10 μM-^{15}N of different labeled substrates (NO_3^-, NH_4^+, and urea; April 16, May 13 and May 27) or 25 μM-^{15}N (April 29) was added to individual aliquots. Containers were placed in water-filled enclosures to maintain ambient temperatures and were covered with 3 layers of neutral density screening to simulate 15% of natural irradiance and the low light conditions in the turbid waters, which may be more frequently observed during the pulsing of nutrients from point sources. The bottles were put in the water-filled enclosures directly after the enrichments. The incubations were removed from the enclosure after ~30 min, filtered onto Whatman precombusted GF/F filters and frozen for ^{15}N uptake. The filtrate was frozen for ambient nutrient analysis, and filters were later analyzed by mass spectrometry. The filters were dried for ~48 hrs, packed into tin capsules, and analyzed on a Sercon mass spectrometer.

Statistical Analysis from Ambient Field Data

Seasonal and spatial patterns were observed using linear interpolation contour maps for ambient nutrients and biomass from 2013-2015. Linear interpolation contour maps were created of NO_3^-, NH_4^+, NH_4^+:NO_3^-, and chl *a* using the Akima package (Akima *et al.*, 2009) in the R software 3.1.2 (R Core Team, 2014).

All available ambient nutrient data and pigment data from 2015 sampling were compiled to determine relationships of ambient nutrients with accessory pigments. The relationship between ambient nutrient concentrations and ratios relative to accessory pigments (denoted as pigment concentration: Chl *a* (μg L^{-1}: μg L^{-1})) were described using a numerical summary correlation (Pearson's r significance testing was performed with the statistical computing and graphics software R using base and statistics packages (R Core Team, 2014). This statistical analysis was chosen since typically parametric tests are used with ratio data.

Statistical Analysis from Uptake Experiments

Biomass-specific uptake rates ($V(h^{-1})$) were calculated for the ^{15}N analyses based on the following formula (Dugdale and Wilkerson, 1986, Glibert and Capone, 1993):

$$V = \frac{(^{15}N \text{ atom \% sample} - {}^{15}N \text{ atom \% normal})}{(^{15}N \text{ atom \% enrichment} \times \text{incubation duration})}$$

where atom % sample is the ^{15}N enrichment in the sample, atom % normal is the natural ^{15}N background enrichment (enrichment concentration divided by the sum of the enrichment concentration and the ambient concentration), and ^{15}N atom % enrichment is the initial isotope enrichment based on added plus ambient substrates (Glibert and Capone, 1993). Since the ^{15}N addition made to these experiments was substantially

elevated, no isotope dilution would be expected and therefore no isotope dilution correction was made (Glibert *et al.*, 1982, Glibert and Capone, 1993). Uptake rates for NH_4^+, NO_3^-, and urea were calculated and summed for samples during the spring of 2015 (April 15th and April 29th). The summed value for N uptake (maximal N-based productivity rates) is used as a physiological index to better understand the potential for total uptake, given that all N forms are provided at or near saturating conditions (Wilkerson *et al.*, 2006).

RESULTS

Ambient Environmental Conditions

Consistent seasonal trends in salinity and temperature measurements were observed in the Anacostia River from 2013 to 2015. Overall, salinity ranged from 0.1 to 0.8. Temperatures ranged from 6.2 to 32.2°C. The average monthly temperature was highest in July (26.36±1.07°C), and the lowest average temperature was observed in March (7.53±0.04°C).

The concentration and proportions of nutrients in the Anacostia River varied substantially over time (Figs. 2-7). The greatest range in nutrient concentrations was observed in NO_3^- concentrations with concentrations from 0 to 83.5 μM (Fig. 2). Maximum concentrations of NO_3^- concentrations were observed from March to May in 2013 and 2014 (Fig. 2). During August of both years, NO_3^- concentrations decreased across all sites from early spring and summer concentrations. As waters moved from the upper Anacostia River to the confluence of the Potomac, concentrations of NO_3^- decreased by approximately 20 μM during July and August (Fig. 2). Concentrations of NH_4^+ ranged from 0 to 62 μM (Fig. 3). Increased concentrations of NH_4^+ were detected

from May through July in 2013 and 2014 (Fig. 3). Increases in NH_4^+ downstream (typically after ANA03) were noted from May to July each year (Fig. 3); however, NH_4^+ concentrations were consistently higher downstream compared to upstream concentrations. Concentrations of urea ranged from 0 to 9.5 μM (Fig. 4). Maximum concentrations of urea concentrations were observed from March to July in 2013 and 2014, with peak concentrations in the lower river (Fig. 4). Concentrations of PO_4^{3-} ranged from 0.01 to 3.16 μM (Fig. 5). Peaks in PO_4^{3-} concentrations were typically observed in July and August, whereas the lowest concentrations were observed in April (Fig. 5).

Changes in nutrient ratios further demonstrate spatial and temporal patterns. The molar ratios of DIN (NO_3^- plus NH_4^+) to PO_4^{3-} were always more than the canonical Redfield ratio (site ANA0082; Fig. 6). Peaks in molar DIN:PO_4^{3-} ratios were noted in May of 2013 and 2015 (~350-525), whereas in 2014 peaks in DIN:PO_4^{3-} were observed in February and May (~250; Fig. 6). Ratios of NH_4^+:NO_3^- were highest from May to September in 2013, with a maximum of 3.5 in July (Fig. 7). In early August 2014, the ratios of NH_4^+:NO_3^- approximately doubled from conditions in June and July, reaching a ratio of 1.25, followed by another peak in late August reaching 1.7 (Fig. 7). The NH_4^+:NO_3^- ratio in the upper river (ANA0082) was typically the lowest, only reaching a maximum of 1.27, whereas ratios increased mid-River (ANA03; at the confluence of Hickey Run and Watts Branch), with maximum ratio of 2.03 (Fig. 7).

Phytoplankton Biomass and Community Composition

Concentrations of chl *a* ranged from 0.18 to 90.4 μg L^{-1} (Fig. 8). In 2013, chl *a* started to increase in May and peaked on September 18 (90.4 μg L^{-1}; Fig. 8A). The

maximum chl *a* concentration in 2014 was recorded in May (90.4 μg L^{-1}) and steadily decreased over the summer and winter. Peaks in chl *a* concentrations consistently occurred at ANA03 (~60 μg L^{-1}), and a secondary peak was observed at ANA22 in July and August of 2014.

2014

During the summer 2014 sampling, specifically from July 9 to August 8, NH_4^+:NO_3^- ratios approximately doubled and chl *a* concentrations declined (Fig. 9A and D). On July 9, the upper and middle river were characterized by peak NO_3^- concentrations (~55 μM) and chl *a* maxima (Fig. 9A and C). On August 8, NH_4^+ concentrations of ~20 μM were found in the upper and middle river, with chl *a* concentrations in the upper river declining from July concentrations from ~30 to ~10μg L^{-1} (Fig. 9A and B). Using the FlowCam during this time period, the phytoplankton total abundance ranged from 145 to 764 cells mL^{-1} (Fig. 10A, C, and E). The highest average phytoplankton abundance was observed on July 9 (410 ± 235 cells mL^{-1}). The average phytoplankton abundances on July 23 and August 8 were approximately two-fold less than observed on July 9 (288 ± 208 cells mL^{-1} and 306 ± 99 cells mL^{-1}, respectively). Along the transect sites, from the upper river (ANA0082) to the lower portion of the river (ANA22), phytoplankton abundance more than doubled. Other than the high abundances near the confluence with the Potomac, blooms were observed in the upper river on July 9 and July 23. On July 9, a bloom occurred in between site ANA0082 and ANA01 and reached a maximum abundance of 2284 cells mL^{-1}. The bloom was still visible and present on July 23; however concentrations were 13% of what they were on July 9 (319 cells mL^{-1}).

The phytoplankton community composition observed using the FlowCam during the summer of 2014 was made up of five major taxonomic groups, with diatoms consistently making up >25% of the community (Fig. 10B, D, and F). The majority of the diatom community was made up of the colonial *Melosira* spp. Cryptophyte abundance (mostly *Cryptomonas* spp.) was greatest on July 9 compared to July 23 and August 8 sampling (Fig. 10B). As cryptophytes decreased, the occurrence of dinoflagellates increased, reaching their highest abundance on July 23 (Fig. 10D). Chlorophyte abundance remained relatively constant over the course of sampling (Fig. 10B, D, and F). The upper river (ANA0082) was dominated by dinoflagellates (likely *Gymnodinium* spp.) on July 23, but on July 9 and August 8 the site was dominated by diatoms, making up >50% (Fig. 10B, D, and F). The middle river (ANA03 and ANA08) was dominated by cryptophytes (>50%) on July 9 (Fig. 10B). Chlorophytes made up ~25% of the community at ANA08 and ANA13 on July 23 and August 8 (Fig. 10D and F).

2015

Large temporal and spatial shifts were observed in community composition based on pigment signatures during 2015 from the upper river to the lower river (ANA0082, ANA08, and ANA22; Fig. 11). The highest accessory pigment concentration in relation to that of chl *a* was suggestive of diatoms in April (0.36 μg L^{-1} fucoxanthin: μg L^{-1} chl *a*; Fig. 11A). Chl *b*, suggestive of chlorophytes, was the next highest accessory pigment detected, with a peak concentration of 0.29 μg L^{-1} chl *b*: μg L^{-1} chl *a* observed in June (Fig. 11C). Overall, peridinin relative to chl *a* (dinoflagellates) was low, less than 0.007 μg L^{-1} peridinin: μg L^{-1} chl *a* throughout 2015. Large seasonal changes in diatoms (as

fucoxanthin: chl *a*) were observed, with concentrations decreasing from March to September. Unlike in 2014, chlorophytes (as chl *b*: chl *a*) increased from May to June. In addition, cryptophytes (as alloxanthin: chl *a*) increased prior to chlorophytes. All sampling sites showed a similar pattern in the shift in community composition from diatoms to chlorophytes; however, in the middle of the river (ANA08) diatoms (as fucoxanthin: chl *a*) began to increase in September (Fig. 11B). Diatoms (as fucoxanthin: chl *a*) were highest in the upper river (ANA0082; 0.36 μg L^{-1}: μg L^{-1}), whereas chlorophytes (as chl *b*: chl *a*) were highest in the lower river (ANA22; 0.29 μg L^{-1}: μg L^{-1}).

Community Composition and N forms

From the accessory pigment analysis, when all ambient nutrient and phytoplankton data from 2015 from all sites analyzed were compiled, the relationships between concentrations of pigment concentrations and nutrients were variable (Table 2). Relationships between NO_3^- concentrations and alloxanthin (indicative of cryptophytes) were negative ($r=0.78$, $p<0.01$). In contrast, NH_4^+ was positively associated with the ambient concentrations of chlorophyll *b*, alloxanthin, and zeaxanthin (chlorophytes, cryptophytes, and cyanobacteria; r=0.91, 0.93, and 0.91; p=0.04, 0.03, and 0.046, respectively). Accordingly, the ratio of NH_4^+:NO_3^- was positively associated with chl *b* and negatively associated with fucoxanthin (chlorophytes and diatoms, respectively). Zeaxanthin (indicative of cyanobacteria) was the only pigment positively associated with urea ($r=.64$, $p=0.03$). PO_4^{3-} concentrations and the ratio of DIN:PO_4^{3-} (NH_4^+ plus NO_3^-; DIN) were not significantly associated with any of the pigments.

Different N-form Additions

In the enrichment experiments using samples from the lower river (ANA22) and cell enumeration performed with the FlowCam, the phytoplankton community changed 24 hours after the addition of a gradient of N concentrations and forms (Fig. 12). The addition of 10 μM NH_4^+ and NO_3^- led to an increase in the total phytoplankton abundance; however, phytoplankton abundance decreased following the addition of 20 and 30 μM NH_4^+ (Fig. 12C).

The addition of different N forms and concentrations also resulted in a change in the phytoplankton relative community composition after 24 hours. A comparison of diatom abundance between the two treatments revealed that the abundance of diatoms was significantly higher in the NO_3^- treatments (365±63 cells mL^{-1}) than the NH_4^+ treatments (204±40 cells mL^{-1}; t=3.76, p=0.013; Fig. 12A and C). The cyanobacteria were significantly more abundant in NH_4^+ treatments than NO_3^- treatments (452±114 cells mL^{-1} and 290±103 cells mL^{-1}, respectively; t=1.83, p=0.07; Fig 12C and A). The relative abundance of dinoflagellates was variable in both nutrient forms treatments, never making up more than 15% of the community composition (Fig 12B and D). In the NO_3^- control, diatoms made up 35% of the community; however, in all of the NO_3^- treatments diatoms made up >45% of the phytoplankton community composition (Fig. 12B). This was not the case for the NH_4^+ treatments, since the percentage of diatoms was reduced in all treatments relative to the control (t=0.50, p=0.35; Fig. 12D). While the diatoms decreased in the NH_4^+ treatments, the percentage of cyanobacteria increased from 47% in the control to > 55% in all treatments (t=0.72, p=0.30; Fig. 12D).

Uptake Rates in the Upper and Lower River and the Effect of NH_4^+

The N-based productivity rates measured on April 15 and May 27 were approximately 2-fold or more higher in the lower river compared to the upper river; however, these rates were more similar to one another on April 29 and May 13 (Table 3). NO_3^- uptake accounted for the majority of N uptake on April 15 and May 27 (>80% and >59%, respectively). On April 29 and May 13, NO_3^- and NH_4^+ made up a similar percentage of N uptake (~40% and ~60%, respectively; an addition of 25 μM ^{15}N was made on the April 29 date compared to 10 μM ^{15}N on other dates). Rates of NO_3^- uptake at both sites on April 15 were approximately 10-fold higher than other sampling dates (Table 3). This was the same time as the peak in fucoxanthin (representing abundance of diatoms) based on accessory pigment analysis. Other than April 15, NO_3^- uptake rates were typically higher in the upper river (ANA0082), which was the site with the higher NO_3^- concentrations (Table 4).

Measurements of NO_3^- uptake in the upper river (ANA0082) and lower river (ANA22) after the addition of a range of NH_4^+ concentrations revealed that different concentrations of NH_4^+ were required to repress NO_3^- uptake in different parts of the river (Fig. 13). On April 15, NO_3^- uptake measurements from the upper river were less sensitive to increasing concentrations of NH_4^+ (0-25 μM) than the lower river, with the upper river experiencing a 93% decrease in NO_3^- uptake only after the addition of 25 μM NH_4^+ (Fig. 13A). Conversely, NO_3^- uptake measured in the lower river (ANA22) on May 27, decreased by 89% after the addition of 10 μM NH_4^+, and remained low after the addition of 25 μM NH_4^+ (Fig. 13D).

DISCUSSION

A range of methods were employed during this work to confirm how N form affects the phytoplankton community composition in the Anacostia River: trends in ambient nutrient concentrations and ratios, community analysis using the FlowCam and accessory pigment analysis, uptake rates as a measure of N-based productivity, and enrichment experiments. All together, phytoplankton community composition, biomass and NO_3^- uptake rates were largely regulated by the changes in relative N forms. Not only was this apparent in seasonal changes in N-forms, but the mesocosm experiments with different N forms (i.e. NO_3^- and NH_4^+) elucidated the strongest evidence of patterns of shifting phytoplankton functional groups. The seasonal and spatial phytoplankton dynamics observed from 2013 to 2015 can be summarized using a conceptual model focused on the relative NH_4^+:NO_3^- ratios in the Anacostia River (Fig. 14). In the spring, the upper Anacostia River was typically dominated by NO_3^- and supported a community of diatoms, which was reduced downstream as NO_3^- declined (Fig. 14). As the relative NH_4^+:NO_3^- increased in the lower river during the summer, with higher ratios reaching the mid-upper river, the shift in the N-form ratio was followed by a shift in the phytoplankton community composition, with diatoms giving way to more chlorophytes and cyanobacteria in the mid-lower river (Fig. 14).

Overall, community composition data and relative NH_4^+:NO_3^- ratios reveal that as N-forms shifted from NO_3^- to more NH_4^+, the phytoplankton community shifted from more diatoms to chlorophytes and cyanobacteria. One of the strongest examples of this was observed during the summer of 2014 from a comparison of nutrient data contours and community composition from the FlowCam (Fig. 9 and 10). On July 9, the chl *a*

maximum in the upper and lower river was dominated by diatoms and occurred at the same time as peak NO_3^- concentrations (Fig. 9C). As relative NH_4^+:NO_3^- increased from July to August, peak chl *a* concentrations decreased in the lower river and consisted of more cryptophytes, chlorophytes and cyanobacteria (Fig. 9D and 10B, D, and E). In the current study, the increasing NH_4^+:NO_3^- ratios (from 0.1 to 0.6 in July and August) supported a shift in the community composition from the diatom bloom that was present in the upper river (around ANA03) to a community of smaller phytoplankton such as chlorophytes and cyanobacteria.

The patterns observed using the FlowCam data were further strengthened by pigment data from sampling in 2015, where the community composition shifted from diatoms to chlorophytes, cryptophytes, and cyanobacteria in the spring (late April to May) and once again in the late summer (late July and August; Fig. 11). When the accessory pigment data from the upper river and lower river were compiled, chl *b*-containing organisms (chlorophytes) were significantly correlated with NH_4^+:NO_3^-, whereas fucoxanthin-containing organisms (diatoms) showed a significant negative correlation with NH_4^+:NO_3^-. In addition, organisms containing chl *b*, alloxanthin, and zeaxanthin (chlorophytes, cryptophytes, and cyanobacteria, respectively) were all significantly correlated with elevated NH_4^+ concentrations.

When interpreted with consideration of prior analyses in the Delaware estuary (Yoshiyama and Sharp, 2006), northern San Francisco Estuary (Glibert *et al.*, 2011), Deep Bay, Hong Kong (Xu *et al.*, 2012), and reservoirs in the Midwestern United States (Harris *et al.*, 2016), the results presented herein support the emerging consensus that N-form plays a part in determining phytoplankton abundance and composition even when

concentrations are at levels that otherwise would be considered saturating for uptake. For instance, work in the urban Delaware estuary using a 26-yr database found that the primary productivity rate per unit chl *a* declined exponentially following increasing NH_4^+ concentrations as low as 10 μM (Yoshiyama and Sharp, 2006). In the northern San Francisco Estuary, the inhibitory effect of NH_4^+ on spring blooms have been documented (Glibert *et al.*, 2011, Dugdale *et al.*, 2012, Parker *et al.*, 2012). Similarly, Xu *et al.* attributed reduced phytoplankton biomass in the nearshore waters of Deep Bay, Hong Kong to ammonium toxicity, but as soon as NH_4^+ was depleted, NO_3^- could support blooms of higher magnitude (Xu *et al.*, 2012). In the Anacostia River, the increases in the number of cyanobacteria with increasing NH_4^+:NO_3^- ratios are similar to findings by Harris *et al.* 2016. Based on data from 4 reservoirs in the Midwestern United States, they found that microcystin-producing cyanobacteria were favored when NO_3^-:NH_4^+ ratios were low and that more secondary metabolites (toxins and compounds that cause taste and odor problems) were produced under these low NO_3^-:NH_4^+ conditions (Harris *et al*., 2016).

Not only was the change in ambient N-forms and resulting shift in phytoplankton community composition observed in the field, but mesocosm enrichments provide experimental support for the relative preference for N-forms by different functional groups in the Anacostia River, even under conditions of non-limiting N. The enrichment of aliquots of water from the lower river site (ANA22), which is the site closest to combined sewer outfalls and was characterized as having overall higher NH_4^+:NO_3^- ratios than other sites, allowed for an assessment of how the phytoplankton community composition would respond to pulses of different N-forms that may result from sewage

effluent and storm-water runoff. The addition of a gradient of NH_4^+ concentrations supported more chlorophytes, whereas diatoms declined following NH_4^+ additions of 20 μM and higher (Fig. 12C). Work by Domingues *et al*. in a tidal fresh estuary in Spain also observed differential preferences for N-forms among phytoplankton functional groups, with chlorophytes and cyanobacteria showing a preference for NH_4^+ (Domingues *et al.*, 2011). In this study, phytoplankton abundances following the addition of increasing NO_3^- concentrations showed that NO_3^- supported diatoms and a decrease in cyanobacteria abundance (Fig. 12A and B). Diatoms have been called "NO_3^- opportunists" because of their abundance in river-dominated estuaries and upwelling systems, where large and frequent additions of NO_3^- occur (Goldman, 1993, Lomas and Glibert, 1999, Glibert *et al.*, 2016). At the other end of the NH_4^+:NO_3^- spectrum, previous freshwater studies have noted the ability of cyanobacteria to assimilate NH_4^+, and their inefficiency at taking up NO_3^- relative to other taxa (Blomqvist *et al.*, 1994, Hyenstrand *et al.*, 1998, McCarthy *et al.*, 2009). This also agrees with findings of mesocosm experiments conducted in the hypereutrophic Wascana Lake in Canada by Donald *et al*., where diatoms responded to NO_3^- enrichments and cyanobacteria responded to NH_4^+ enrichments (Donald *et al.*, 2011, Donald *et al.*, 2013). Additionally, experiments in the San Francisco Bay Delta showed that treatments enriched with NO_3^- produced more fucoxanthin (indicative of diatoms) and NH_4^+ enrichments produced more chl *b* and zeaxanthin (representative of chlorophytes and cyanobacteria, respectively; Glibert *et al.* 2014b). The observations of dichotomous phytoplankton communities in the Anacostia River and other comparative studies validate that the preference for NH_4^+ is not absolute among the phytoplankton taxa (Glibert *et al.* 2016).

The preference for NH_4^+ exhibited by some phytoplankton is generally assumed to be a function of the greater cellular energetic costs of assimilating oxidized N than reduced N (NO_3^- and NH_4^+, respectively) and that NH_4^+ represses NO_3^- uptake and assimilation (Dortch 1990 and references therein). The NH_4^+ concentration tipping point that exerts the NH_4^+ repression on NO_3^- metabolism in phytoplankton depends on a suite of factors from the presence of specific phytoplankton taxa and their physiological status to their previous environmental conditions (Glibert *et al.* 2016 and references therein). The Anacostia River is an N-rich environment and NO_3^- uptake rate measurements at sites experiencing contrasting NH_4^+ concentrations show that the concentration of NH_4^+ required to repress NO_3^- metabolism depends on the initial NO_3^- concentration of the sample and by inference the cellular NO_3^- concentration. The upper portion of the Anacostia River was characterized by overall lower NH_4^+:NO_3^- ratios and NO_3^- concentrations that averaged 48.42± 22.85 μM . As a result, the addition of higher NH_4^+ concentrations was required to decrease NO_3^- uptake rates in the upper river compared to the lower river. The resilient NO_3^- uptake rates in the upper river provide insight into why a higher proportion of diatoms are supported in the upper river. In addition, peak concentrations of fucoxanthin-containing organisms (diatoms) were measured on April 16 (Fig. 11A), which most likely contributed to the highest total uptake rates and highest percentage of NO_3^- uptake observed (Table 3). These results are consistent with mesocosm experiments by Glibert and Berg (2009) in which the percent NO_3^- uptake was directly related to the fraction of the community as diatoms. It is apparent from the uptake rates that the ambient N-forms play a role in determining how the community composition shifts.

Depending on how elevated NO_3^- concentrations were, increases in the relative concentration of NH_4^+ repressed NO_3^- uptake and most likely resulted in the shift in phytoplankton community structure (Fig. 14). NO_3^- supported a phytoplankton community dominated by diatoms and as the concentration of NH_4^+ increased, the community was made up of more cyanobacteria and chlorophytes. Taking into account the global reports of N-form determining phytoplankton community structure, this work presents a new case of NH_4^+ supporting a community comprised of cyanobacteria, chlorophytes and cryptophytes in an urban tidal-fresh waterway. Although the annual "State of the Anacostia River Report Card" includes water quality indicators such as chl *a* and stormwater runoff volume to guide decision makers in meeting the ultimate goal of a "fishable and swimmable" river (DDOE, 2008, AWS, 2015), this work demonstrates that the Anacostia River water quality is much more complicated and would benefit from other measures of ecosystem health, such as N-forms. Given hopes in the watershed for improving water quality and stimulating the use of the river by kayakers, boaters and recreational fisherman, a greater focus on nutrients as a source of pollution and their removal, especially with an emphasis on N-form, may have beneficial implications for the trajectory of eutrophication in this system.

Table 1. An overview of the data used and the time period that samples were collected.

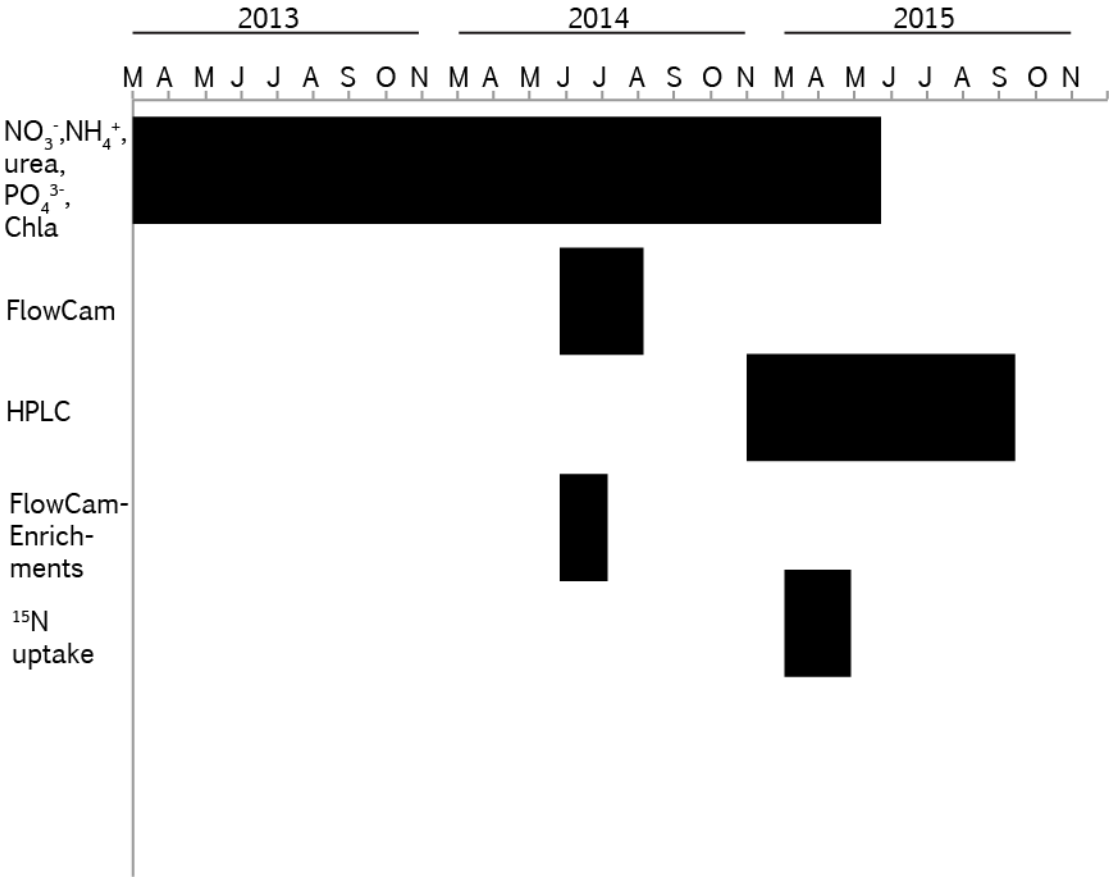

Table 2. Comparison of correlation statistics for individual accessory pigments (concentration of accessory pigments in relation to Chlorophyll *a* (μg L^{-1}: μg L^{-1})) relative to ambient nutrient concentrations for samples from the Anacostia River.

Response variable and ambient nutrient conditions; statistical parameter	**Chlorophyll *b***	**Alloxanthin**	**Fucoxanthin**	**Zeaxanthin**
NO_3^-				
Regression coefficient (slope)	-0.0001	-0.0012	0.005	-0.0002
Correlation coefficient	0.0009	**0.78****	0.32	0.08
Significance (p) of r	0.94	0.007	0.18	0.53
N	7	7	7	7
NH_4^+				
Regression coefficient (slope)	0.0034	0.0016	-0.012	0.0006
Correlation coefficient	**0.91***	**0.93***	0.89	**0.91***
Significance (p) of r	0.04	0.03	0.054	0.046
N	4	4	4	4
Urea				
Regression coefficient (slope)	0.007	-0.001	-0.005	0.002
Correlation coefficient	0.35	0.07	0.02	**0.64***
Significance (p) of r	0.16	0.55	0.717	0.03
N	7	7	7	7
PO_4^{3-}				
regression coefficient (slope)	0.031	-0.005	-0.017	-0.001
correlation coefficient	0.12	0.008	0.018	0.001
significance (p) of r	0.052	0.618	0.47	0.819
N	31	31	31	31
DIN:PO_4^{3-}				
Regression coefficient (slope)	0.002	0.0009	-0.007	0.0006
Correlation coefficient	0.48	0.34	0.379	0.83
Significance (p) of r	0.3	0.4	0.38	0.08
N	4	4	4	4
NH_4^+:NO_3^-				
Regression coefficient (slope)	0.155	0.072	-0.54	0.029
Correlation coefficient	**0.96***	0.89	**0.93***	0.89
Significance (p) of r	0.02	0.055	0.03	0.057
N	4	4	4	4

Correlation coefficients (r) that were significant at $p<0.01$ are indicated by **; whereas those that are significant at $p<0.05$ are indicated by *; all significant values are also shown in bold font.

Table 3. Comparison of Nitrate uptake rates and N-based productivity rates (Sum of NO_3^-, NH_4^+, and urea uptake, V_{max} h^{-1}) for samples taken from the upper Anacostia River (ANA0082) and the lower river (ANA22) in 2015.

Date	Site	Nitrate uptake (h^{-1})	Sum Uptake (h^{-1})	% NO3 uptake	% NH4 uptake	% Urea uptake
15-Apr	ANA0082	0.34	0.4270	80.21	15.81	3.98
15-Apr	ANA22	0.67	0.7431	89.57	7.72	2.70
29-Apr	ANA0082	0.03	0.0700	41.71	40.86	17.43
29-Apr	ANA22	0.03	0.0861	40.19	46.34	13.47
13-May	ANA0082	0.07	0.1062	66.20	26.00	7.82
13-May	ANA22	0.05	0.0872	63.19	28.10	8.72
27-May	ANA0082	0.07	0.1116	59.59	27.06	13.35
27-May	ANA22	0.05	0.5683	90.62	6.93	2.45

Table 4. Ambient environmental conditions of sites sampled in the upper Anacostia River (ANA0082) and lower river (ANA22) in 2015. These samples were subsequently used in enrichment experiments to measure NO_3^- uptake.

Date	Site	Temperature (°C)	Chlorophyll *a* (µg L)	Nitrate (µM)	Ammonium (µM)	Urea (µM)	Phosphate (µM)
4/15	ANA0082	15.2	39.39	24.70	5.84	2.66	1.84
4/15	ANA22	15.1	7.89	34.70	16.42	0.23	1.91
4/29	ANA0082	13.1	42.90	37.00	2.70	0.00	2.56
4/29	ANA22	15.0	7.31	42.50	16.73	1.86	1.46
5/13	ANA0082	19.1	9.62	79.20	12.91	0.73	1.16
5/13	ANA22	23.5	16.90	44.70	21.11	0.00	1.66
5/27	ANA0082	23.3	12.20	48.11	6.70	1.25	1.14
5/27	ANA22	24.5	26.20	43.66	34.59	4.64	2.03

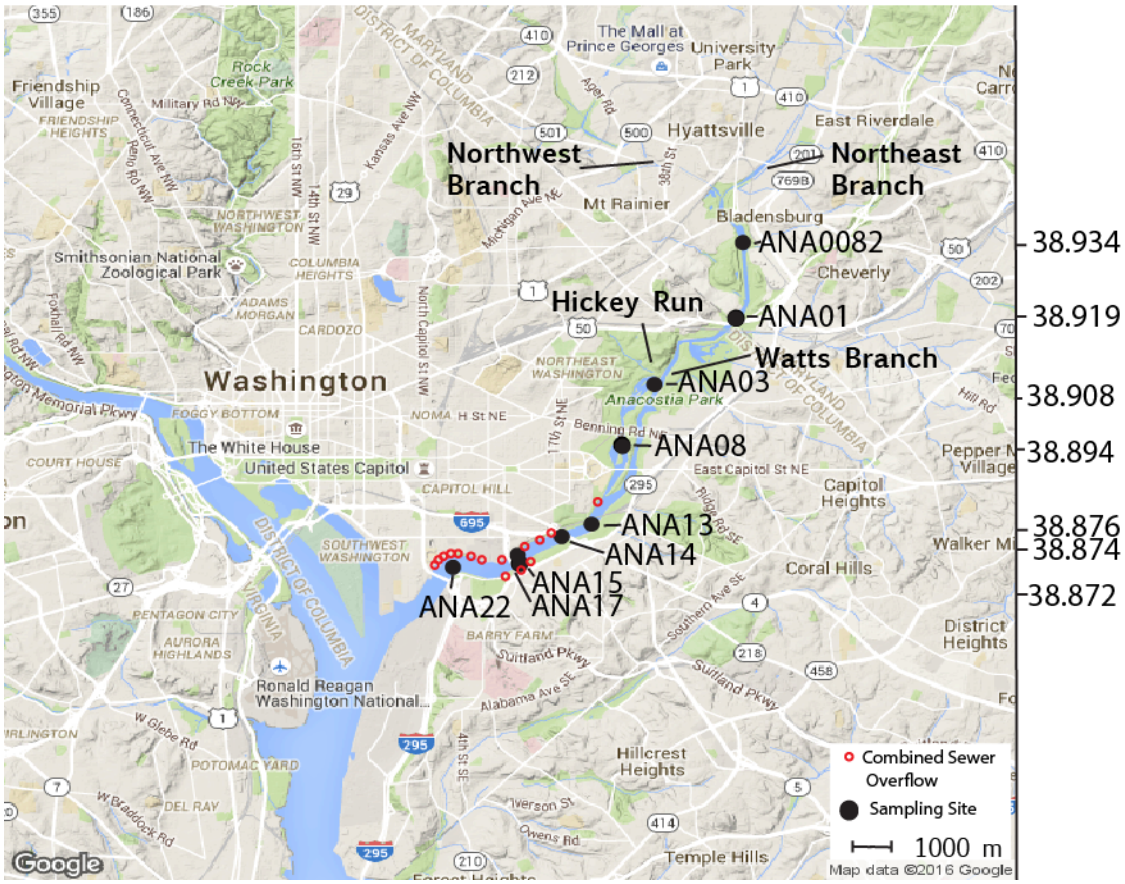

Figure 1. Map of study sites in the Anacostia River, Washington, D.C., USA showing the combined sewer overflow sites, Northeast Branch, Northwest Branch, Hickey Run, and Watts Branch.

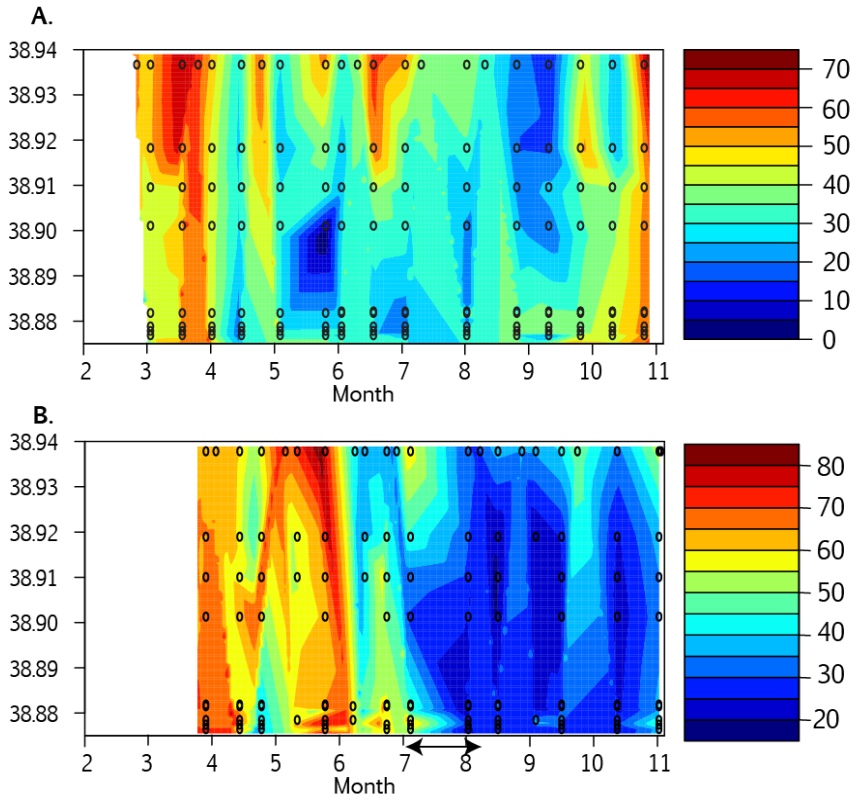

Figure 2. Surface contours of NO_3^- (μmol L^{-1}) plotted versus sampling latitude on the Anacostia River (y-axis) from ANA22 (downstream) to ANA0082 (upstream) and time (x-axis) from 2013 (A) and 2014 (B). Open circles indicate actual sampling locations. The arrow from July 9 to August 8, 2014 sampling indicates the period that community composition was tracked using the FlowCam.

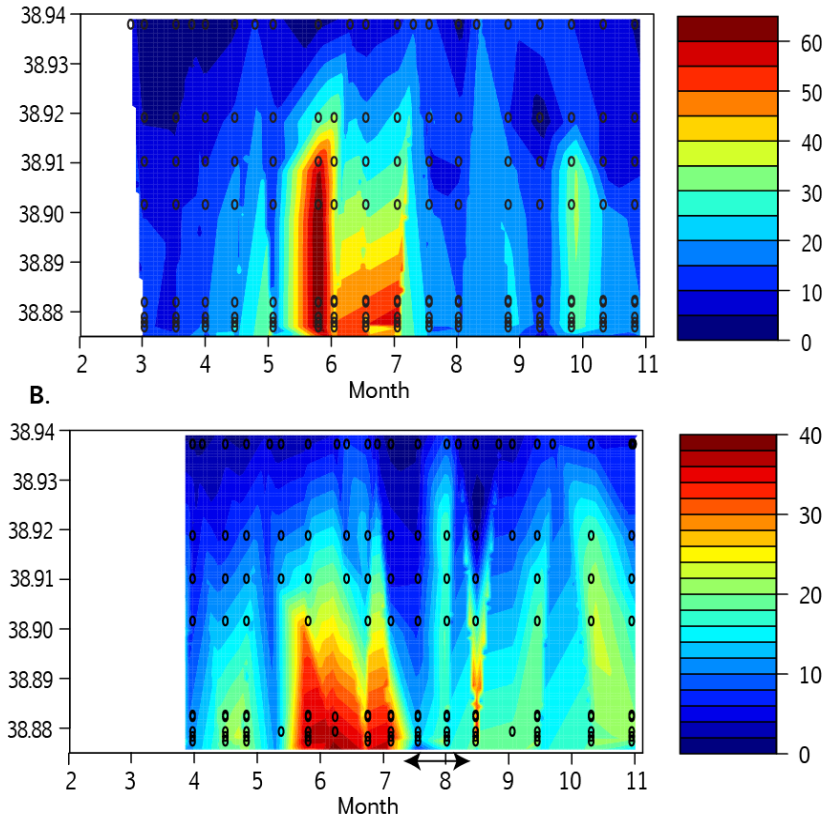

Figure 3. Surface contours of NH_4^+ (µmol L^{-1}) plotted versus sampling latitude on the Anacostia River (y-axis) from ANA22 (downstream) to ANA0082 (upstream) and time (x-axis) from 2013 (A) and 2014 (B). Open circles indicate actual sampling locations. The arrow from July 9 to August 8, 2014 sampling indicates the period that community composition was tracked using the FlowCam.

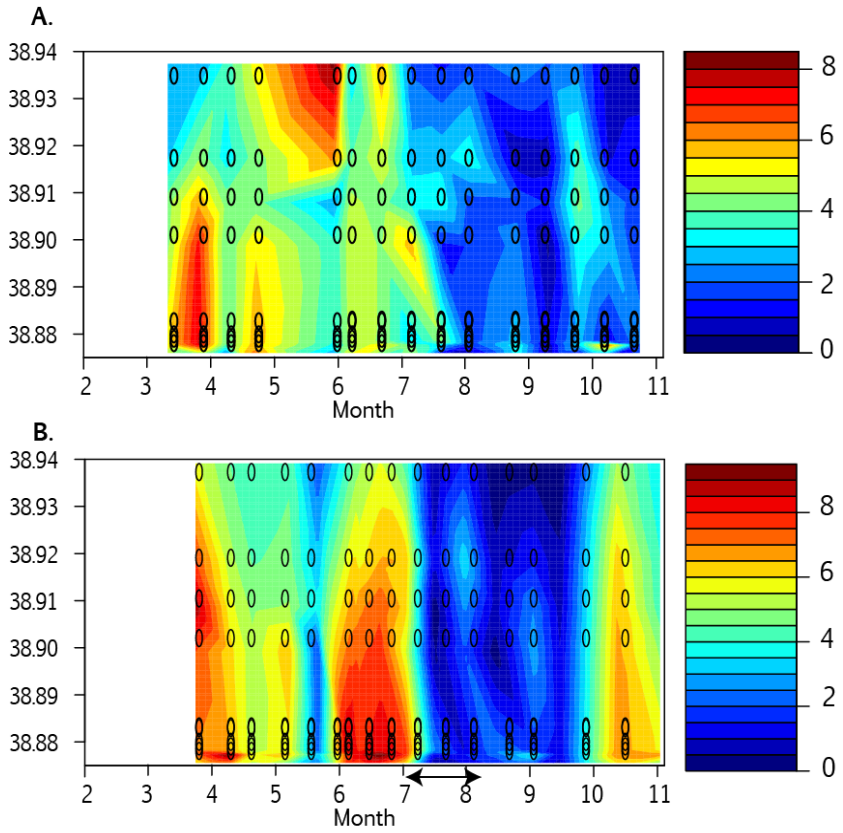

Figure 4. Surface contours of urea (μmol L^{-1}) plotted versus sampling latitude on the Anacostia River (y-axis) from ANA22 (downstream) to ANA0082 (upstream) and time (x-axis) from 2013 (A) and 2014 (B). Open circles indicate actual sampling locations. The arrow from July 9 to August 8, 2014 sampling indicates the period that community composition was tracked using the FlowCam.

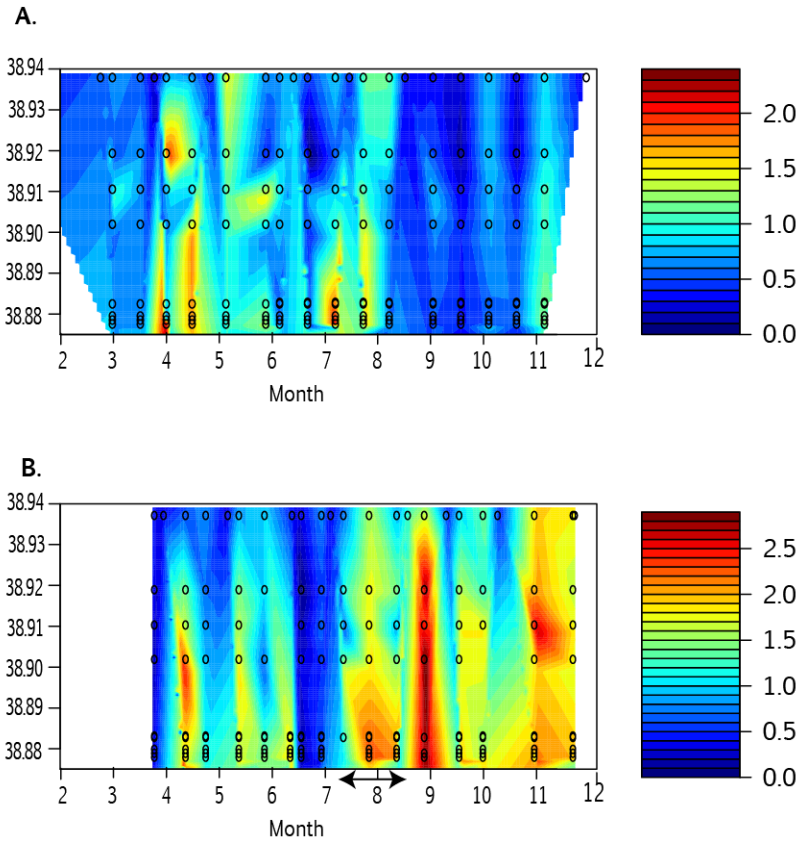

Figure 5. Surface contours of PO_4^{3-} (μmol L^{-1}) plotted versus sampling latitude on the Anacostia River (y-axis) from ANA22 (downstream) to ANA0082 (upstream) and time (x-axis) from 2013 (A) and 2014 (B). Open circles indicate actual sampling locations. The arrow from July 9 to August 8, 2014 sampling indicates the period that community composition was tracked using the FlowCam.

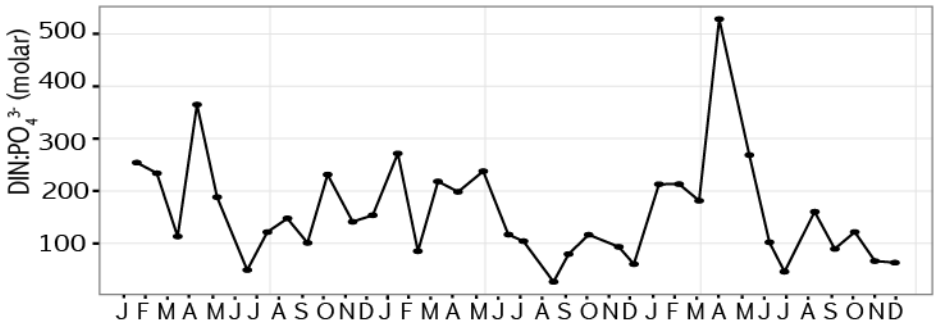

Figure 6. Temporal changes in relative DIN (NO_3^- plus NH_4^+) to PO_4^{3-} (molar; D) ratios near the Bladensburg Bridge (ANA0082) from 2013 to 2015.

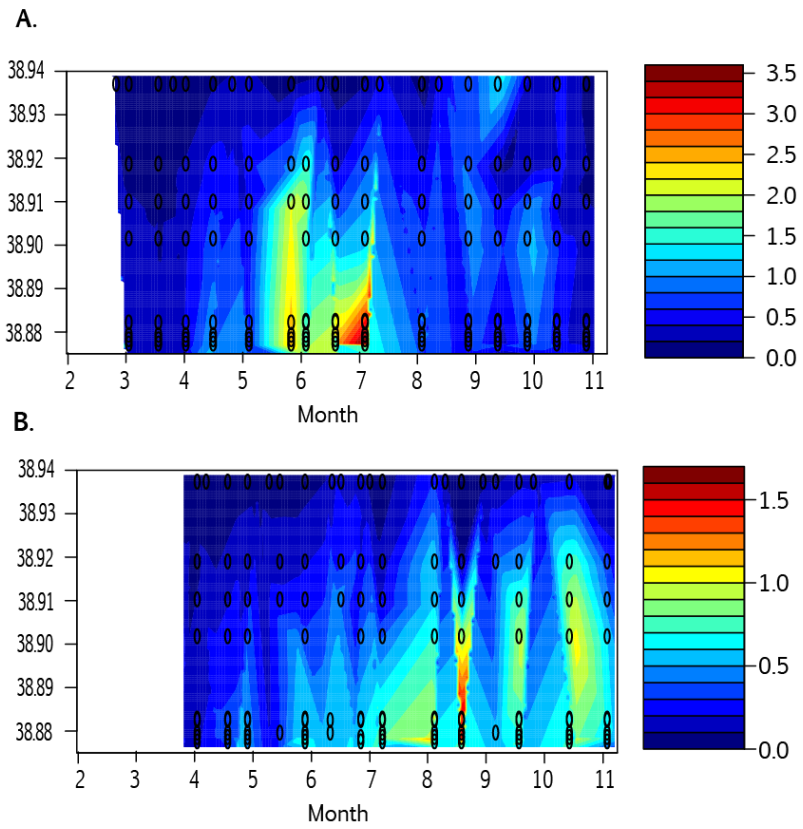

Figure 7. Surface contours of NH_4^+:NO_3^- (molar) plotted versus sampling latitude on the Anacostia River (y-axis) from ANA22 (downstream) to ANA0082 (upstream) and time (x-axis) from 2013 (A) and 2014 (B). Open circles indicate actual sampling locations. The arrow from July 9 to August 8, 2014 sampling indicates the period that community composition was tracked using the FlowCam.

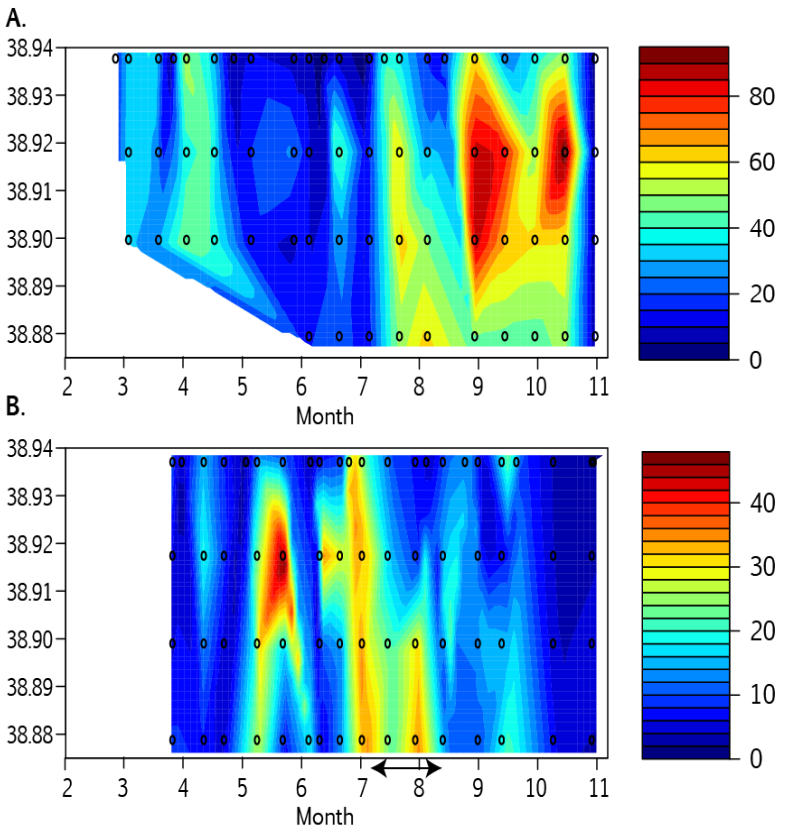

Figure 8. Surface contours of Chl *a* (μg L^{-1}) plotted versus sampling latitude on the Anacostia River (y-axis) from ANA22 (downstream) to ANA0082 (upstream) and time (x-axis) from 2013 (A) and 2014 (B). Open circles indicate actual sampling locations. The arrow from July 9 to August 8, 2014 sampling indicates the period that community composition was tracked using the FlowCam.

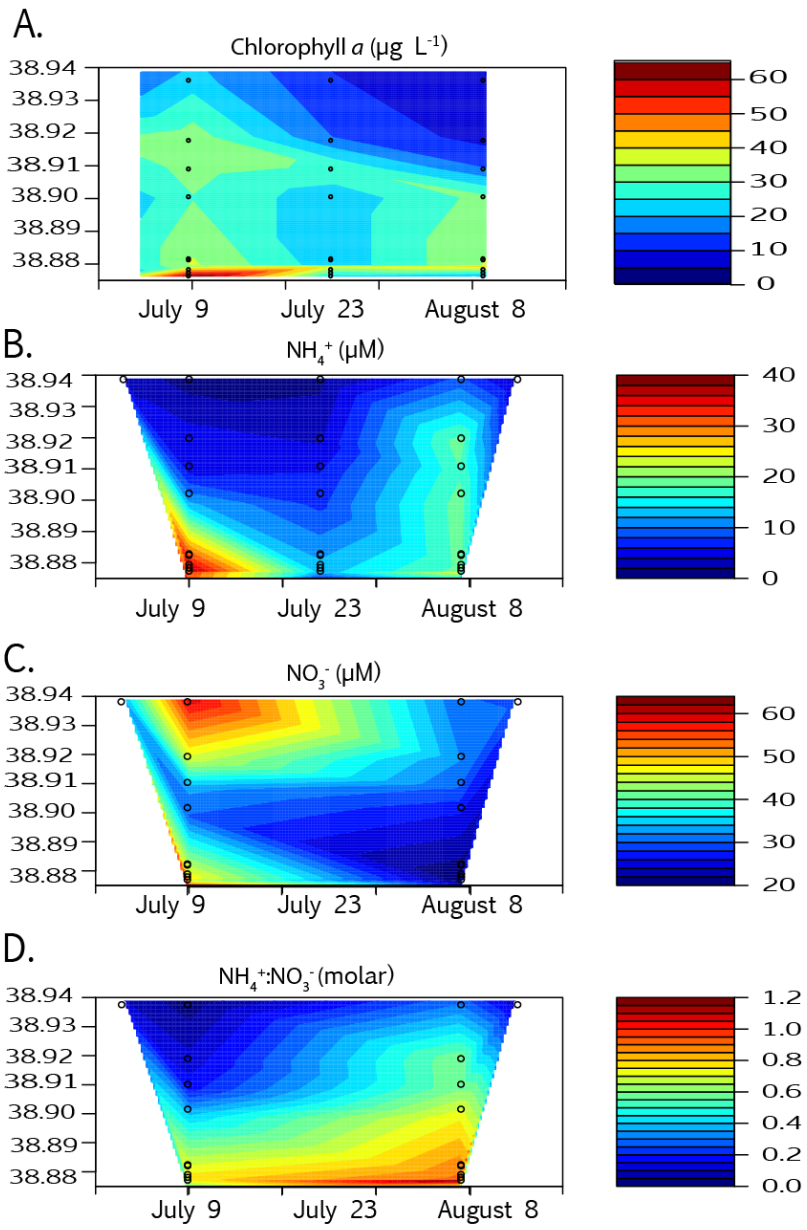

Figure 9. Surface contours from summer of 2014 of chl *a* (µg L^{-1}; A), NH_4^+ (µM; B), NO_3^- (µM; C), and NH_4^+:NO_3^- (molar; D) plotted versus sampling latitude on the Anacostia River (y-axis) from ANA22 (downstream) to ANA0082 (upstream) and time (x-axis). Open circles indicate actual sampling locations.

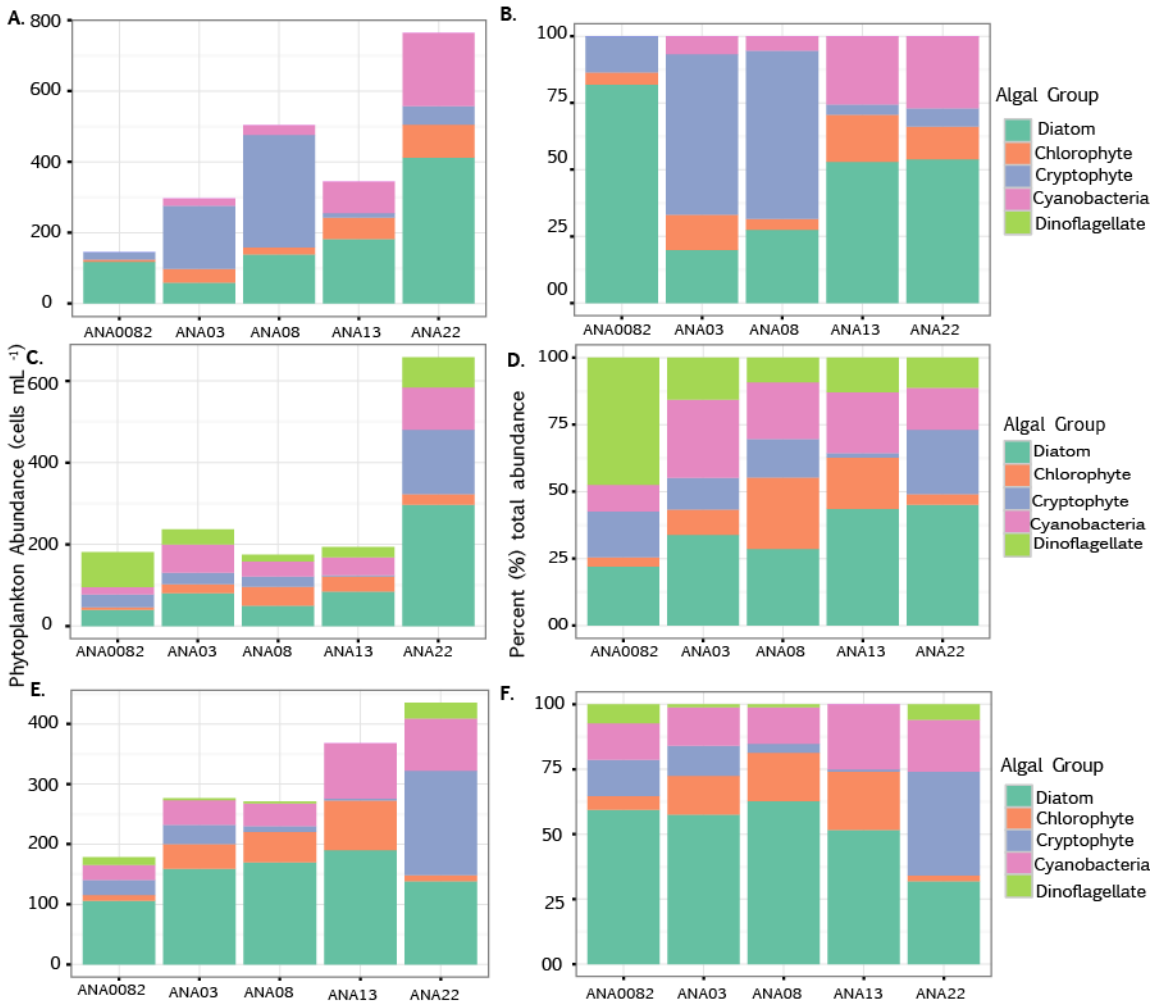

Figure 10. Absolute and relative phytoplankton abundance based on cell enumeration using FlowCam during 2014 from the upper-river (ANA0082) to lower-river (ANA22; x-axis) on July 9 (A and B), July 23 (C and D), and August 8 (E and F). Note the changes in scales from panel to panel.

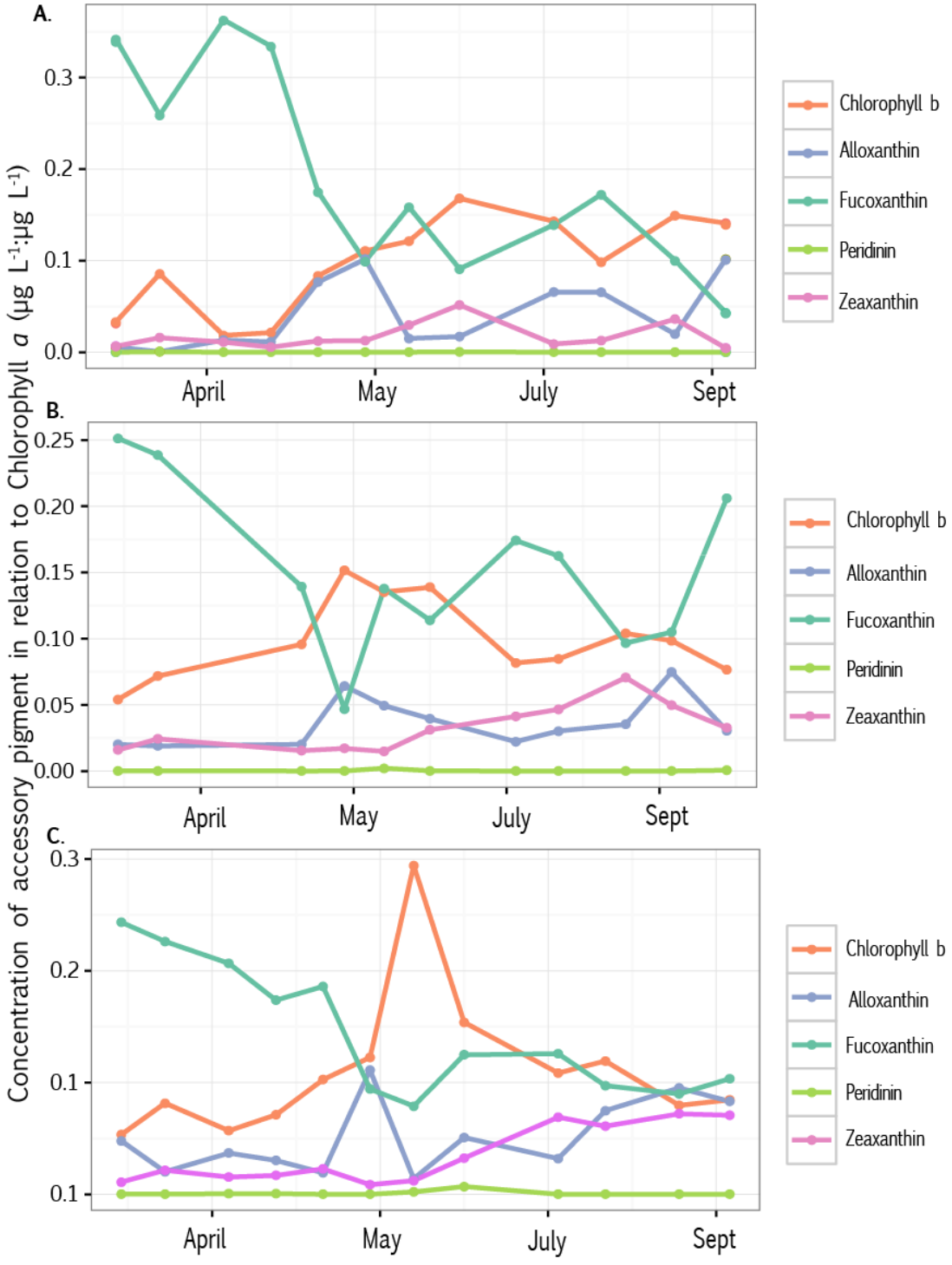

Figure 11. Changes in concentrations of accessory pigments from March to September 2015 along the Anacostia River from sites from the upper river to the lower river: ANA0082 (A), ANA08 (B), and ANA22 (C).

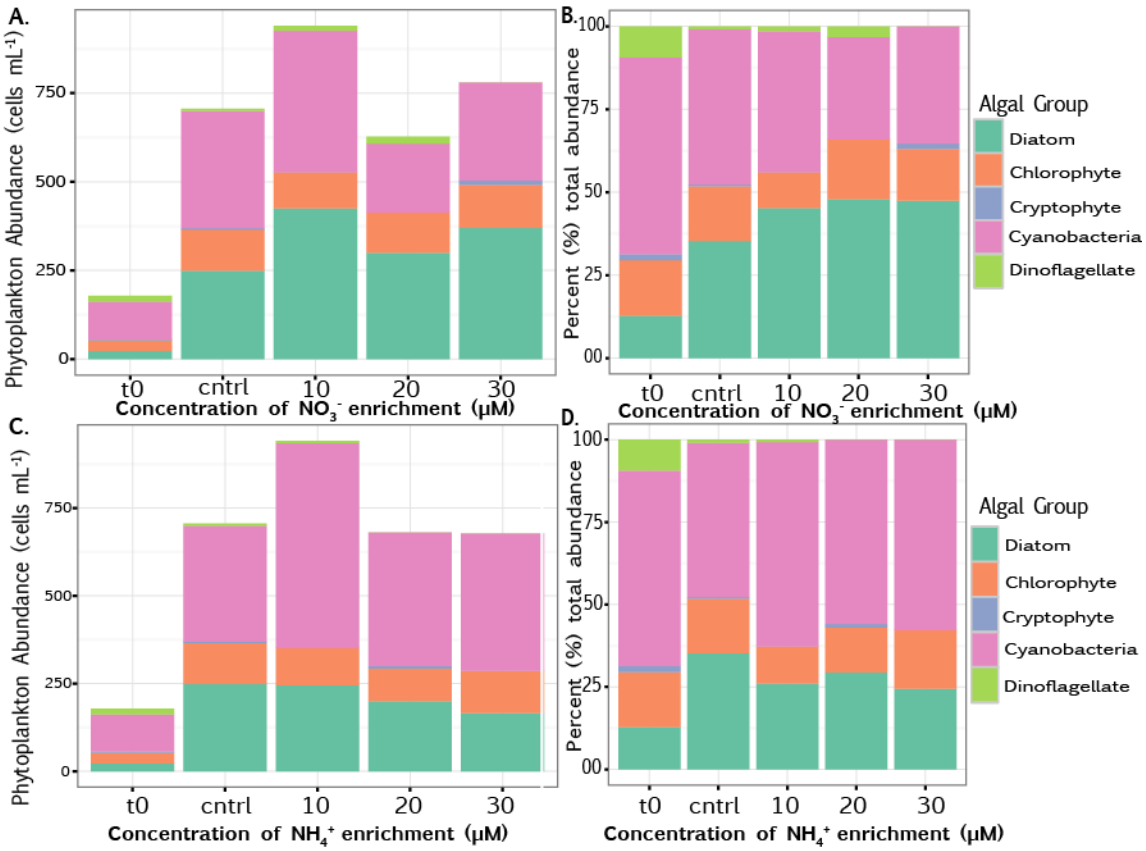

Figure 12. Absolute and relative phytoplankton abundance based on cell enumeration using FlowCam after the addition of a gradient of concentrations of either NO_3^- (A and B) and NH_4^+ (C and D) and incubation for 24 h, with t0 representing the initial phytoplankton community before the enrichment.

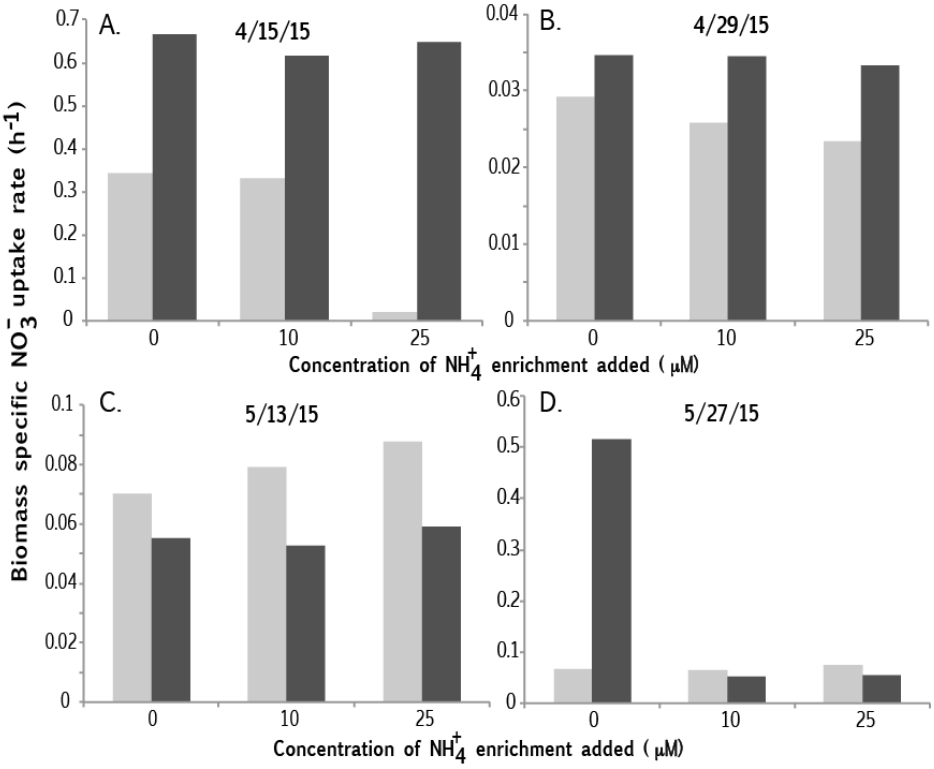

Figure 13. Comparison of NO_3^- uptake for samples enriched with 10 and 25 μM NH_4^+ in the upper river (ANA0082; pale bars) and the lower river (ANA22; dark bars). The uptake rates were taken on four sampling dates in 2015: April 15 (A), April 29 (B), May 13 (C), and May 27 (D).

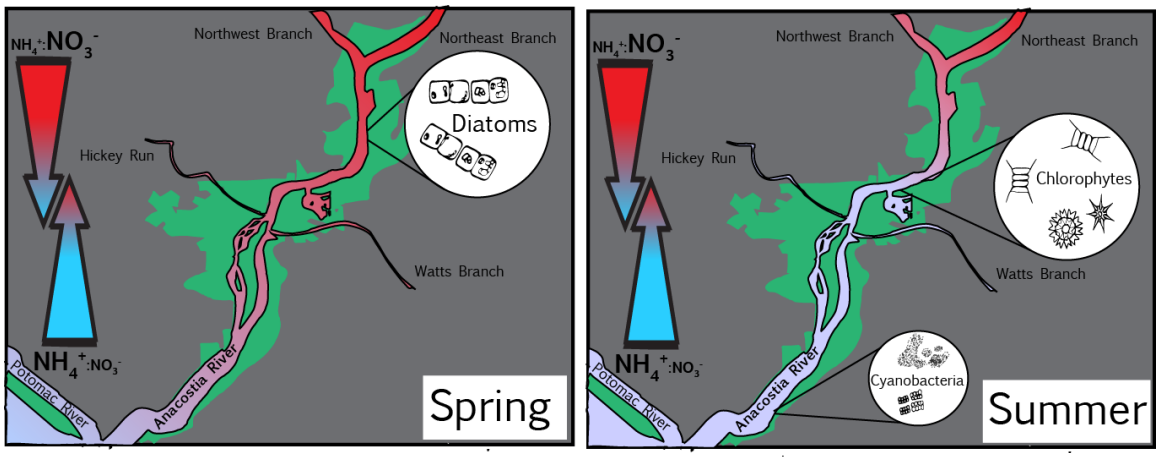

Figure 14. Conceptual model of the spring and summer NH_4^+:NO_3^- ratios in the Anacostia River regulating the shifts in phytoplankton community composition from a diatom-dominated system in the spring to more chlorophytes and cyanobacteria in the summer. Note the map is not drawn exactly to scale and that at no time does the river have only NO_3^- or NH_4^+.

REFERENCES

Akima, H., Gebhardt, A., Petzoldt, T. and Maechler, M. 2009. akima: Interpolation of irregularly spaced data. R package version 0.5-4, R Foundation for Statistical Computing Vienna, Austria.

Anacostia Watershed Society (AWS). 2015. 2015: State of the Anacostia River Report Card. Bladensburg, MD. Web <https://www.anacostiaws.org/programs/publicaffairs/2015-state-river-report-card>.

Behm, P., Buckley, A. and Schultz, C. L. 2003. TAM/WASP Toxics Screening Level Model for the Tidal Portion of the Anacostia River. Prepared for District of Columbia Department of Health Environmental Health Administration Bureau of Environmental Quality Water Quality Division. Final Report, Interstate Commission on the Potomac River Basin Report No. 03-2

Berg, G. M., Balode, M., Purina, I., Bekere, S., Béchemin, C. and Maestrini, S. 2003. Plankton community composition in relation to availability and uptake of oxidized and reduced nitrogen. *Aquatic Microbial Ecology* **30**, 263-274.

Blomqvist, P., Petterson, A. and Hyenstrand, P. 1994. Ammonium-nitrogen: a key regulatory factor causing dominance of non-nitrogen-fixing cyanobacteria in aquatic systems. *Archiv für Hydrobiologie,* **132,** 141-164.

Bran and Luebbe, Inc. 1999. *Bran Luebbe Autoanalyzer Applications: AutoAnalyzer Method No. G-175-96 Phosphate in Water and Seawater*. Buffalo Grove, IL: Bran Luebbe, Inc.

Chesapeake Bay Program (CBP). 2002. The State of the Chesapeake Bay: A Report to the Citizens of the Bay Region. Annapolis, MD. Web. <http://www.chesapeakebay.net/documents/0659_001.pdf>.

Cloern, J. E. 2001. Our evolving conceptual model of the coastal eutrophication problem. *Marine Ecology Progress Series* **210**, 223-253.

District of Columbia Water and Sewer Authority (DC Water). 2016. DC Water Breaks Ground on $2.6 Billion Clean Rivers Project- Largest Construction Project Since Building of Metro. Web. <http://www.dcwater.com/news/listings/>.

District Department of the Environment (DDOE). 2008. Anacostia 2032: Plan for a Fishable and Swimmable Anacostia River. Web. <http://doee.dc.gov/sites/default/files/dc/sites/ddoe/publication/attachments/Anacostia2032.pdf>.

Doane, T. A. and Horwáth, W. R. 2003. Spectrophotometric Determination of Nitrate with a Single Reagent. *Analytical Letters*, **36**, 2713-2722.

Domingues, R. B., Barbosa, A. B., Sommer, U. and Galvão, H. M. 2011. Ammonium, nitrate and phytoplankton interactions in a freshwater tidal estuarine zone: potential effects of cultural eutrophication. *Aquatic Sciences,* **73,** 331-343.

Donald, D. B., Bogard, M. J., Finlay, K., Bunting, L. and Leavitt, P. R. 2013. Phytoplankton-specific response to enrichment of phosphorus-rich surface waters with ammonium, nitrate, and urea. *PloS one,* **8,** e53277.

Donald, D. B., Bogard, M. J., Finlay, K. and Leavitt, P. R. 2011. Comparative effects of urea, ammonium, and nitrate on phytoplankton abundance, community composition, and toxicity in hypereutrophic freshwaters. *Limnology and Oceanography,* **56,** 2161-2175.

Dortch, Q. 1990. The interaction between ammonium and nitrate uptake in phytoplankton. *Marine Ecology Progress Series,* **61,** 183-201.

Dugdale, R., Wilkerson, F., Parker, A. E., Marchi, A. and Taberski, K. 2012. River flow and ammonium discharge determine spring phytoplankton blooms in an urbanized estuary. *Estuarine, Coastal and Shelf Science,* **115,** 187-199.

Dugdale, R. C. and Wilkerson, F. P. 1986. The use of 15N to measure nitrogen uptake in eutrophic oceans; experimental considerations1, 2. *Limnology and Oceanography,* **31,** 673-689.

Dugdale, R. C., Wilkerson, F. P., Hogue, V. E. and Marchi, A. (2007) The role of ammonium and nitrate in spring bloom development in San Francisco Bay. *Estuarine, Coastal and Shelf Science,* **73,** 17-29.

Environmental Protection Agency (EPA). 2011. Reactive nitrogen in the United States: an analysis of inputs, flows, consequences, and management options. Scientific Advisory Board Publication No. EPA-SAB-11-013. Washington, D.C.

Environmental Protection Agency (EPA). 2016. Anacostia River Watershed District of Columbia. Web. <water.epa.gov>.

Friedrichs, C. T. and Aubrey, D. G. 1994. Tidal propagation in strongly convergent channels. *Journal of Geophysical Research,* **99,** 3321-3321.

Galloway, J. N. and Cowling, E. B. 2002. Reactive nitrogen and the world: 200 years of change. *AMBIO: A Journal of the Human Environment,* **31,** 64-71.

Glibert, P. M., Lipschultz, F., McCarthy, J. J. and Altabet, M. A. 1982. Isotope dilution models of uptake and remineralization of ammonium by marine plankton. *Limnology and Oceanography,* **27,** 639-650.

Glibert, P. M. 1998. Interactions of top-down and bottom-up control in planktonic nitrogen cycling, pp. 1-12. In T., Tamminen and H., Kuosa [eds], Eutrophication in planktonic ecosystems: Food web dynamics and elemental cycling. Springer.

Glibert, P. M., Allen, J. I., Bouwman, A. F., Brown, C. W., Flynn, K. J., Lewitus, A. J. and Madden, C. J. 2010. Modeling of HABs and eutrophication: status, advances, challenges. *Journal of Marine Systems,* **83,** 262-275.

Glibert, P. M. and Berg, G.M. 2009. Nitrogen form, fate and phytoplankton composition, pp. 183-189. In V. S. Kennedy, W. M. Kemp, J. E. Peterson and W. C. Dennison [eds], Experimental ecosystems and scale: Tools for understanding and managing coastal ecosystems. New York, NY: Springer.

Glibert, P. M. and Burkholder, J. M. 2006. The complex relationships between increasing fertilization of the earth, coastal eutrophication and porliferation of harmful algal blooms, pp. 341-354. In E., Granéli and J. T., Turner [eds], Ecology of Harmful Algae. Springer.

Glibert, P. M. and Capone, D. G. 1993. Mineralization and assimilation in aquatic, sediment, and wetland systems, pp. 243-272. In R. Knowles and T. H., Blackburn [eds], Nitrogen Isotope Techniques. San Diego, CA: Academic.

Glibert, P. M., Fullerton, D., Burkholder, J. M., Cornwell, J. C. and Kana, T. M. 2011. Ecological stoichiometry, biogeochemical cycling, invasive species, and aquatic food webs: San Francisco estuary and comparative systems. *Reviews in Fisheries Science,* **19,** 358-417.

Glibert, P. M., Heil, C. A., Hollander, D., Revilla, M., Hoare, A., Alexander, J., Murasko, S. 2004. Evidense for dissolved organic nitrogen and phosphorus uptake during a cyanobacterial bloom in Florida Bay. *Marine Ecological Progress Series*, **280**, 73-83.

Glibert, P. M., Maranger, R., Sobota, D. and Bouwman, L. 2014a. The Haber Bosch-harmful algal bloom (HB-HAB) link. *Environmental Research Letters*, **9**, 105001.

Glibert, P. M., Wilkerson, F. P., Dugdale, R. C., Parker, A. E., Alexander, J., Blaser, S. and Murasko, S. 2014b. Phytoplankton communities from San Francisco Bay Delta respond differently to oxidized and reduced nitrogen substrates - even under conditions that would otherwise suggest nitrogen sufficiency. *Frontiers in Marine Science,* **1**, 1-16.

Glibert, P. M., Wilkerson, F. P., Dugdale, R. C., Raven, J. A., Dupont, C. L., Leavitt, P. R., Parker, A. E., Burkholder, J. M. and Kana, T. M. 2016. Pluses and minuses of ammonium and nitrate uptake and assimilation by phytoplankton and implications for productivity and community composition, with emphasis on nitrogen‐enriched conditions. *Limnology and Oceanography,* **61,** 165-197.

Goldman, J. C. 1993. Potential role of large oceanic diatoms in new primary production. *Deep Sea Research Part I: Oceanographic Research Papers,* **40,** 159-168.

Hall, S. R. 2009. Stoichiometrically explicit food webs: feedbacks between resource supply, elemental constraints, and species diversity. *Annual Review of Ecology, Evolution, and Systematics,* **40,** 503-528.

Harris, T. D., Smith, V. H., Graham, J. L., Van De Waal, D. B., Tedesco, L. P. and Clercin, N. 2016. Combined effects of nitrogen to phosphorus ratios and nitrogen speciation on cyanobacterial metabolite concentrations in eutrophic Midwestern USA reservoirs. *Inland Waters,* **6,** 199-210.

Heil, C. A., Revilla, M., Glibert, P. M. and Murasko, S. 2007. Nutrient quality drives differential phytoplankton community composition on the southwest Florida shelf. *Limnology and Oceanography,* **52,** 1067-1078.

Heisler, J., Glibert, P. M., Burkholder, J. M., Anderson, D. M., Cochlan, W., Dennison, W. C., Dortch, Q., Gobler, C. J., Heil, C. A. and Humphries, E. 2008.

Eutrophication and harmful algal blooms: a scientific consensus. *Harmful Algae,* **8,** 3-13.

Houlton, B. Z., Boyer, E., Finzi, A., Galloway, J., Leach, A., Liptzin, D., Melillo, J., Rosenstock, T. S., Sobota, D. and Townsend, A. R. 2013. Intentional versus unintentional nitrogen use in the United States: trends, efficiency and implications. *Biogeochemistry,* **114,** 11-23.

Hwang, H. M. and Foster, G. D. 2006. Characterization of polycyclic aromatic hydrocarbons in urban stormwater runoff flowing into the tidal Anacostia River, Washington, DC, USA. *Environmental Pollution,* **140,** 416-426.

Hyenstrand, P., Nyvall, P., Pettersson, A. and Blomqvist, P. 1998. Regulation of non-nitrogen-fixing cyanobacteria by inorganic nitrogen sources-experiments from Lake Erken. *Archiv fur Hydrobiologie Spec. Issues: Advances in Limnology,* **51,** 29-40.

Jeffrey, S. W., and Vesk, M. 1997. Introduction to marine phytoplankton and their pigments signatures, p. 37-84. In S. W., Jeffrey *et al.* [eds] Phytoplankton Pigments in Oceanography: Guidelines to Modern Methods. Paris: UNESCO.

Jeffrey, S. W., and Wright, S. W. 1994. Photosynthetic pigments in the Haptophyta, p. 111-132. In J. C., Green and B. S. C., Leadbeater [eds], The Haptophyte Algae. Oxford, UK: Clarendon Press.

Jones, M. N. 1984. Nitrate reduction by shaking with cadmium: Alternative to cadmium columns. *Water Research*, **18**, 643-646.

Kemp, W. M. *et al.*, 2005. Eutrophication of Chesapeake Bay: Historical trends and ecological interactions. *Marine Ecology Progress Series*, **303**, 1-19.

Legendre, L. and Rassoulzadegan, F. 1995. Plankton and nutrient dynamics in marine waters. *Ophelia,* **41,** 153-172.

Logan, W. S. 1999. Estimation of Shallow Groundwater Flux to the Anacostia River. Draft Report for D.C. Department of Health.

Lomas, M. W. and Glibert, P. M. 1999. Interactions between NH_4^+ and NO_3^- uptake and assimilation: comparison of diatoms and dinoflagellates at several growth temperatures. *Marine Biology,* **133,** 541-551.

Maryland Department of the Environment (MDE). 2010. Total maximum daily loads of PCBs in the Northeast and Northwest branches of the non-tidal Anacostia River, Montgomery and Prince George's Counties, Maryland. Public Draft. Baltimore, MD.

Maryland Department of the Environment (MDE). 2012. Maryland's final 2012 integrated report of surface-water quality. Web. <http://www.mde.state.md.us/programs/Water/TMDL/Integrated303dReports/Pages/2012_IR.aspx.>.

McCarthy, J. J. 1981. The kinetics of nutrient utilization. *Canadian Bulletin of Fisheries and Aquatic Sciences*, 211-233.

McCarthy, M. J., James, R. T., Chen, Y., East, T. L. and Gardner, W. S. 2009. Nutrient ratios and phytoplankton community structure in the large, shallow, eutrophic, subtropical Lakes Okeechobee (Florida, USA) and Taihu (China). *Limnology,* **10,** 215-227.

Miller, C. V., Chanat, J. G. and Bell, J. M. 2013. Water quality in the Anacostia River, Maryland and Rock Creek, Washington, D.C.: Continuous and discrete monitoring with simulations to estimate concentrations and yields of nutrients, suspended sediment, and bacteria. U.S. Geological Survey Open-File Report 2013-1034. 37. < http://pubs.usgs.gov/of/2013/1034.>.

Miranda, K. M., Espey, M. G., Wink, D. A. 2001. A rapid simple spectrophotometric method for simultaneous detection of nitrate and nitrite. *Nitric Oxide*, **5,** 62-71.

Mousseau, L., Klein, B., Legendre, L., Dauchez, S., Tamigneaux, E., Tremblay, J. E. and Ingram, R. G. 2001. Assessing the trophic pathways that dominate planktonic food webs: an approach based on simple ecological ratios. *Journal of Plankton Research,* **23,** 765-777.

Nixon, S. W. 1995. Coastal marine eutrophication: a definition, social causes, and future concerns. *Ophelia,* **41,** 199-219.

NRC (National Research Council). 2000. Clean coastal waters-understanding and reducing the effects of nutrient pollution. National Academy Press.

Parker, A. E., Dugdale, R. C. and Wilkerson, F. P. 2012. Elevated ammonium concentrations from wastewater discharge depress primary productivity in the

Sacramento River and the Northern San Francisco Estuary. *Marine Pollution Bulletin,* **64,** 574-586.

Parson, T. R., Maita, Y. and Lalli, C. M. 1984. A Manual of Chemical and Biological Methods for Seawater Analyses. Pergamon Press, New York: 173.

Peñuelas, J., Poulter, B., Sardans, J., Ciais, P., Van Der Velde, M., Bopp, L., Boucher, O., Godderis, Y., Hinsinger, P. and Llusia, J. 2013. Human-induced nitrogen–phosphorus imbalances alter natural and managed ecosystems across the globe. *Nature Communications,* **4**, 2934. doi:10.1038/ncomms3934.

R Core Team. 2014. *R: A language and environment for statistical computing. R Foundation for Statistical Computing*. R Foundation for Statistical Computing, Vienna, Austria.

Raven, J. A., Linda, B. W. and Handley, L. 1992. Ammonia and ammonium fluxes between photolithotrophs and the environment in relation to the global nitrogen cycle. *New Phytologist,* **121,** 5-18.

Revilla, M., Alexander, J., and Glibert, P. M. 2005. Urea analysis in coastal waters: comparison of enzymatic and direct methods. *Limnology Oceanography Methods*, **3**, 290-299.

Sterner, R. W. and Elser, J. J. 2002. *Ecological Stoichiometry: The Biology of Elements From Molecules to the Biosphere.* Princeton University Press, Princeton, NJ.

Syracuse Research Corporation (SRC). 2000. Interpretive summary of existing data relevant to potential contaminants of concern within the Anacostia River watershed. Syracuse Research Corporation, New York.

Tetra Tech (TT). 2014. Remedial Investigation Work Plan: Anacostia River Sediment Project, Washington, D.C. District Department of the Environment, Washington, D.C. Web. <doee.dc.gov>.

Van Heukelem, L. and Thomas, C. S. 2001. Computer-assisted high-performance liquid chromatography method development with applications to the isolation and analysis of phytoplankton pigments. *Journal of Chromatography A,* **910,** 31-49.

Velinsky, D. J., Riedel, G. F., Ashley, J. T. F. and Cornwell, J. C. 2011. Historical contamination of the Anacostia River, Washington, DC. *Environmental Monitoring and Assessment,* **183,** 307-328.

Vitousek, P. M., Aber, J. D., Howarth, R. W., Likens, G. E., Matson, P. A., Schindler, D. W., Schlesinger, W. H., and Tilman, D. G. 1997. Human alternation of the global nitrogen cycle: sources and consequences. *Ecological Applications*, **7**, 737-750.

Warner, A., Shepp, D. L., Corish, K. and Galli, J. 1997. An Existing source assessment of pollutants to the Anacostia watershed. Department of Environmental Programs, MW COG, Final Report, Washington, D.C.

Wilkerson, F. P., Dugdale, R. C., Hogue, V. E., and Marchi, A. 2006. Phytoplankton blooms and nitrogen productivity in the San Francisco Bay. *Estuaries and Coasts*, **29**, 401-416.

Xu, J., Glibert, P. M., Liu, H., Yin, K., Yuan, X., Chen, M., and Harrison, P. J. 2012. Nitrogen sources and rates of phytoplankton uptake in different regions of Hong Kong waters win summer. *Estuaries and Coasts*, **35**, 559-571.

Yoshiyama, K. and Sharp, J. H. 2006. Phytoplankton response to nutrient enrichment in an urbanized estuary: Apparent inhibition of primary production by overeutrophication. *Limnology and Oceanography,* **51**, 424-434.

Chapter 2. Phytoplankton composition responses to changes in nutrient concentration, form, and proportion: a study of nutrient-rich West Lake, Hangzhou, China

INTRODUCTION

The marine and freshwater systems of China are among the most nitrogen (N) polluted in the world (Ti and Yan, 2013, Glibert *et al.* 2014a). The response to nutrient pollution, eutrophication, in China's freshwaters waters include high biomass cyanobacterial blooms, particularly those of *Microcystis aeruginosa*, changes in species diversity of both primary and secondary producers, reductions in dissolved oxygen resulting in fish kills, and increased frequency of toxic and nontoxic harmful algal blooms (HABs) (Nixon, 1995, Pu *et al.*, 1998, Chen *et al.*, 2003a, Glibert *et al.*, 2014a). China has become an "endmember" of extreme N pollution as a result of both sewage effluent from expanding populations and from escalating applications of N fertilizer (Li and Zhang, 1999, Van Drecht *et al.,* 2009, Glibert *et al.*, 2014a).

Eutrophication in China has been linked with the rise in N fertilizer use as well as declining soil retention (Cui *et al.*, 2013, Glibert *et al.*, 2014a). China's fertilizer N use has escalated from approximately ~0.5 MT in the 1960s to 42 MT around 2010 with some of this N "leaking" into aquatic systems, considering the inefficient incorporation of N into agricultural products (Glibert *et al*., 2014a and references therein). Although phosphorus (P) is also associated with fertilizer runoff, the stoichiometry of fertilizer has changed in recent decades, resulting in increasing N:P reaching waters (Glibert *et* al., 2012). Not only are N loads rising in China, but relative N forms reaching aquatic ecosystems are changing, resulting in increasing chemically-reduced (e.g. NH_4^+,

dissolved organic N) compared to chemically-oxidized forms of N (NO_3^-) (Chen *et al.*, 2010, Xu *et al.*, 2011, Glibert *et al.,* 2014a). NH_4^+ has long thought to be the preferred form of N for phytoplankton uptake (McCarthy, 1981, Raven *et al.*, 1992); however, NH_4^+ may actually suppress overall growth when concentrations are sufficiently high (Morris and Syrett, 1963, Dortch, 1990, Lomas and Glibert, 1999a, 1999b, Glibert *et al.*, 2016).

The availability of different forms of N has often been used to understand ecosystem fates, such as biotic responses propagating through the food web from phytoplankton to fish. A classic concept within oceanographic phytoplankton ecology, based on the idea of "new" and "regenerated" production, is that NO_3^- generally supports higher food web production, while NH_4^+ more often supports microbial food webs in nutrient depleted marine systems (Dugdate and Goering, 1967). Declines in productivity, specifically diatoms, have been observed in systems experiencing increasing NH_4^+ loads, as well as mesocosm experiments enriched with NH_4^+ (Sharp *et al.*, 2009, Donald *et al.,* 2011, Parker *et al.* 2012, Glibert *et al.*, 2014b). In addition, cyanobacteria and dinoflagellate communities have been associated with NH_4^+ enrichment and field observations of reduced N dominated nutrient concentrations (Berg *et al.*, 2003, Glibert *et al.*, 2006, Heil *et al.*, 2007, Glibert and Berg, 2009, Donald *et al.*, 2011). In contrast to nutrient-poor marine waters, the ecosystem fate of different forms of N in nutrient-rich environments has been comparatively rarely examined (Glibert *et al.*, 2012). This raises questions as to whether the changes in the nutrient availability or form affects phytoplankton at the base of the food web similarly in nutrient-rich, compared to nutrient-poor systems, and if so, to what extent current shifts in N form may contribute to

primary producers that are less efficiently transferred to higher trophic levels, such as HABs.

The marine and freshwaters in and around Hangzhou, China, are heavily enriched in N. West Lake is a shallow polymictic lake in Hangzhou, the capitol of Zhejiang Province in eastern China and it used for drinking water and irrigation, and it attracts tourists worldwide (Fig. 1). The accumulation of nutrients and resulting degradation of West Lake's waters has been of concern since the 1970s considering its small volume and the rapid development of the economy and drainage basin (Hongping and Jianyi, 2002). Despite the implementation of water supply and dredging projects in West Lake in the 1980s to improve water quality, blooms continue to appear (Hongping and Jianyi, 2002). Some of these blooms taint and discolor the waters and increase water purification costs for treatment.

Bloom formation may also be influenced by episodic weather-related events such as tropical cyclones (hurricanes or typhoons; McGillicuddy *et al.*, 2007, Zhao *et al.,* 2009, Chen and Tang, 2012) as a result of enhanced nutrient pulses, resuspension of benthic phytoplankton, and changes in water temperature and water column stratification (Zhu *et al.*, 2014a). Typhoons and hurricanes are important drivers of biogeochemical and water quality perturbations (Burkholder *et al.*, 2006, Paerl *et al.*, 2006, Rabalais *et al.*, 2009, Zhu *et al.*, 2014a).

This study aimed to determine the extent to which phytoplankton community composition is altered as changes in N loading occur. First, the natural phytoplankton community (species composition, biomass, and chemical composition) was characterized along an N gradient in West Lake. Second, patterns in phytoplankton communities

observed in the lake were compared to those observed in enrichment experiments with N of varying forms with and without P. The period of our sampling also allowed us to examine effects of typhoons on nutrients and therefore on phytoplankton. We hypothesized that shifts in phytoplankton community composition in the enrichment experiments would mirror the phytoplankton assemblages observed along the ambient N gradient in West Lake. It was expected that in the environments enriched with N and increasing NH_4^+ there would be a shift in phytoplankton assemblages with large diatoms giving way to cyanobacteria and dinoflagellates.

MATERIALS AND METHODS

Study Site

West Lake, located west of downtown Hangzhou, China, receives freshwater from the Qiantang River in the south and is a shallow lake (average depth of 1.56 m) that has a total area of 5.66 km^2 and watershed area of 27.25 km^2 (Fig. 1; Hongping and Jianyi, 2002). On average, West Lake receives ca. 4.6 m^3 s^{-1} from six inflow sites in the southwest portion of the lake, while the water exits the river through nine outflow sites in the northeast. Samples were taken at 3 sites, with site 1 closest to the inflow of water from the Qiantang River and site 3 closest to the outflow sites. These sites were chosen based on preliminary nutrient analysis that indicated the sites had contrasting nutrient regimes, as well as the presence of phytoplankton blooms at site 3.

This study took place during the 2015 Asian typhoon season, with two typhoons occurring during the period of this study, Typhoon Chan-hom in July and Typhoon Soudelor in August. Thus, the 2015 typhoon season provided a unique opportunity to

study the effect of changes in nutrient form on the phytoplankton community in West Lake. Monthly precipitation and temperature data were acquired from National Oceanic and Atmospheric Administration's National Climatic Data Center (NOAA NCDC) Data Online (http://www7.ncdc.noaa.gov/CDO/) for Hangzhou, China.

Sample Collection

Samples were collected at three different bridge-accessible sites on seven separate sampling dates from May to September of 2015 (May 5, June 6, June 26, July 12, July 26, August 6, September 8). At each site, water was taken from the surface using a clean bucket and immediately brought back to the laboratory for processing and to initiate 48 h enrichment experiments. Upon return to the laboratory, samples were filtered through Whatman GF/F filters (nominally 0.7 μm; precombusted 2 h 450 °C) for the determination of chlorophyll *a* (chl *a*). Filters for the latter analyses were kept frozen for a week prior to drying. The GF/F filtrates of these filtrations were frozen for later analysis of NH_4^+, NO_3^-, and PO_4^{3-}. In addition, aliquots of water from each of the sites were prepared for nutrient enrichment experiments as described in the following sections.

Community Composition

Phytoplankton composition and abundance were determined for each field site and each experimental treatment. Samples were fixed and preserved in 2% formaldehyde, covered and stored at 20°C until each sample was counted on a Sedgewick Rafter cell. Replicate cell counts were made using a Smart-e Digital Microscope (Chongqing Optec Instrument Co., Ltd) at 100x and dilutions were made to avoid clustering of organisms. Phytoplankton were identified to genus level, and characterized into groups based on phylum.

Experimental Treatments

Enrichment experiments were conducted to determine changes in phytoplankton community composition under conditions in which N form and P were manipulated. Approximately 2 L of water was taken from the three sites and was returned to the laboratory. Then, acid washed plastic bottles were filled with 200 mL aliquots of sample, which were variably enriched with either NH_4^+, NH_4^+ plus P, NO_3^-, NO_3^- plus P, urea, and P only, to produce a range of nutrient supply ratios. Additions of 100 μM-N and 2 μM-P were made for the first three sampling dates (May 7, June 5, and June 26, 2015), while 40 μM-N and 2 μM-P additions were added to the samples for the final four sampling dates (July 12, July 26, August 6, September 8, 2015). The level of nutrient enrichment was aimed to increase the total available N to a value >40 μM-N, which would be >2-fold larger than the observed ambient NH_4^+ concentrations at the 3 sites. The six different enriched treatments were incubated in water-filled enclosures directly after the enrichments under natural light and temperature conditions for a period of 48 h. After 24 h and 48 h subsamples were taken from each treatment container to track phytoplankton community composition, biomass accumulation, and nutrients. Bottles were removed from the enclosure after 24 and 48 h, contents were then filtered onto Whatman precombusted GF/F filters and frozen for chl *a* and the filtrate was frozen for ambient nutrient analysis.

Analytical Protocols

Samples were stored for a period of a week and then thawed at room temperature for nutrient analysis. Ambient nutrients were analyzed using manual colorimetric assays (NH_4^+) and autoanalysis techniques (NO_3^- and PO_4^{3-}). Concentrations of NH_4^+ were

analyzed according to Zhu *et al*. (2014b). Concentrations of NO_3^- were analyzed according to Whitledge *et al.* (1981) and Bran and Luebbe (1999a) Method G-172-96, and PO_4^{3-} following Bran and Luebbe (1999b) Method G-175-96. Samples for chl *a* were analyzed using a Turner Designs Model 10-AU fluorometer following a 24 h 90% acetone extraction at 4°C (Arar and Collins, 1992).

Data Analysis

All available ambient nutrient data were compiled at sites 1 and 2 to determine their relationship with chl *a* at the downstream sites 2 and 3. The relationship between ambient nutrient concentrations and chl *a* ($\mu g\ L^{-1}$) were described using a numerical summary correlation (Pearson's r significance testing was performed with the statistical computing and graphics software R using base and statistics packages (R Core Team, 2014).

Non-metric multi-dimensional scaling (NMDS), an ordination technique, was performed to detect the relationship between phytoplankton assemblages and environmental data. Each sample (21 samples total) was reordered according to species composition rank (10 taxa) to carry out the correlation between the distance matrix and 2-dimensional space (Clarke, 1993). The dissimilarity matrix was made using the Gower metric, based on its high rank order similarity with gradient separation. The data were transformed with a square root transformation to balance the abundance data (Oksanen, 2014). NMDS was chosen since the interpretation of data is more straightforward and it works well when species have large differences in abundance (Gardener, 2014). In addition, NMDS can be used with non-normal and discontinuous distributions, and is considered the most effective ordination technique in community ecology (McCune and

Grace, 2002). The closer the samples are to one another in "taxa space" the more similar the samples are. Separate analyses based on 1-4 dimensions revealed that the 2-dimensional solution had a low stress value of 0.17 (low stress value implies better fit between data and ordination; Clarke, 1993). Vectors were applied to the ordination to show the direction of most rapid change using the R-function *envfit*, and the length is proportional to the correlation between the ordination and the environmental variable (Oksanen, 2014). A contour plot of environmental variables allows for the visualization of the relationship between the ordination and the environmental variables. The dissimilarity matrix calculation for NMDS was performed using the software R 3.1.2 (R Core Team, 2014) with the vegan 2.3 package (Oksanen *et al.*, 2015). The influence of different sites on phytoplankton diversity was tested on the basis of the distance matrix with Adonis, implementing 999 permutations.

An indicator species analysis was performed for each species and each site to determine whether any phytoplankton taxa were significantly associated with a site. In addition this analysis was performed for each treatment, to determine whether any phytoplankton taxa were significantly associated with an enrichment treatment. The Dufrene-Legendre indicator values (Dufrêne and Legendre, 1997) were calculated using the *indicspecies* package in R (De Cáceres, 2013), as a product of the relative frequency and relative average abundance at each site or treatment. A maximum value of 100% indicates that the species is recorded in all samples taken at one site, or that species is recorded in all samples after the addition of a particular treatment. Differences in species abundance were compared among the sites as well as the treatments using a MANOVA test and by one-way ANOVA, followed by *post hoc* multiple comparisons of treatment

means with Tukey's least significant difference procedure with α=0.05 using the software R. All calculations and figures were performed with the statistical computing and graphics software R using base and statistics packages, unless otherwise noted.

RESULTS

Ambient Environmental Conditions

Seasonal changes in precipitation and air temperature were summarized by NOAA in Hangzhou (Network:ID, GHCND:CHM00058457; 30.233° N, 120.167° E) during the sampling period . The extreme maximum in daily precipitation throughout the period of sampling occurred in August (8 cm); however, the total monthly precipitation was greatest in July (39 cm) (NOAA NCDC). The mean air temperature ranged from a minimum of 17.8 °C in May to a maximum of 32.4 °C in August. Typhoons occurred on July 11 and August 5.

Large changes in nutrient concentrations were observed across the three sampling sites. Overall, all inorganic N forms were high; NH_4^+ concentrations ranged from 3.57 to 24.4 μM-N, and NO_3^- concentrations ranged from 17.66 to 89.62 μM-N (Fig. 2A and B). Ambient PO_4^{3-} concentrations ranged from near 0 to 0.74 μM-P (Fig. 2C). An increase in PO_4^{3-} was observed at site 1 on July 12 and at all sites on August 6, which co-occurred with Typhoon conditions on these dates (Fig. 2C).

A gradient in NO_3^- concentrations across the three sites was apparent (Fig. 2A). The concentration of NO_3^- was the highest at site 1 and remained somewhat constant (~ 80 μM), since this is the site adjacent to the inflow of water from the Qiantang River. At site 3, NO_3^- concentrations were the lowest and approximately half of those at site 1 (~ 40 μM, Fig. 2A). Overall, the NO_3^- concentrations generally decreased as the water

moved from site 1 to site 3. Site 3 had the highest NH_4^+ concentrations (~10 μM, Fig. 2B), until August 6 when concentrations at site 2 increased 5-fold (~25 μM) (Fig. 2B). Similar to the NO_3^- gradient, PO_4^{3-} was the highest at site 1 on all dates (Fig. 2C). In general, it appeared that concentrations of all of the nutrients, except for NH_4^+, decreased from site 1 to site 3.

Molar ratios of DIN (NO_3^- plus NH_4^+) to PO_4^{3-} were always more than the canonical Redfield ratios at all sites and during all sampling dates (Fig. 2D). Molar DIN:DIP ratios varied the most at site 1 (Fig. 2D). Sites 2 and 3 experienced a gradual increase in DIN:DIP (Fig. 2D). The ratio of NH_4^+:NO_3^- increased throughout the majority of the sampling period, with the highest ratio noted on August 6 (0.81, Fig. 2E).

Phytoplankton Biomass and Community Composition

Phytoplankton biomass varied substantially during the sampling season. Concentrations of chl *a* ranged from 5 μg L^{-1} in May to a maximum of 152 μg L^{-1} in September (Fig. 2F). Chl *a* values were the highest at site 3, followed by site 2 and site 1, with the exception of September 8 when the highest chl *a* value (~160 μg L^{-1}) was observed at site 2. In general, concentrations of chl *a* were >20 μg L^{-1} at sites 2 and 3, with chl *a* reaching a peak of ~140 and 150 μg L^{-1} during the months of July and September, respectively.

Total phytoplankton abundance ranged from 31-3601 cells mL^{-1}, with the lowest abundance observed in May and the highest on July 12 (Fig. 3). The absolute abundance of phytoplankton increased from site 1 to site 3 (Fig. 3). A peak in phytoplankton abundance occurred at site 1 on July 26 (Fig. 3A), whereas peak abundance at site 2 occurred on June 26, with a secondary peak on July 26 (Fig. 3B). The maximum

abundance of phytoplankton at site 3 was on July 12 and abundance was slightly reduced on July 26 (Fig. 3C).

There were 10 major phytoplankton taxa identified from preserved samples (Table 1). Overall, *Nitzschia* sp. were the most abundant (8,124 cells ml^{-1}), followed by *Tribonema* sp. (5,208 cells ml^{-1}), *Chlorella* spp. (778 cells ml^{-1}), and *Merismopedia* sp. (731 cells ml^{-1}; Fig. 3). There was a heterogenous phytoplankton community at site 1 from May to September (Fig. 4A), whereas sites 2 and 3 were mostly homogenous (Fig. 4B and C). Site 2 was dominated by *Nitzschia* sp. (>50%), except on June 26 (~65% *Tribonema* sp.), August 6 (30% *Chlorella* spp.), and September 8 (30% *Tribonema* sp. and 30% *Merismopedia* sp.) (Figs. 3B and 4B). Contrastingly, the phytoplankton community at site 3 shifted from a community dominated by a diatom *Nitzschia* sp. (Bacillariophyta; ~85%) in May to a filamentous yellow-green benthic algae, *Tribonema* sp., by September (Xanthophyceae; ~50%; Figs. 3C and 4C). On all sampling dates the abundance of the large cryptophyte *Cryptomonas* spp. was reduced at site 3 compared to site 1 (Fig. 4A and C).

When all ambient nutrient and chl *a* data were compiled, chl *a* at site 2 and different nutrients from site 1 (Fig. 5A, C, E, G, and I) and chl *a* at site 3 and different nutrients from site 2 (Fig. 5B, D, F, H, and J) were related (Table 2 and Fig. 5). NO_3^- concentrations at the prior station had a positive linear relationship with chl *a* at both sites 2 and 3 (Fig. 5A and B), whereas the relationship of NH_4^+ at the prior station with chl *a* was different between the two sites (Fig. 5C and D). The differences in productivity between sampling locations indicates that the influence of ambient NH_4^+ concentrations also depends on other ambient nutrients. PO_4^{3-} concentrations had a negative linear

relationship with chl *a* at both sites, but only chl *a* at site 2 showed a significant relationship with PO_4^{3-} at site 1 ($r=0.69$, $p=0.01$; Fig. 5E and F). The ratio of DIN:PO_4^{3-} at the prior sites had a positive linear relationship with chl *a* at both sites, but only chl *a* at site 2 had a significant relationship ($r=0.86$, $p=0.002$; Fig. 5G and H). The ratio of NH_4^+:NO_3^- did not show a significant trend or association with chl *a* at either site (Fig. 5I and J).

Indicator Species and Cluster Analysis

The indicator species analysis performed across the three sites using all species, revealed differences between site 1 and sites 2 and 3. The abundance of the chlorophytes, *Scenedesmus* spp., *Pediastrum* spp. and *Tetrastrum* sp., were strongly and significantly associated with sites 2 and 3 ($p<0.001$ for *Scenedesmus* spp. and *Pediastrum* spp., $p<0.05$ for *Tetrastrum* sp.). The cyanobacteria, *Merismopedia* sp. was also characterized as an indicator species at sites 2 and 3 ($p<0.05$). There were no distinct indicator species from site 1.

The results of the multi-dimensional scaling analyses demonstrated a gradient change in phytoplankton community similarity associated with the sampling location, with site 1 separated from sites 2 and 3 (stress=0.17, Fig. 6). Although sites 1 and 2 were closer in distance to one another, the nutrient data also showed that sites 2 and 3 were more similar (Fig. 2). Adonis calculations revealed a significant influence of the site ($p=0.04$) on the phytoplankton community composition. The multivariate analyses showed that the biomass was most highly correlated with the phytoplankton community structure ($p<0.01$, $r^2=0.38$), followed by DIN and DIN:DIP ($p<0.5$ and $p<0.07$, $r^2=0.27$ and $r^2=0.23$, respectively; Fig. 7A and B). This indirect gradient approach puts the

environmental variables in perspective with bi-plot environmental vector arrows representing gradients and pointing in the direction of rapid change in the environmental variable. The biomass (chl *a*) and DIN:DIP vectors rapidly increased towards sites 2 and 3, while the DIN vector rapidly changed (increasing) towards the direction of site 1 (Fig. 7A and B).

The species scores showed that several species were correlated with the NMDS axes and associated nutrient conditions (Fig. 6 and 7). *Cryptomonas* spp., *Thalassiosira* sp., and *Chlorella* spp. displayed a significant correlation with samples from site 1, indicating that they were positively associated with DIN. The bloom forming species *Tribonema* sp. was found in the center of the NMDS, representative of the fact that they dominated most samples. Cyanobacteria, such as *Merismopedia* sp. and *Microcystis* sp. were positively associated with NMDS axis 2, which is also associated with rapidly increasing DIN:DIP and chl *a*.

Contours of ambient nutrient concentrations and ratios associated with the ambient phytoplankton community composition were fitted to the ordination (Fig. 8A-C). NO_3^- contours showed a linear influence of concentration associated with the community composition (Fig. 8A). Concentrations of ~60 μM NO_3^- were associated with species observed at site 1 (*Chlorella* spp., *Thalassiosira* sp., and *Cryptomonas* spp.; Fig. 8A). A non-linear influence of NH_4^+ concentrations associated with community composition were also fitted to the ambient community composition ordination, reflecting the higher NH_4^+ concentrations at site 1 than sites 2 and 3 (Figure 8B). Contours of DIN:DIP fitted to the ordination also showed a non-linear influence of DIN:DIP on community composition, with the highest DIN:DIP contours of ~1500 associated with Cyanobacteria

(Fig. 8C). The filamentous yellow-green alga *Tribonema* sp. was found between DIN:DIP contours of 0 and 500 (Fig. 8C). Species consistently observed at site 1 (*Chlorella* spp., *Thalassiosira* sp., and *Cryptomonas* spp.) were grouped together within the DIN:DIP 500 contour (Fig. 8C).

Community Response to N Forms

The response of chl *a* to N and P enrichments in experimental treatments depended on the sampling date (Fig. 9). At site 1, only one of the sampling dates (July 26) had a significant difference in chl *a* concentrations between the enrichment treatments compared to the control (Fig. 9A). On that date, the addition of combined NH_4^+ and P additions had the greatest positive influence on chl *a* (~5-fold increase, p=0.12), while the addition of P and combined NO_3^- and P also had a positive influence on chl *a* (p=0.16 and p=0.30, respectively; Fig. 9A). At site 2, significant differences in chl *a* concentrations following enrichments were observed on two sampling dates (May 7 and September 8; p<0.001and p<0.001; Fig. 9B). On those dates, the addition of combined NH_4^+ and P had the greatest positive influence on chl *a* concentration (p=0.01), while the addition of combined NO_3^- and P and P addition also had a positive, but not significant, influence on chl *a* concentrations (p=0.06 and p=0.08, respectively; Fig. 9B). The most frequent significant differences in chl *a* concentrations were observed at site 3 (May 7, July 12, July 26, and September 8; Fig. 9C). The significant differences between treatments at sites 2 and 3 were also the sampling dates with the lowest NH_4^+:NO_3^- ratios (Fig. 2E). The addition of combined NH_4^+ and P at site 3 had a positive influence on chl *a* on all sampling dates; however, it was only significant on May 7 and September 8 (p=0.06 and p=0.01, respectively; Fig. 9C). The additions had the strongest effect on chl

a on June 26 and July 26, when ambient PO_4^{3-} and NO_3^- concentrations were at their lowest (Figs. 2A and C, 9). Overall, the combined N and P additions and P additions led to the strongest positive responses.

In the enrichment experiments, when all data were compiled for each site separately from May through September 2015, the addition of N and P promoted the growth of the community as a whole at all sites (Fig. 10). However, the change in total community abundance differed for those samples enriched with NH_4^+ and P compared to those enriched with NO_3^- and P depending on the site (Fig. 10). When examined over time for phytoplankton community composition, the control water sample (no nutrient addition) typically showed increases in the xanthophyceae and bacillariophyta groups relative to initial conditions, whereas cryptophytes and cyanobacteria were reduced. At site 1, the NH_4^+ plus P, NO_3^- plus P, and P treatments resulted in increases in total community abundance. Among these three treatments, there were comparatively small differences in community composition; however, treatments with NH_4^+ plus P consisted of more chlorophytes than the other treatments (Fig. 10A). The addition of NO_3^- plus P at site 2 showed the highest increase in phytoplankton community abundance, and resulted in a community dominated by bacillariophyta (diatoms; Fig. 10B). At site 3, the addition of NH_4^+ plus P had the highest increase in phytoplankton community abundance, with a community dominated by xanthophyceae (Fig. 10C). Multivariate analysis of variance (MANOVA) for combined abundance data from all sites revealed a significant effect of nutrient form on phytoplankton abundance, as measured by each phytoplankton group abundance ($F(6, 280)=4.40$, $p<0.001$; Fig. 10). Univariate F-tests for each of the 5 phytoplankton groups showed that the abundance of chlorophytes and cryptophytes

among the different treatments was significantly different ($F(6, 280)=2.52$, $p<0.01$ and $F(6,280)=0.98$, $p<0.05$, respectively; Fig. 10).

The nutrient enrichment experiments revealed temporal differences in phytoplankton growth from May to September 2015, yet consistent changes in phytoplankton groups were observed following the different treatments (Figs. 11-13). The highest percent change in phytoplankton abundance was observed in treatments receiving P, with or without the different forms of N (Figs. 11-13). Samples receiving P, with or without N, had a percent change that was 2- to 10-fold greater than those treatments that did not receive P (Figs. 12 and 13). Cryptophytes had the highest percent change after just the addition of P (1800 %; Fig. 12C), responding approximately 4-fold more than other algal groups, such as chlorophytes and cyanobacteria (Figs. 13C).

Phytoplankton abundance after enrichment with NO_3^- and NH_4^+ and P differed. The enrichment of site 3 with NH_4^+ plus P resulted in a 2000-12500 % increase in cryptophytes on June 26, July 26, and August 6 (Fig. 11I). After cryptophytes, cyanobacteria experienced the next highest percent change after the addition of NH_4^+ plus P with a maximum percent change ranging from ~500-1500% consistently at site 2 (Fig. 11H). Following cyanobacteria, chlorophytes growth was stimulated by the addition of NH_4^+ plus P on all dates and all sampling locations (Fig. 11G-H and 13A). The cryptophytes response to NO_3^- plus P at site 3 ranged from ~1250 to 5000 % (Fig. 11L). The addition of NO_3^- plus P had a maximum cyanobacteria response at site 2 of ~3000% that varied significantly across the sampling dates (Figs. 11K), whereas the addition of P resulted in a maximum increase in cyanobacteria by ~500% at all sites (Figs. 12 and 13C). A comparison of chlorophyta response to different N-forms reveal that they were

stimulated by treatments with NH_4^+ more often than NO_3^- treatments (Figs. 11 and 13A-B). Xanthophyceae responded in 66% of the NH_4^+ treatments, compared to 29% of the NO_3^- treatments (Figs. 11A-F). The addition of NO_3^- plus P and NH_4^+ plus P stimulated bacillariophyceae at sites 1 and 3; however, the addition of NO_3^- plus P at site 2 showed an approximately two-fold greater percent change than samples treated with NH_4^+ plus P (Figs. 11G-L).

The community response to N forms at site 3 was incorporated with the ambient community composition data into two separate NMDS ordination plots to observe shifts in community composition. After the addition of NH_4^+ to site 3, species community composition shifted further away from the ambient community composition more typical of all the sites (Fig. 14A). The shift observed in the community composition was associated with cyanobacteria species and chlorophyta species (Fig. 14A). In contrast, the addition of NO_3^- to site 3 resulted in a community that was very similar to sites 2 and 3, whereas some samples shifted closer to site 1 samples (Fig. 14B).

DISCUSSION

Community Compositional Changes and Biomass

This work has shown that phytoplankton community composition changes in response to nutrient form and nutrient ratios in lake water that - based on nutrient concentrations alone - was presumably not limited by nutrients. Spatial and temporal shifts in phytoplankton community composition observed in the field mirrored responses to N forms in enrichment mesocosms. Changes in N form were significantly associated with shifts in phytoplankton community composition, most notably after the addition of

NH_4^+ plus P. NMDS was used to discern patterns in abundance, considering the large separation between species showed the range of environmental preferences among species. However, the overlap of some species in the NMDS analysis indicated that there were similarities in environmental preferences between species, which were indicative of their relative functional groups. Responses to different N forms observed during enrichment experiments confirm that there are clear differences between the algal groups.

The most consistent community composition responses were seen in samples enriched in NH_4^+ and NH_4^+ plus P, leading to increased abundance of chlorophytes and cyanobacteria. This was seen for example, in site 3 at all times with maximum responses in enrichment experiments in August (Figs. 11C and I, 13A). This pattern matches the NMDS analysis, where the NH_4^+ treatment in the enrichment experiments at site 3 showed a shift from ambient community composition more typical of all sites towards a community influenced by greater chlorophyte abundance (*Tetrastrum* sp., *Pediastrum* spp., and *Scenedesmus* spp.; Fig.14A). Similarly, indicator species analysis recognized that chlorophytes were associated with sites 2 and 3, the sites with the highest NH_4^+:NO_3.

The increase in the number of chlorophytes and cyanobacteria in the field and enrichment experiments following increasing NH_4^+ concentrations indicate that these functional groups are supported by NH_4^+. These responses are comparable to those shown by Donald *et al.* (2013) in Wascana Lake, Saskatchewan, Canada, enrichment experiments in the nutrient polluted San Francisco Bay Delta, and a freshwater tidal estuary in Spain (Domingues *et al.*, 2011, Donald *et al.*, 2013, Glibert *et al.*, 2014b). Mesocosm experiments using combined additions of NO_3^- and NH_4^+ in a tidal estuary in Spain yielded consistent results, showing a preference for NH_4^+ over NO_3^- by

chlorophytes (Domingues *et al.*, 2011). In Wascana Lake, chlorophytes and cyanobacteria increased by 400-800% following the addition of NH_4^+ in a series of 3-week nutrient enrichment experiments (Donald *et al.*, 2013). Similarly, mesocosm experiments conducted in the San Francisco Bay Delta revealed greater responses by zeaxanthin and chl *b*-containing organisms, which are indicative of cyanobacteria and chlorophytes, after the addition of NH_4^+ (Glibert *et al.*, 2014b). The assessment of the phytoplankton community in Vancouver Lake, Washington, also found that chlorophytes were associated with greater NH_4^+ levels (Lee *et al.*, 2015). Across the globe, from hypereutrophic Lake Taihu, China to Lake Okechobee, Florida, cyanobacteria have been recognized for their dominance in systems when N is supplied in chemically reduced forms (McCarthy *et al.*, 2009, Glibert *et al.,* 2014a, 2016). Moreover, the responses observed in West Lake are consistent with extensive reviews of culture work and field measurements by Collos and Harrison (2014) and Glibert *et al*. (2016) which support the emerging consensus that chlorophytes and cyanobacteria are more tolerant of high NH_4^+ conditions than are diatoms.

Not only did ambient N-forms change the community composition in West Lake, but they supported different chl *a* yields. NO_3^- consistently supported a chl *a* yield ranging from ~1 μg chl *a*: 1 μM N to ~2 μg chl *a*: 1 μM N, which are similar to values reported in a range of aquatic ecosystems (Gowen *et al.*, 1992, Edwards *et al.*, 2003, Glibert *et al.*, 2014b). A median yield of 1.1 μg chl *a*: 1 μM N was collected from work by Gowen *et al.*, 1992 and Edwards *et al.*, 2003 with samples collected from Scottish waters (Gowen *et al.,* 1992, Edwards *et al.*, 2003). Likewise, Glibert *et al.*, 2014b describe a similar range, particularly noting the greater yield in chl *a* following the

enrichment of samples with NO_3^- (Glibert *et al.*, 2014b). Although the relationship of NH_4^+ concentration with biomass was not as clear, differences in yields were most likely due to shifts in community composition with different N-forms.

Responses to Typhoons

During the course of sampling in West Lake, two typhoons were followed by changes in phytoplankton community composition. The shifts in community composition suggest that the typhoons contributed to runoff and high nutrient concentrations that supported the change. The typhoons led to increases in PO_4^{3-} that approximately doubled ambient PO_4^{3-} concentrations (July 12 and August 6; Fig. 2C). At the same time, the typhoons were most likely responsible for elevated NH_4^+ concentrations observed on August 6 (Fig. 2B). Therefore, the increase in the ambient chlorophyte and cyanobacteria groups in August is thought to have been a response to the pulse of nutrients (NH_4^+ and PO_4^{3-}) following the typhoon (Fig. 4B). Such responses were again mirrored in the enrichment experiments days after the typhoon in which the addition of NH_4^+ resulted in some of the highest percent changes in cyanobacteria, chlorophytes and cryptophytes compared to other sampling dates (Fig. 11A-C). This was also supported by the regression analysis of chl *a* from offset site nutrients, since the highest biomass was present at low PO_4^{3-} concentrations, which is indicative of rapid PO_4^{3-} uptake and assimilation following the pulse of the limiting nutrient (Fig. 5E and F).

The typhoons encountered during sampling in West Lake may have contributed to runoff and high winds, which resulted in nutrient concentrations that supported a shift in phytoplankton community composition. Episodic weather events have been associated with algal bloom events, long-term changes, and shifts in phytoplankton community

composition in the Neuse River Estuary, the Chesapeake Bay, San Francisco Bay Delta and many other estuaries (Burkholder *et al.*, 2006, Mallin and Corbett, 2006, Paerl *et al.*, 2006, Briceño and Boyer, 2010, Voynova and Sharp, 2012, Glibert *et al.*, 2014c, 2014d). For instance, the increased frequency and magnitude of tropical storms and hurricanes since 1996 in the Neuse River Estuary and Pamlico Sound have been associated with long term shifts in phytoplankton communities from the occurrence of winter-spring dinoflagellate blooms to increases in chlorophytes (Paerl *et al.*, 2006). In the Delaware Estuary, an abrupt increase in phytoplankton biomass was observed following a large discharge event in June 2006, which supplied nutrients to mid- and lower bay regions (Voynova and Sharp, 2012). Additionally, it has been hypothesized in the Maryland Coastal Bays that large episodic storms and associated freshwater flows, wind, or benthic resuspension, caused elevated PO_4^{3-} and NH_4^+ concentrations followed by increases in cyanobacterial picoplankton (Glibert *et al.*, 2014d).

Implications

Pollution problems due to N loading in China are severe; over 40% of all state-monitored rivers are considered "grade 4" (unsuitable for human contact), with West Lake most recently receiving a grade of 3 (slight eutrophication; Anonymous, 2010, MEP, 2011). One of the most well studied lakes in China is Taihu, where the duration of cyanobacterial *Microcystis* blooms has increased from ~1 month yr^{-1} to approximately 10 months yr^{-1} over the past 15 years (Duan *et al.*, 2009, Glibert *et al.*, 2014a). In the Taihu watershed (Changjiang River watershed), the use of N fertilizers for manure and mineral fertilizer has increased 8 to 10-fold since the 1950s (Chen *et al.*, 2008); and the change in harmful algal blooms in Taihu is strongly related to this increase in urea, as well as the

ratio of urea:P_2O_5 use scaled to the Changjiang watershed (Glibert *et al.*, 2014a). The trends in phytoplankton community composition in West Lake are not like those in Taihu. In West Lake, *Microcystis* sp. only made up 0% to 10% of the total phytoplankton abundance out of all sampling dates and sites, whereas *Microcystis* sp. can contribute anywhere from 40% to 98% of the total biovolume in Taihu from May to October (Chen *et al.*, 2003b). West Lake's phytoplankton community composition shifted from a community dominated by diatoms (bacillariophyceae) in the early summer to filamentous yellow-green (xanthophyceae), chlorophytes, and cyanobacteria surface blooms in the late summer, which were attributed the rise in NH_4^+:NO_3^-. This work demonstrates that with increasing N loads particularly when the N form is disproportionately in NH_4^+ relative to NO_3^-, the environment favors nuisance algal blooms, particularly those of cyanobacteria. West Lake may be on a trajectory of having blooms similar to those of Taihu if N pollution continues.

Conclusions

Given the global and regional trends and magnitude of N loads, and especially in China, these findings have important implications for the proliferation of HABs and the future of water quality management. Understanding the relationships between N forms and phytoplankton groups when nutrient loads and concentrations exceed those of "saturation" has consequences for the stoichiometry of aquatic ecosystems, in that imbalances can negatively influence trophic transfers and biogeochemistry (Glibert *et al.*, 2013). Changes in nutrient loads and forms have repercussions for competition and species success, which result in changes in species dominance and biodiversity (Glibert, 2012). The indicator species, including *Scenedesmus* spp., *Pediastrum* spp., *Tetrastrum*

sp. and *Merismopedia* sp., reported in this work may provide a useful target for managers in West Lake to monitor the ecosystem health and set restoration goals. More importantly, current nutrient criteria are largely focused on total N or P and total biomass measures of chl *a* (Bricker *et al.*, 2008, Harding Jr *et al.*, 2014). The classic view of phytoplankton response to eutrophication that more nutrients leads to more biomass neglects the importance of changes in nutrient form on phytoplankton succession and phytoplankton "quality" that ultimately determine the success of higher trophic levels.

Table 1 Most common phytoplankton taxa determined in West Lake, China, in summer 2015

Bacillariophyceae
Nitzschia sp.
Thalassiosira sp.
Chlorophyta
Tetrastrum sp.
Pediastrum spp.
Scenedesmus spp.
Chlorella spp.
Cryptophyta
Cryptomonas spp.
Cyanobacteria
Merismopedia sp.
Microcystis sp.
Xanthophyceae
Tribonema sp.

Table 2. Comparison of correlation statistics for Chlorophyll *a* (μg L^{-1}) at sites 2 and 3 relative to ambient nutrient concentrations for samples from West Lake.

Response variable and ambient nutrient conditions; statistical parameter		**Chlorophyll *a* @ 2**	**Chlorophyll *a* @ 3**
NO_3^-			
	regression coefficient (slope)	1.97	0.95
	correlation coefficient	0.27	0.14
	significance (p) of r	0.23	0.4
	N	7	7
NH_4^+			
	regression coefficient (slope)	5.48	-2.62
	correlation coefficient	0.13	0.17
	significance (p) of r	0.43	0.36
	N	7	7
PO_4^{3-}			
	regression coefficient (slope)	-145.48	-122.61
	correlation coefficient	**0.69***	0.50
	significance (p) of r	0.01	0.07
	N	7	7
DIN:PO_4^{3-}			
	regression coefficient (slope)	0.15	0.07
	correlation coefficient	**0.86****	0.25
	significance (p) of r	0.002	0.26
	N	7	7
NH_4^+:NO_3^-			
	regression coefficient (slope)	33.59	-93.50
	correlation coefficient	0.001	0.21
	significance (p) of r	0.94	0.30
	N	7	7

Correlation coefficients (r) that were significant at $p<0.01$ are indicated by **; whereas those that are significant at $p<0.05$ are indicated by *; all significant values are also shown in bold font.

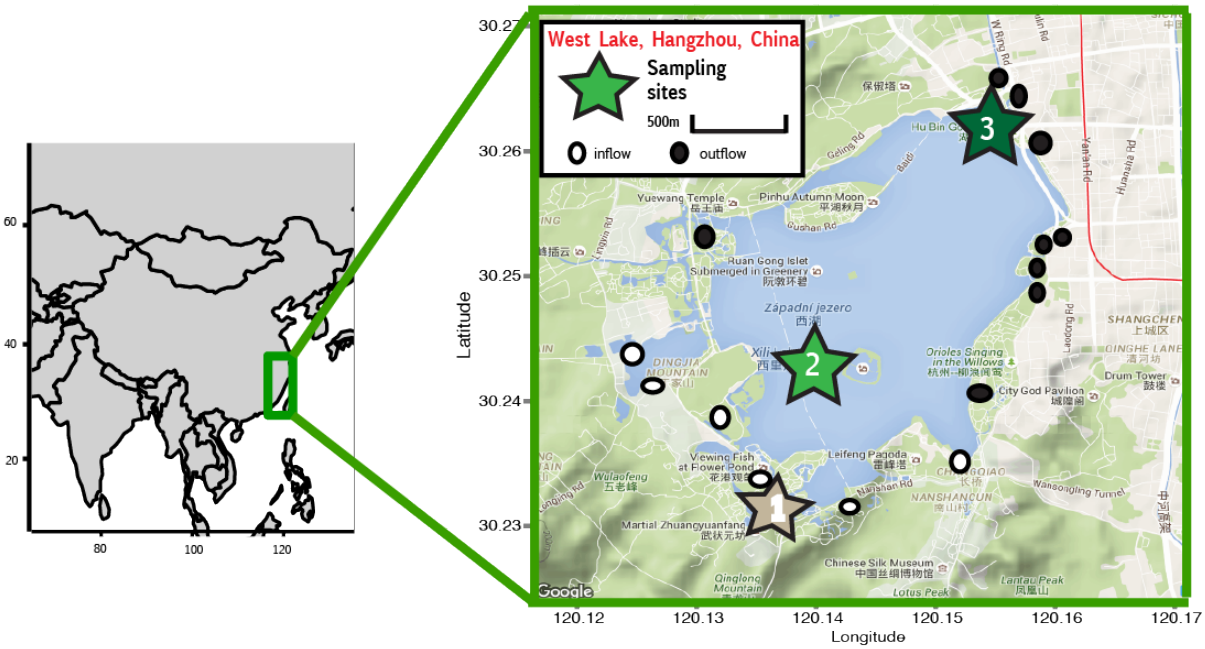

Figure 1. Map of West Lake in Hangzhou, China, showing the three sampling sites. Open circles show source of inflow from Qiantang River and black circles show sites of outflow.

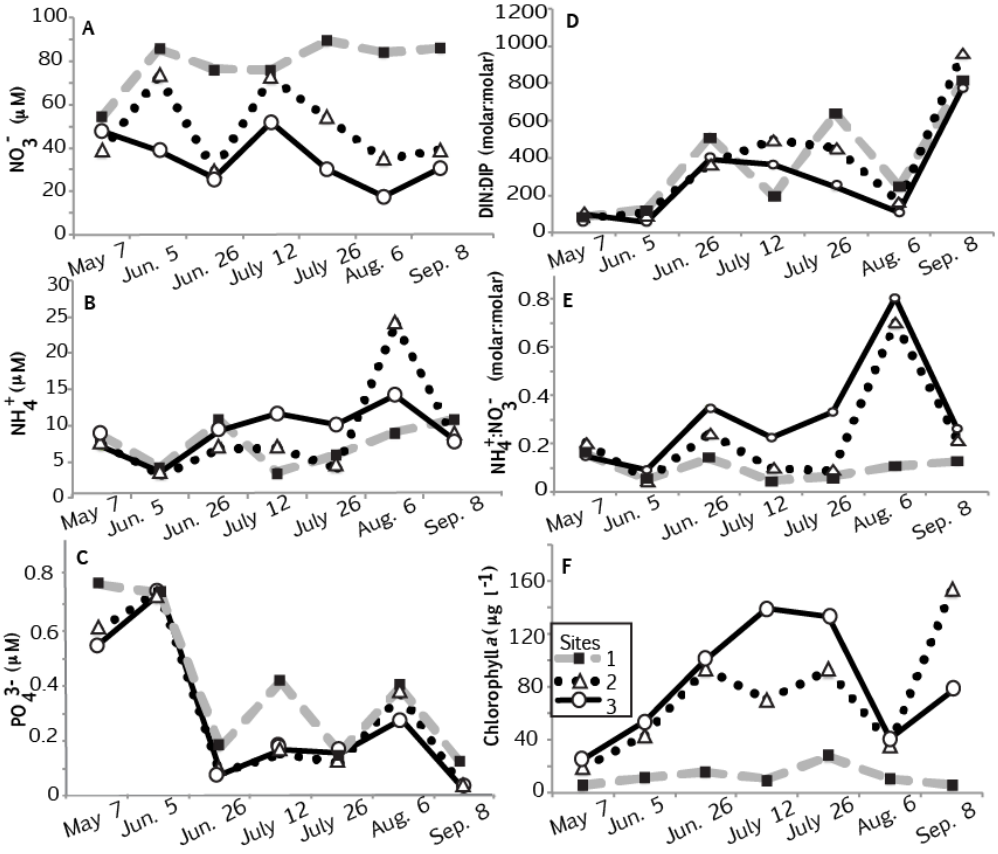

Figure 2. Concentration of NO_3^- (panel A), NH_4^+ (panel B) PO_4^{3-} (panel C), and dissolved inorganic N (NO_3^- and NH_4^+; DIN) relative to P (PO_4^{3-}; panel D), and NH_4^+ relative to NO_3^- (NH_4^+:NO_3^-; panel E), and Chlorophyll *a* (panel F) for the 3 sites sampled over 7 dates in 2015. All data shown are from near-surface samples. Note that the scale is different for all six panels.

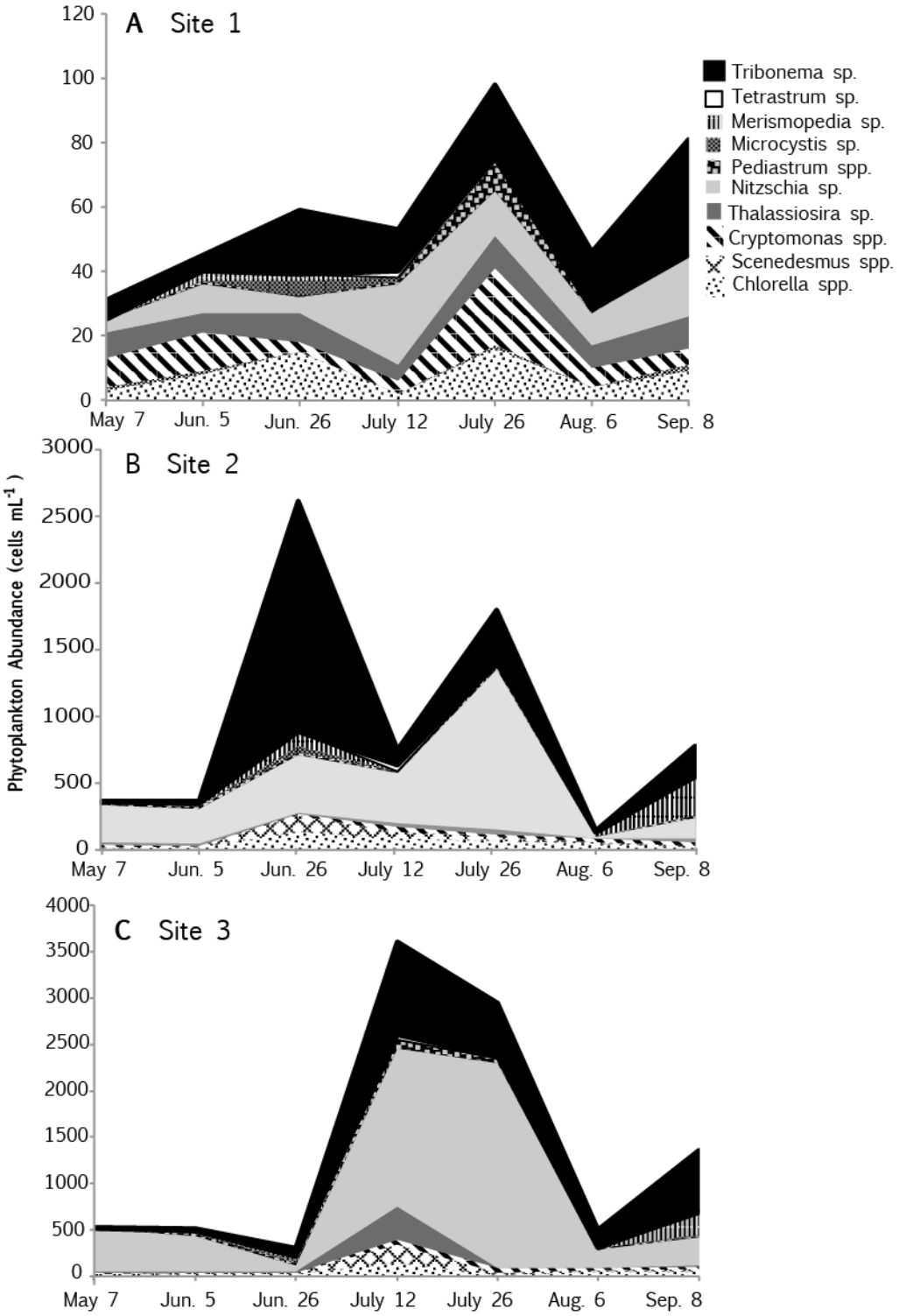

Figure 3. Absolute phytoplankton abundance from May 7 through September 8 at site 1(A), site 2(B), and site 3 (C). Note the changes in scales from panel to panel.

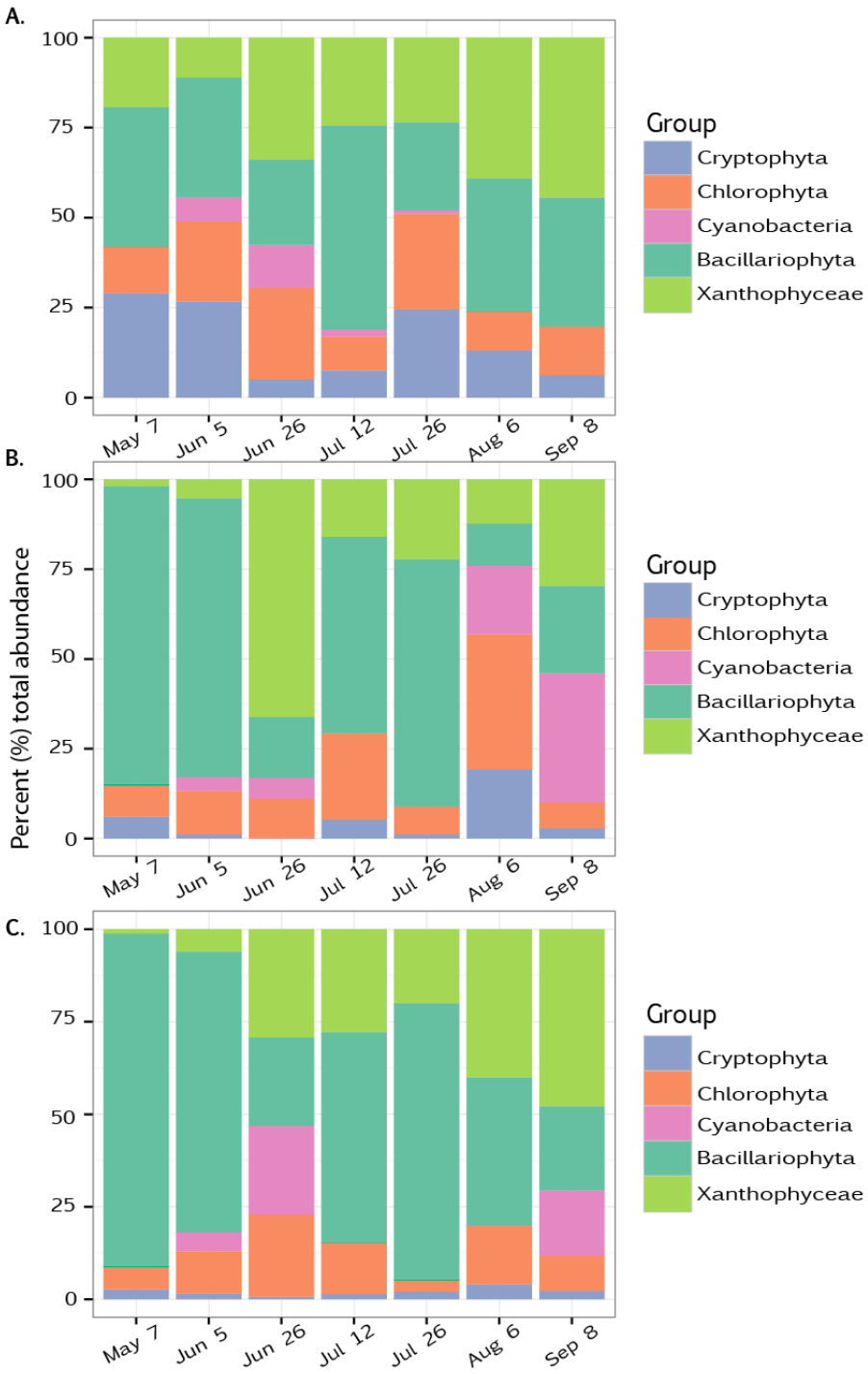

Figure 4. Relative phytoplankton abundance from May 7 through September 8 at site 1 (A), site 2 (B), and site 3 (C).

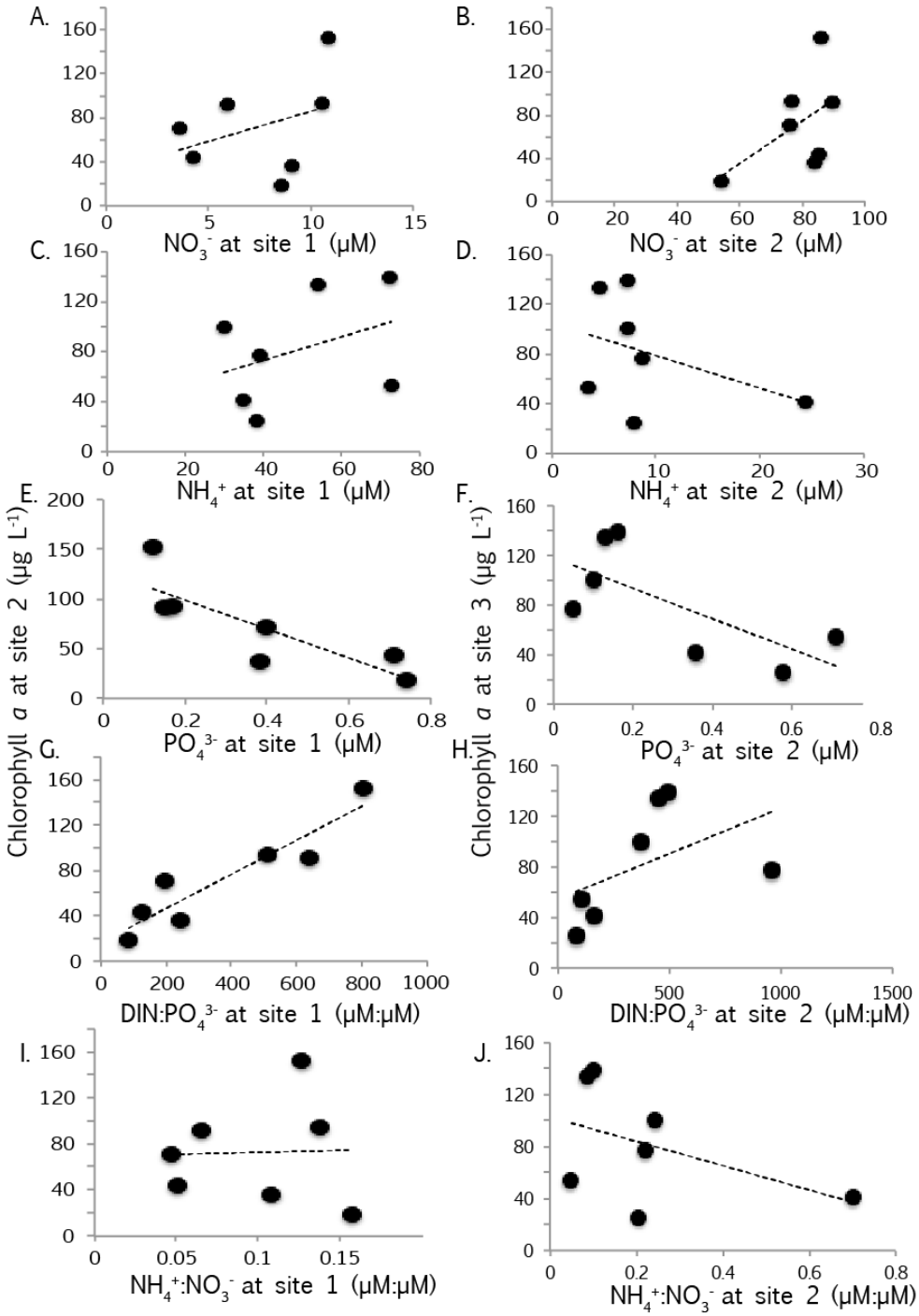

Figure 5. Chlorophyll *a* at site 2 (A, C, E, G, and I) and site 3 (B, D, F, H, and J) in relation to nutrients at upstream site 1 (A, C, E, G, and I) and site 2 (B, D, F, H, and J). Each point represents ambient data from sampling from May 7 to September 8. Regression statistics are given in Table 2.

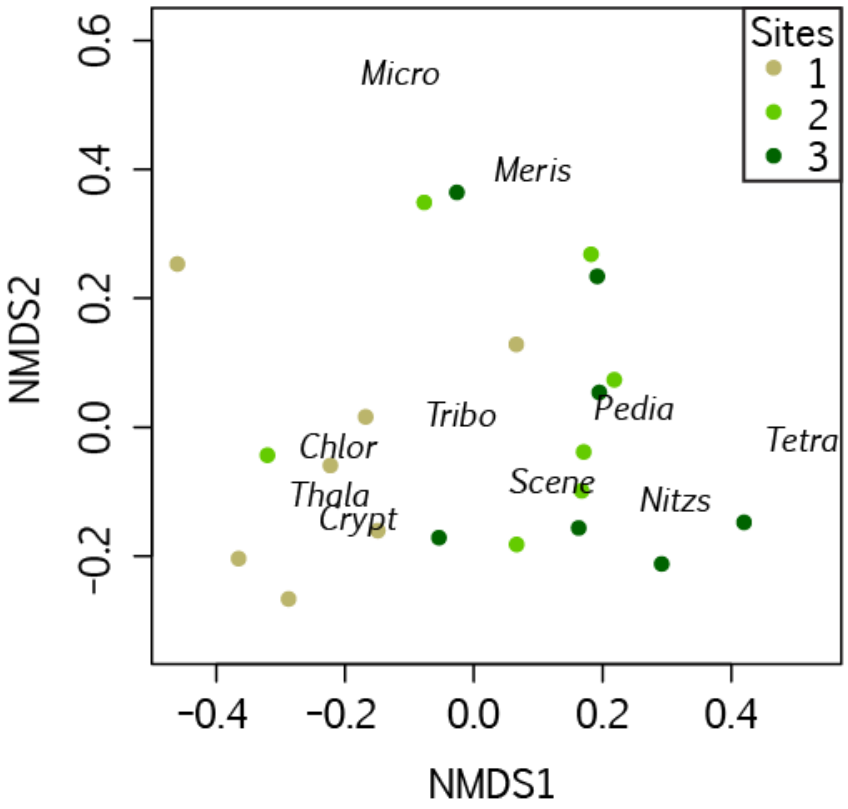

Figure 6. NMDS plot for phytoplankton abundance. Circles are samples and are color-coded depending on which site they came from, while species abundances are labeled.

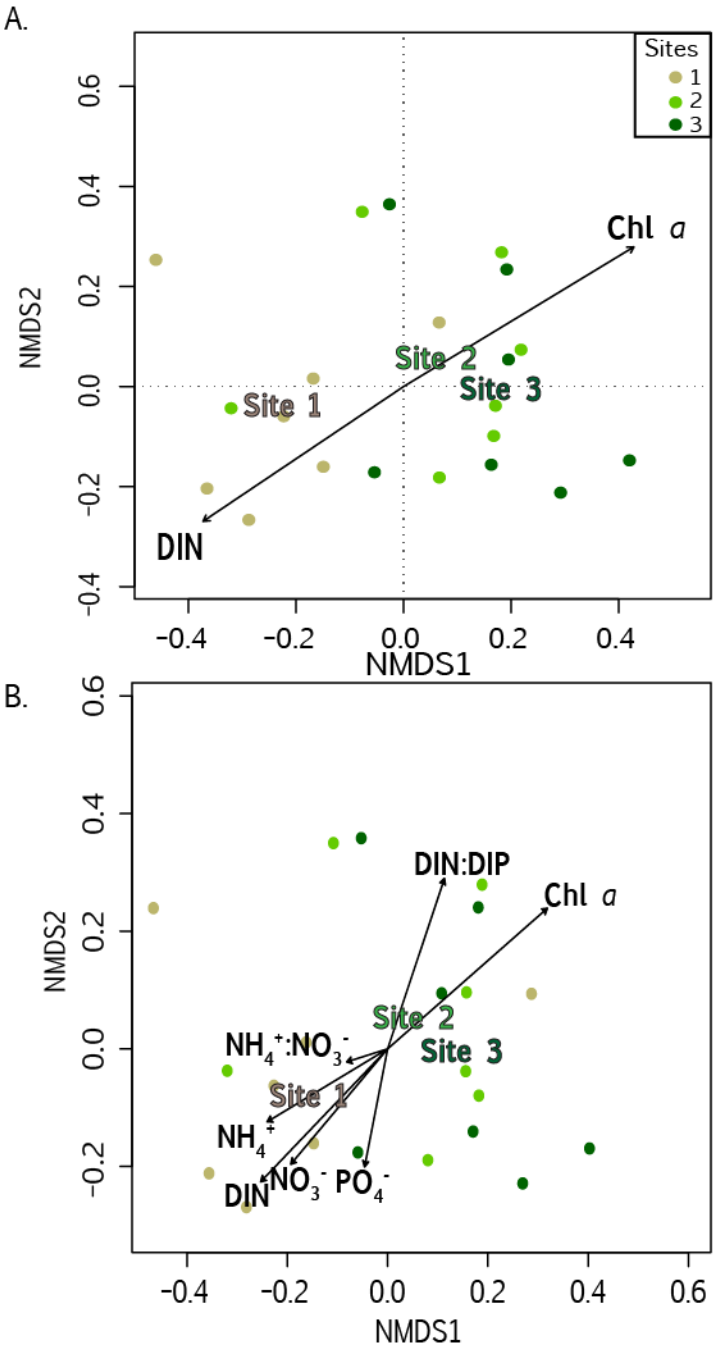

Figure 7. NMDS plot for phytoplankton abundance. Circles are samples and are color-coded depending on which site they came from. Vectors are fitted on top of the ordination plot showing the direction of most rapid change in the significant environmental variable. The separate panels show the environmental vectors that were significant ($p<0.05$) (A) and all of the environmental variables measured (B). The length of the arrow is proportional to the correlation between the ordination and environmental variables.

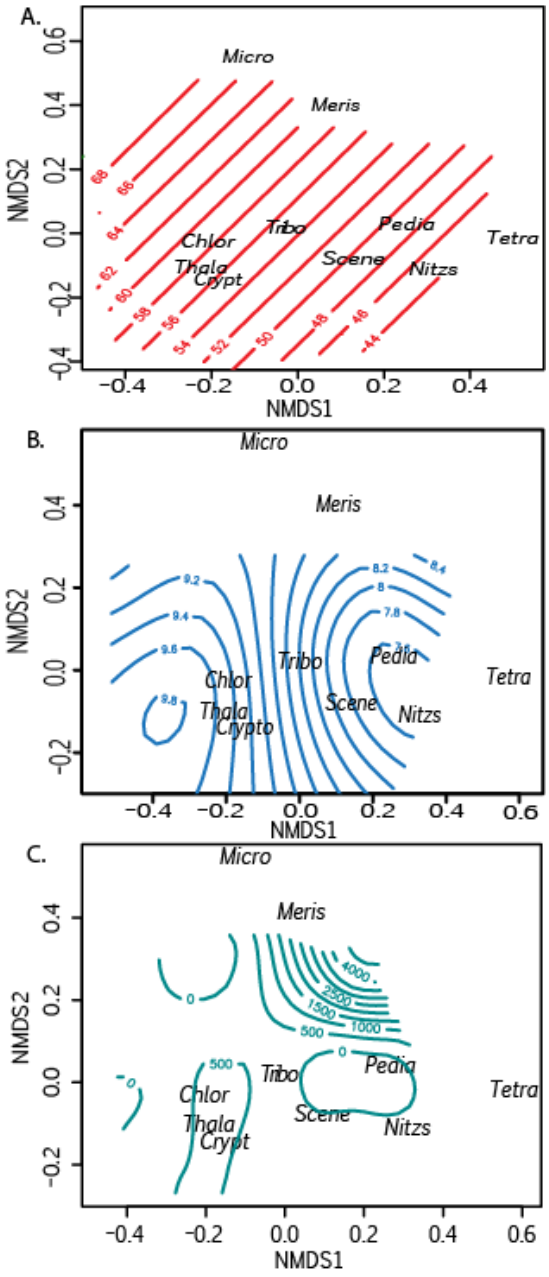

Figure 8. NMDS plot for phytoplankton abundance. Dominant genera are labeled. The red contours in (A) represent the gradient of NO_3^- (µM) in relation to ambient phytoplankton community composition. The blue contours in (B) represent the gradient of NH_4^+ (µM) in relation to ambient phytoplankton community composition. The teal contours in (C) represent the gradient of DIN:DIP (molar) in relation phytoplankton community composition.

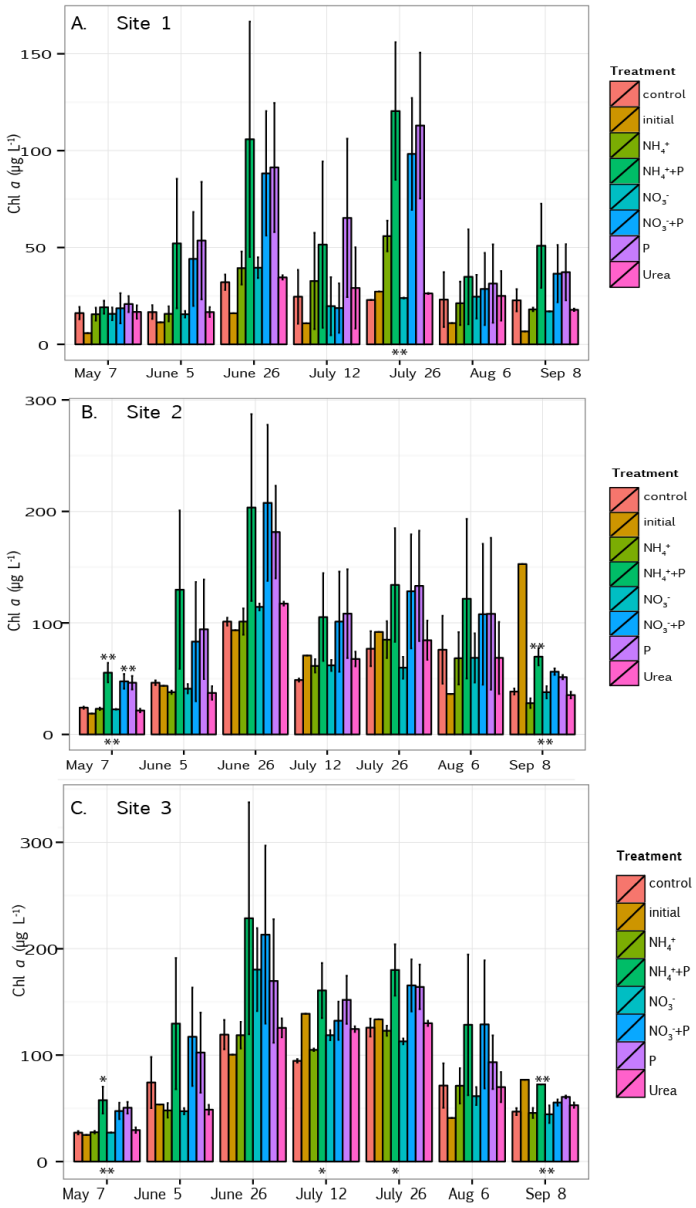

Figure 9. Initial and average of phytoplankton biomass (chl *a*) after 1 and days incubation in enrichments conducted from May 7 to September 8 with samples collected from site 1(A), site 2 (B), and site 3 (C). Error bars represent ± 1 SD of duplicate samples. Differences between the treatment and control are shown on the basis of ANOVA tukey post hoc test, with significance at the $p<0.01$ level indicated by **; those that are significant at the $p<0.05$ levels are indicated by *. Significant differences between all treatments is signified by either * or ** ($p<0.01$ and $p<0.05$, respectively) below the sampling date based on ANOVA f-test.

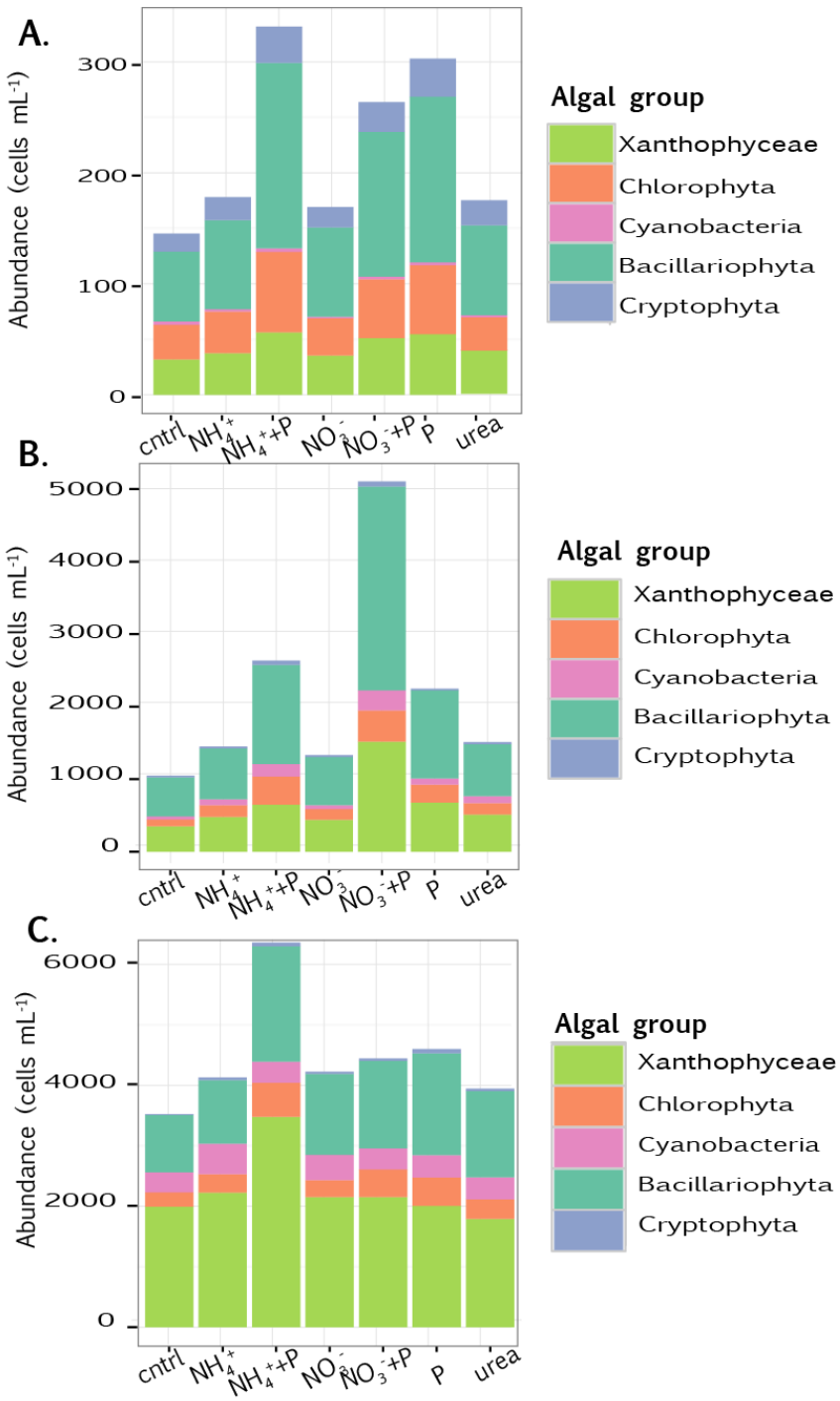

Figure 10. Mean abundance of each algal group at the end of the two-day enrichment experiment for each treatment at sampling sites 1 (A), 2 (B), and 3 (C). The mean combines abundance data from the seven enrichment experiment dates.

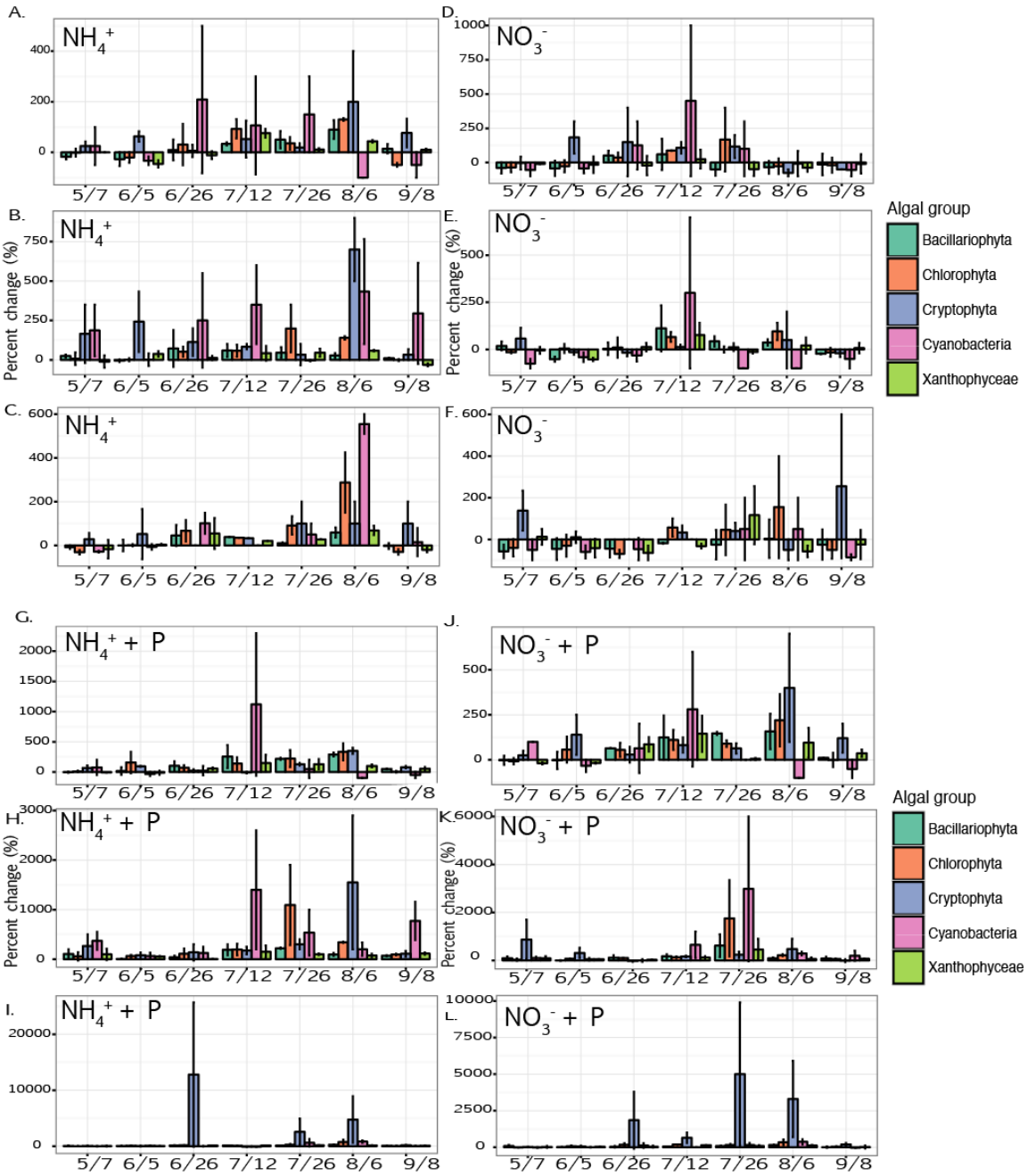

Figure 11. Percent change in abundance of each phytoplankton group after the addition of NH_4^+ (Panels A, B, C), of NO_3^- (panels D, E, F), of NH_4^+ plus P (panels G, H, I), and of NO_3^- plus P (panels J, K, L) relative to the control at sites 1, 2, and 3, respectively. Error bars represent ± 1 SE of two time points (T24 and T48).

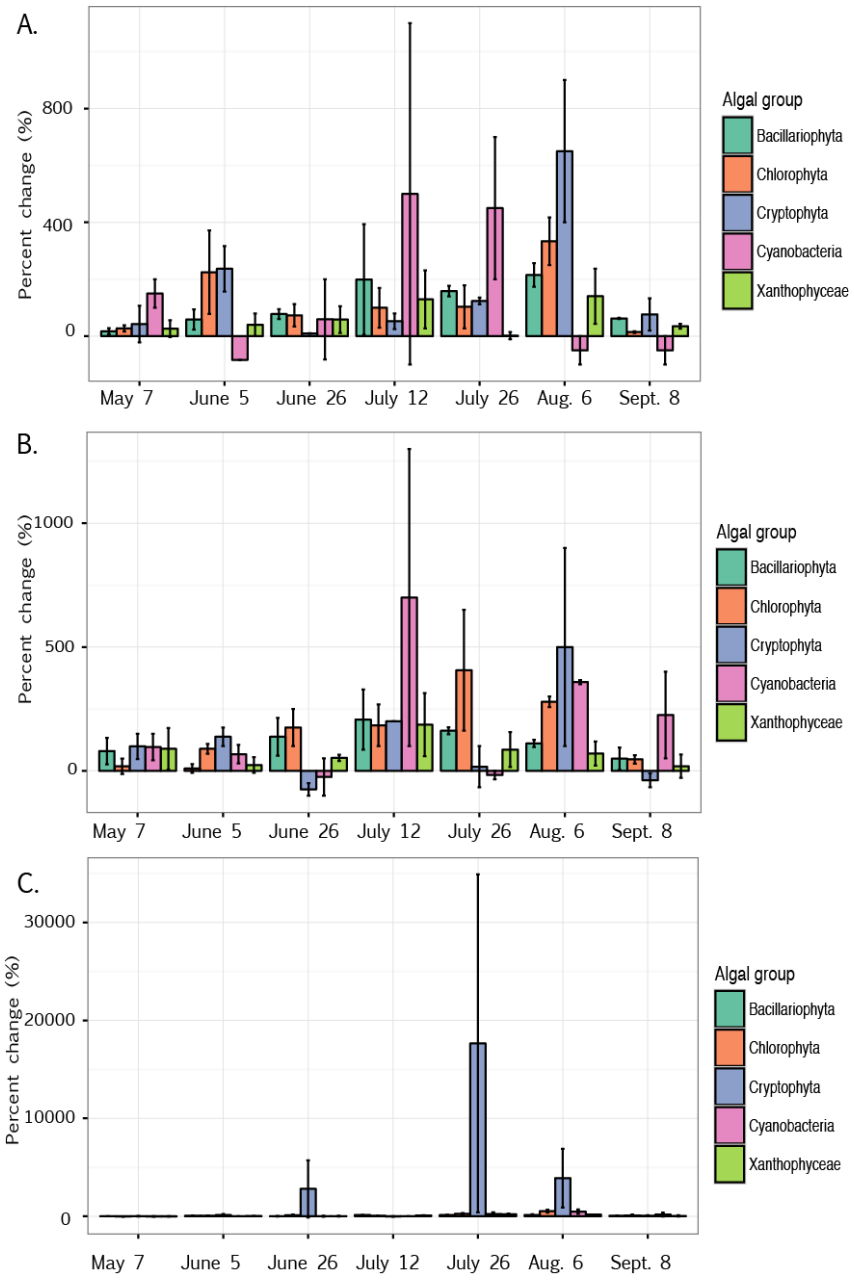

Figure 12. Percent change in abundance of each phytoplankton group after the addition of P relative to the control at sites 1 (A), 2 (B), and 3 (C). Error bars represent ± 1 SE of two time points (T24 and T48).

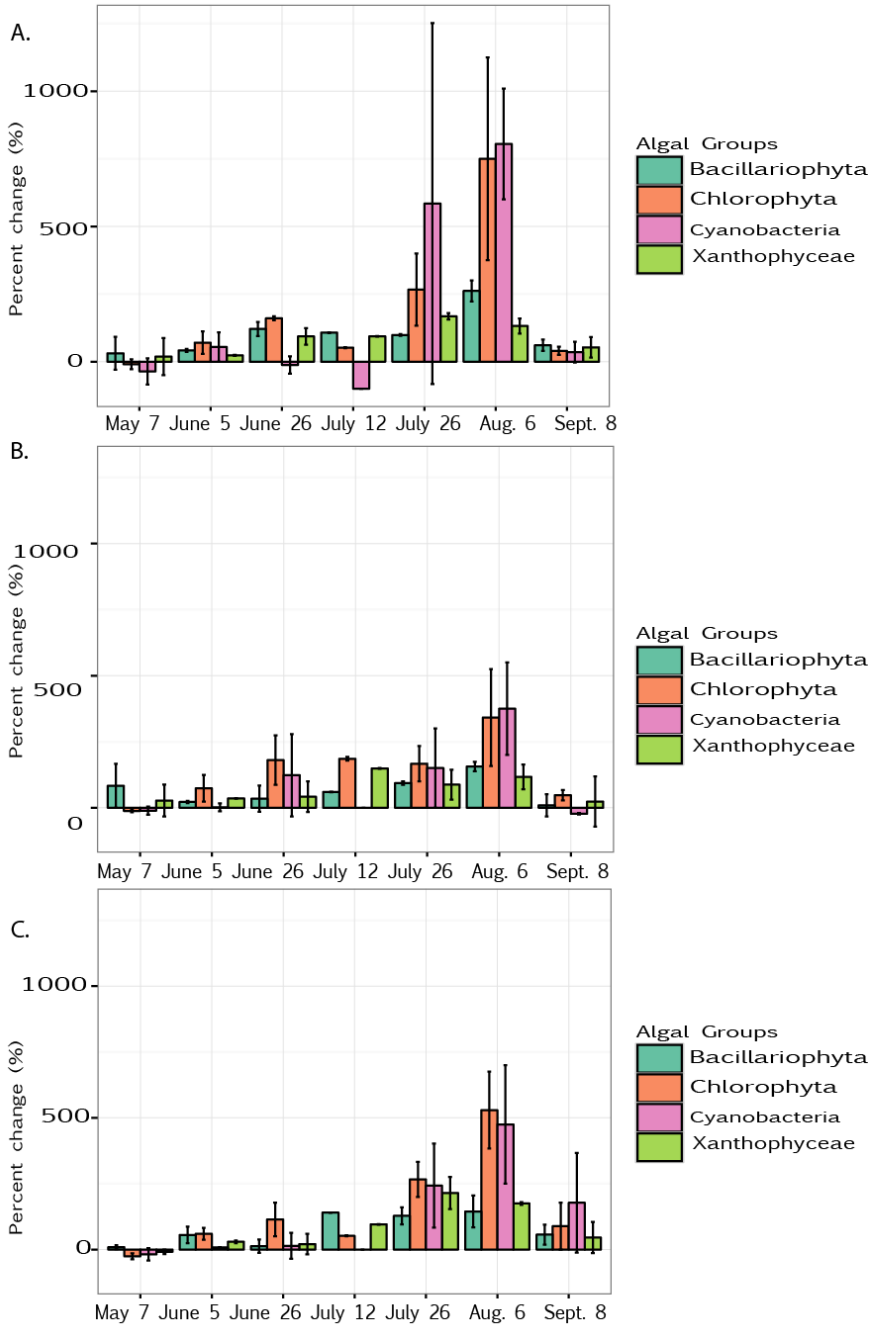

Figure 13. Percent change in abundance of each phytoplankton group except for cryptophyta after the addition of NH_4^+ plus P (A), NO_3^- plus P (B), and P (C) relative to the control at site 3. Error bars represent ± 1 SE of two time points (T24 and T48).

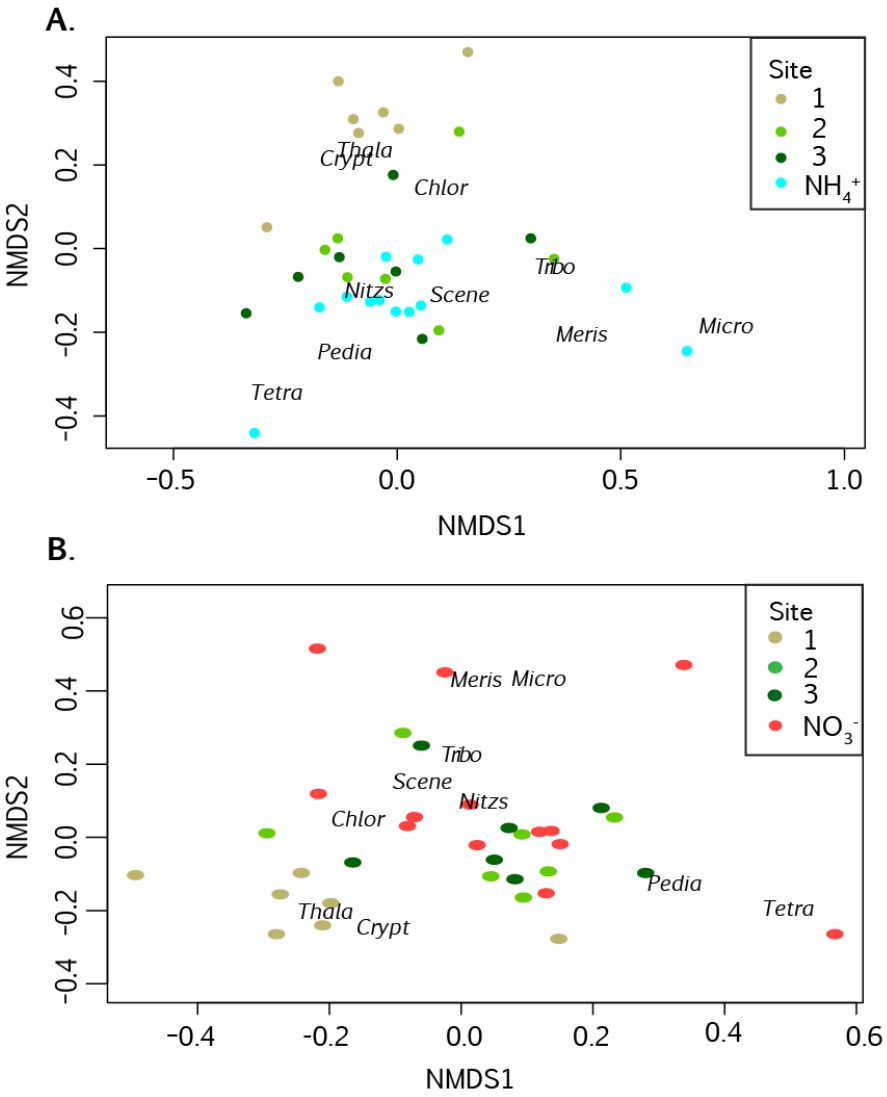

Figure 14. NMDS plot for phytoplankton abundance. Circles are samples and are color-coded depending on which site they came from, while species abundances are labeled. The blue dots in (A) represent the phytoplankton abundance on each sampling date after the addition of NH_4^+ to site 3 samples. The red dots in (B) represent the phytoplankton abundance on each sampling date after the addition of NO_3^- to site 3 samples.

REFFERENCES

Anonymous. 2010. Raising a Stink. The Economist. <http://www.economist.com/node/16744110>.

Arar, E. J., Collins, G.B. 1992. In vivo determination of chlorophyll *a* and phaeophytin *a* in marine and freshwater phytoplankton by fluorescence. Methods for the Determination of Chemical Substances in Marine and Estuarine Samples. Environmental Monitoring and Support Laboratory, Office of Research and Development, Cincinnati, OH (U.S. EPA, OH EPA/600/R-92/121.)

Berg, G. M., Balode, M., Purina, I., Bekere, S., Béchemin, C. and Maestrini, S. 2003. Plankton community composition in relation to availability and uptake of oxidized and reduced nitrogen. *Aquatic Microbial Ecology* **30**, 263-274.

Bran and Luebbe, Inc. 1999a. Bran Luebbe Autoanalyzer Applications: AutoAnalyzer Method No. Nitrate and Nitrite in Water and Seawater. Buffalo Grove, IL: Bran Luebbe, Inc.

Bran and Luebbe, Inc. 1999b. Bran Luebbe Autoanalyzer Applications: AutoAnalyzer Method No. G-175-96 Phosphate in Water and Seawater. Buffalo Grove, IL: Bran Luebbe, Inc.

Briceño, H. O. and Boyer, J. N. 2010. Climatic controls on phytoplankton biomass in a sub-tropical estuary, Florida Bay, USA. *Estuaries and Coasts,* **33**(2), 541-553.

Bricker, S. B., Longstaff, B., Dennison, W., Jones, A., Boicourt, K., Wicks, C. and Woerner, J. 2008. Effects of nutrient enrichment in the nation's estuaries: a decade of change. *Harmful Algae,* **8,** 21-32.

Burkholder, J. M., Dickey, D. A., Kinder, C. A., Reed, R. E., Mallin, M. A., Mciver, M. R., Cahoon, L. B., Melia, G., Brownie, C. and Smith, J. 2006. Comprehensive trend analysis of nutrients and related variables in a large eutrophic estuary: A decadal study of anthropogenic and climatic influences. *Limnology and Oceanography,* **51,** 463-487.

Chen, H., Yu, Z., Yao, Q., Mi, T. and Liu, P. 2010. Nutrient concentrations and fluxes in the Changjiang Estuary during summer. *Acta Oceanologica Sinica,* **29,** 107-119.

Chen, N., Hong, H., Zhang, L. and Cao, W. 2008. Nitrogen sources and exports in an agricultural watershed in Southeast China. *Biogeochemistry,* **87,** 169-179.

Chen, Y., Fan, C., Teubner, K. and Dokulil, M. 2003a. Changes of nutrients and phytoplankton chlorophyll-a in a large shallow lake, Taihu, China: an 8-year investigation. *Hydrobiologia,* **506,** 273-279.

Chen, Y., Qin, B., Teubner, K. and Dokulil, M. T. 2003b. Long-term dynamics of phytoplankton assemblages: Microcystis-domination in Lake Taihu, a large shallow lake in China. *Journal of Plankton Research,* **25,** 445-453.

Chen, Y. and Tang, D. 2012. Eddy-feature phytoplankton bloom induced by a tropical cyclone in the South China Sea. *International Journal of Remote Sensing,* **33,** 7444-7457.

Clarke, K. R. 1993. Non-parametric multivariate analyses of changes in community structure. *Australian Journal of Ecology,* **18,** 117-143.

Collos, Y. and Harrison, P. J. 2014. Acclimation and toxicity of high ammonium concentrations to unicellular algae. *Marine Pollution Bulletin,* **80,** 8-23.

Cui, S., Shi, Y., Groffman, P. M., Schlesinger, W. H. and Zhu, Y. G. 2013. Centennial-scale analysis of the creation and fate of reactive nitrogen in China (1910–2010). *Proceedings of the National Academy of Sciences,* **110,** 2052-2057.

De Cáceres, M. 2013. How to use the indicspecies package (ver. 1.7.1). <http://cran.r-project.org/web/packages/indicspecies>.

Domingues, R. B., Barbosa, A. B., Sommer, U. and Galvão, H. M. 2011. Ammonium, nitrate and phytoplankton interactions in a freshwater tidal estuarine zone: potential effects of cultural eutrophication. *Aquatic Sciences,* **73,** 331-343.

Donald, D. B., Bogard, M. J., Finlay, K., Bunting, L., and Leavitt, P. R. 2013. Phytoplankton-specific response to enrichment of phosphorus-rich surface waters with ammonium, nitrate, and urea. *PLoS ONE*, **8**: e53277.

Donald, D. B., Bogard, M. J., Finlay, K. and Leavitt, P. R. 2011. Comparative effects of urea, ammonium, and nitrate on phytoplankton abundance, community composition, and toxicity in hypereutrophic freshwaters. *Limnology and Oceanography,* **56,** 2161-2175.

Dortch, Q. 1990. The interaction between ammonium and nitrate uptake in phytoplankton. *Marine Ecology Progress Series.* **61,** 183-201.

Duan, H., Ma, R., Xu, X., Kong, F., Zhang, S., Kong, W., Hao, J. and Shang, L. 2009. Two-decade reconstruction of algal blooms in China's Lake Taihu. *Environmental Science & Technology,* **43,** 3522-3528.

Dufrêne, M. and Legendre, P. 1997. Species assemblages and indicator species: the need for a flexible asymmetrical approach. *Ecological Monographs,* **67,** 345-366.

Dugdale, R. C. and Goering, J. J. 1967. Uptake of new and regenerated forms of nitrogen in primary productivity. *Limnology and Oceanography,* **12,** 196-206.

Edwards, V. R., Tett, P., and Jones, K. J. 2003. Changes in the yield of chlorophyll from dissolved available inorganic nitrogen after an enrichment event-applications for predicting eutrophication in coastal waters. *Continental Shelf Research*, **23**, 1771-1786.

Gardener, M. 2014. *Community Ecology: Analytical Methods Using R and Excel,* (Pelagic Publishing), 447-463.

Glibert, P. M. 2012. Ecological stoichiometry and its implications for aquatic ecosystem sustainability. *Current Opinion in Environmental Sustainability,* **4,** 272-277.

Glibert, P. M. and Berg, G.M. 2009. Nitrogen form, fate and phytoplankton composition, p. 183-189. In V. S. Kennedy, W. M. Kemp, J. E. Peterson and W. C. Dennison [eds], Experimental ecosystems and scale: Tools for understanding and managing coastal ecosystems. New York, NY: Springer.

Glibert, P. M., Dugdale, R. C., Wilkerson, F., Parker, A. E., Alexander, J., Antell, E., Blaser, S., Johnson, A., Lee, J. and Lee, T. 2014c. Major–but rare–spring blooms in 2014 in San Francisco Bay Delta, California, a result of the long-term drought, increased residence time, and altered nutrient loads and forms. *Journal of Experimental Marine Biology and Ecology,* **460,** 8-18.

Glibert, P. M., Harrison, J., Heil, C. and Seitzinger, S. 2006. Escalating worldwide use of urea–a global change contributing to coastal eutrophication. *Biogeochemistry,* **77,** 441-463.

Glibert, P. M., Hinkle, D. C., Sturgis, B. and Jesien, R. V. 2014d. Eutrophication of a Maryland/Virginia coastal lagoon: a tipping point, ecosystem changes, and potential causes. *Estuaries and Coasts,* **37,** 128-146.

Glibert, P. M., Kana, T. M. and Brown, K. 2013. From limitation to excess: the consequences of substrate excess and stoichiometry for phytoplankton physiology, trophodynamics and biogeochemistry, and the implications for modeling. *Journal of Marine Systems*, **125**, 14-28.

Glibert, P. M., Manager, R., Sobota, D. J. and Bouwman, L.. 2014a. The Haber-Bosch-Harmful algal bloom (HB-HAB) link. *Environmental Research Letters.* **9**, 105001(13 pp).

Glibert, P. M., Wilkerson, F. P., Dugdale, R. C., Parker, A. E., Alexander, J., Blaser, S. and Murasko, S. 2014b. Microbial communities from San Francisco Bay Delta respond differently to oxidized and reduced nitrogen substrates - even under conditions that would otherwise suggest nitrogen sufficiency. *Frontiers in Marine Science,* **1**, article 17.

Glibert, P. M., Wilkerson, F. P., Dugdale, R. C., Raven, J. A., Dupont, C. L., Leavitt, P. R., Parker, A. E., Burkholder, J. M. and Kana, T. M. 2016. Pluses and minuses of ammonium and nitrate uptake and assimilation by phytoplankton and implications for productivity and community composition, with emphasis on nitrogen-enriched conditions. *Limnology and Oceanography,* **61,** 165-197.

Gowen, R. J., Tett, P., and Jones, K. J. 1992. Predicting marine eutrophication: the yield of chlorophyll from nitrogen in Scottish coastal waters. *Marine Ecology Progress Series*, **85**, 153-161.

Harding Jr, L. W., Batiuk, R. A., Fisher, T. R., Gallegos, C. L., Malone, T. C., Miller, W. D., Mulholland, M. R., Paerl, H. W., Perry, E. S. and Tango, P. 2014. Scientific bases for numerical chlorophyll criteria in Chesapeake Bay. *Estuaries and Coasts,* **37,** 134-148.

Heil, C. A., Revilla, M., Glibert, P. M. and Murasko, S. 2007. Nutrient quality drives differential phytoplankton community composition on the southwest Florida shelf. *Limnology and Oceanography,* **52,** 1067-1078.

Hongping, P. and Jianyi, M. 2002. Study on the algal dynamic model for West Lake, Hangzhou. *Ecological Modelling,* **148,** 67-77.

Lee, T. A., Rollwagen-Bollens, G. and Bollens, S. M. 2015. The influence of water quality variables on cyanobacterial blooms and phytoplankton community composition in a shallow temperate lake. *Environmental Monitoring and Assessment,* **187,** 1-19.

Li, Y. and Zhang, J. 1999. Agricultural diffuse pollution from fertilisers and pesticides in China. *Water Science and Technology,* **39,** 25-32.

Lomas, M. W. and Glibert, P. M. 1999a. Interactions between NH_4^+ and NO_3^- uptake and assimilation: comparison of diatoms and dinoflagellates at several growth temperatures. *Marine Biology,* **133,** 541-551.

Lomas, M. W. and Glibert, P. M. 1999b. Temperature regulation of nitrate uptake: a novel hypothesis about nitrate uptake and reduction in cool-water diatoms. *Limnology and Oceanography,* **44,** 556-572.

Mallin, M. A. and Corbett, C. A. 2006. How Hurricane Attributes Determine the Extent of Environmental Effects: Multiple Hurricanes and Different Coastal Systems. *Estuaries and Coasts,* **29,** 1046-1061.

McCarthy, J. J. 1981. The kinetics of nutrient utilization. *Canadian Bulletin of Fisheries and Aquatic Sciences,* **210,** 211-233.

McCarthy, M. J., James, R. T., Chen, Y., East, T. L. and Gardner, W. S. 2009. Nutrient ratios and phytoplankton community structure in the large, shallow, eutrophic, subtropical Lakes Okeechobee (Florida, USA) and Taihu (China). *Limnology,* **10,** 215-227.

McCune, B. and Grace, J. B. 2002. Analysis of Ecological Communities. MjM Software Design, Oregon, USA.

McGillicuddy, D. J., Anderson, L. A., Bates, N. R., Bibby, T., Buesseler, K. O., Carlson, C. A., Davis, C. S., Ewart, C., Falkowski, P. G., Goldthwait, S. A., Hansell, D. A., Jenkins, W. J., Johnson, R., Kosnyrev, V. K., Ledwell, J.

R., Li, Q. P., Siegel, D. A. and Steinberg, D. K. 2007. Eddy/Wind Interactions Stimulate Extraordinary Mid-Ocean Plankton Blooms. *Science,* **316,** 1021-1026.

Ministry of Environmental Protection the People's Republic of China (MEP). 2011. State of the Environment: Water Environment. Ministry of Environmental Protection The Peope's Republic of China. <http://english.mep.gov.cn>.

Morris, I. and Syrett, P. J. 1963. The development of nitrate reductase in Chlorella and its repression by ammonium. *Archiv für Mikrobiologie,* **47,** 32-41.

Nixon, S. W. 1995. Coastal marine eutrophication: a definition, social causes, and future concerns. *Ophelia,* **41,** 199-219.

Oksanen, J. 2014. *Multivariate analysis of ecological communities in R: vegan tutorial*. <http://cc.oulu.fi/~jarioksa/opetus/metodi/vegantutor.pdf>.

Oksanen, J., Blanchet, F. G., Kindt, R., Legendre, P., Minchin, P. R., O'hara, R. B., Simpson, G. L., Solymos, P., Stevens, M. H. H. and Wagner, H. 2015. *vegan: Community Ecology Package.* R package version 2.0-10.

Paerl, H. W., Valdes, L. M., Peierls, B. L., Adolf, J. E. and Harding, L. W. 2006. Anthropogenic and climatic influences on the eutrophication of large estuarine ecosystems. *Limnology and Oceanography,* **51,** 448-462.

Parker, A. E., Dugdale, R. C., and Wilkerson, F. P. 2012. Elevated ammonium concentrations from wastewater discharge depress primary productivity in the Sacramento River and the Northern San Francisco Estuary. *Marine Pollution Bulletin*, **64**, 574-586.

Pu, P., Hu, W., Yan, J., Wang, G. and Hu, C. 1998. A physico-ecological engineering experiment for water treatment in a hypertrophic lake in China. *Ecological Engineering,* **10,** 179-190.

R Core Team. 2014. *R: A language and environment for statistical computing. R Foundation for Statistical Computing*. R Foundation for Statistical Computing, Vienna, Austria.

Rabalais, N. N., Turner, R. E., Díaz, R. J. and Justić, D. 2009. Global change and eutrophication of coastal waters. *ICES Journal of Marine Science: Journal du Conseil,* **66,** 1528-1537.

Raven, J. A., Linda, B. W. and Handley, L. 1992. Ammonia and ammonium fluxes between photolithotrophs and the environment in relation to the global nitrogen cycle. *New Phytologist,* **121,** 5-18.

Sharp, J. H., Yoshiyama, K., Parker, A. E., Schwartz, M. C., Curless, S. E., Beauregard, A. Y., Ossolinski, J. E. and Davis, A. R. 2009. A biogeochemical view of estuarine eutrophication: seasonal and spatial trends and correlations in the Delaware Estuary. *Estuaries and Coasts,* **32,** 1023-1043.

Ti, C. and Yan, X. 2013. Spatial and temporal variations of river nitrogen exports from major basins in China. *Environmental Science and Pollution Research,* **20,** 6509-6520.

Van Drecht, G. A., Bouwman, A. F., Harrison, J. and Knoop, J. M. 2009. Global nitrogen and phosphate in urban wastewater between 1970 and 2050, *Global Biogeochemical Cycles*, **23**, GB0A03.

Voynova, Y. G. and Sharp, J. H. 2012. Anomalous biogeochemical response to a flooding event in the Delaware Estuary: a possible typology shift due to climate change. *Estuaries and Coasts,* **35,** 943-958.

Whitledge, T. E., Malloy, S. C., Patton, C. J. and Wirick, C. D. 1981. Automated nutrient analyses in seawater. Brookhaven National Lab., Upton, NY (USA).

Xu, J., Glibert, P. M., Liu, H., Yin, K., Yuan, X., Chen, M. and Harrison, P. J. 2011. Nitrogen Sources and Rates of Phytoplankton Uptake in Different Regions of Hong Kong Waters in Summer. *Estuaries and Coasts,* **35,** 559-571.

Zhao, H., Tang, D. and Wang, D. 2009. Phytoplankton blooms near the Pearl River estuary induced by Typhoon Nuri. *Journal of Geophysical Research: Oceans,* **114**, C12027.

CONCLUSIONS

This research elucidates how changes in N-forms and N:P-ratios determine phytoplankton communities in two urban freshwater systems, the Anacostia River, USA, a tributary to the Potomac River feeding into the Chesapeake Bay, and West Lake, Hangzhou, Zhejiang Province, China. This work assessed the response of phytoplankton communities to changing N-form by posing questions: Do different N-forms support different phytoplankton functional groups? More specifically, do sites with higher NH_4^+:NO_3^- ratios, even against a background of elevated nutrients, support more cyanobacteria, while lower NH_4^+:NO_3^- ratios support more diatoms? Finally, does the community composition after the enrichment of waters with different N-forms mirror the observations expected in the field? Although the Anacostia River and West Lake differ significantly in terms of hydrology, climate, and socio-economic uses, these systems share interests of economic development, healthy residential areas and resource management. These mutual interests and contrasting freshwater environments provide a unique opportunity to learn about the influence of N-form on phytoplankton community composition and ecosystem productivity.

Characterizations of the ambient phytoplankton communities and N-forms in both of the studied freshwater systems illustrate similar seasonal and spatial patterns. Following the >2-fold increase in NH_4^+:NO_3^- ratios observed from the early spring to late summer in the Anacostia River, the phytoplankton community shifted from more diatoms to chlorophytes and cyanobacteria. In general, a similar pattern was also observed in West Lake; however, in addition to the increase in chlorophytes and cyanobacteria following increasing NH_4^+:NO_3^- ratios , a filamentous yellow-green algae

(xanthophyceae) also became more abundant in the late summer. The NH_4^+:NO_3^- ratios and the dominant phytoplankton functional groups also differed across the sampling sites in the Anacostia River and West Lake. In the Anacostia River, the upper river typically had smaller NH_4^+:NO_3^- ratios than the lower portion of the river. It is expected that the smaller ratios in the upper river supported more diatoms, whereas higher ratios in the lower river supported more cryptophytes, chlorophytes and cyanobacteria. Likewise in West Lake, the site-averaged NH_4^+:NO_3^- ratios more than doubled from the entrance of the Lake, receiving water from the Qiantang River, to the point of outflow. As the NH_4^+:NO_3^- ratio increased in West Lake, a higher abundance of chlorophytes was observed at the sites with higher NH_4^+:NO_3^- ratios.

Overall, the enrichment experiments conducted here from both parts of the globe add further evidence to the growing consensus that N-form plays a significant role in determining phytoplankton community structure even when N is not at levels considered limiting for phytoplankton production. The addition of a gradient of NH_4^+ concentrations to water from the Anacostia River resulted in the proliferation of chlorophytes and a reduction in the number of diatoms. A similar pattern was observed in West Lake when samples enriched with NH_4^+ and NH_4^+ plus P lead to increased abundance of chlorophytes and cyanobacteria. The findings that changes in N-form supported differential phytoplankton communities is compatible with previous findings in lakes and estuaries, such as Wascana Lake, Canada, San Francisco Estuary, a tidal estuary in Spain, and reservoirs in the Midwestern United States (Donald *et al.* 2011, Domingues *et al.*, 2011, Glibert *et al.*, 2014a, Harris *et al.*, 2016).

The availability of different forms of N has often been used to understand ecosystem fates, such as biotic responses propagating through the food web from phytoplankton to fish. A classic concept within oceanographic phytoplankton ecology, based on the idea of "new" and "regenerated" production, is that NO_3^- supports fish production, while NH_4^+ supports microbial food webs in nutrient depleted marine systems (Dugdale and Goering, 1967). It has not been clear how this dichotomous control of food webs fits into the framework of systems experiencing chronic nutrient-enrichment. This work reveals that in both of these systems experiencing nutrient enrichment that NH_4^+ supports communities dominated by more chlorophytes and cyanobacteria than other phytoplankton groups.

The phytoplankton community in the Anacostia River and West Lake showed similar responses in community composition following changes in NH_4^+:NO_3^- ratios, yet there were some obvious dissimilarities in terms of how the systems responded to their specific environments. For example, West Lake experienced more stochastic weather events than the Anacostia River during the period of sampling encompassed here, considering the rapid changes in phytoplankton community composition following the expected pulsing of nutrients during the 2015 typhoons. For the most part, the upper Anacostia River showed a gradual change in phytoplankton community following the continuous delivery of nutrients from its tributaries and groundwater. On the other hand, the sharp changes in community structure in the lower portion of the Anacostia may be due to the pulsing of nutrients from combined sewer overflow effluent during rain events. In addition to N-forms, differences in the community composition in these contrasting

parts of the globe are also attributed to their environmental conditions, such as temperature and the existing community at the time of nutrient delivery.

Anthropogenic forces are likely to continue forcing nutrient stoichiometry of ecosystems into new stable states (Glibert *et al.*, 2013). Although this analysis only focused on two nutrient-enriched freshwater systems, the need for consistent monitoring of N-forms rather than simply N and P extends to other coastal waters. As demonstrated by the formation of dichotomous phytoplankton communities in the Anacostia River and West Lake, understanding community structure in nutrient enriched systems is complex, and requires an improved understanding of the N-forms from both continuous and more detailed monitoring of N-forms, as well as modeling efforts.

REFERENCES

Domingues, R. B., Barbosa, A. B., Sommer, U. and Galvão, H. M. 2011. Ammonium, nitrate and phytoplankton interactions in a freshwater tidal estuarine zone: potential effects of cultural eutrophication. *Aquatic Sciences,* **73,** 331-343.

Donald, D. B., Bogard, M. J., Finlay, K. and Leavitt, P. R. 2011. Comparative effects of urea, ammonium, and nitrate on phytoplankton abundance, community composition, and toxicity in hypereutrophic freshwaters. *Limnology and Oceanography,* **56,** 2161-2175.

Dugdale, R. C. and Goering, J. J. 1967. Uptake of new and regenerated forms of nitrogen in primary productivity. *Limnology and Oceanography,* **12,** 196-206.

Glibert, P. M., Kana, T. M. and Brown, K. 2013. From limitation to excess: the consequences of substrate excess and stoichiometry for phytoplankton physiology, trophodynamics and biogeochemistry, and the implications for modeling. *Journal of Marine Systems*, **125**, 14-28.

Glibert, P. M., Wilkerson, F. P., Dugdale, R. C., Parker, A. E., Alexander, J., Blaser, S. and Murasko, S. 2014a. Microbial communities from San Francisco Bay Delta respond differently to oxidized and reduced nitrogen substrates - even under conditions that would otherwise suggest nitrogen sufficiency. *Frontiers in Marine Science,* **1**, article 17.

Harris, T. D., Smith, V. H., Graham, J. L., Van De Waal, D. B., Tedesco, L. P. and Clercin, N. 2016. Combined effects of nitrogen to phosphorus ratios and nitrogen speciation on cyanobacterial metabolite concentrations in eutrophic Midwestern USA reservoirs. *Inland Waters,* **6,** 199-210.